Demand Response Enabling Technology Development

Phase I Report: June 2003-November 2005

Overview and Reports from the Four Project Groups:

Thermostat/Controls
Communications/Network
Metering/Sensors
Energy Scavenging

April 4, 2006

Edward Arens: Center for Built Environment, Architecture Dept.
David Auslander: Mechanical Engineering Dept.
David Culler: Electrical Engineering and Computer Science (EECS) Dept.
Cliff Federspiel: Center for the Built Environment, Architecture Dept.
Charlie Huizenga: Center for the Built Environment, Architecture Dept.
Jan Rabaey: Berkeley Wireless Research Center, EECS Dept.
Paul Wright: Mechanical Engineering Dept.
Dick White: Berkeley Sensor and Actuator Center, EECS Dept.

Graduate Student Researchers: Eric Carleton, Xue Chen, Alex Do, Jonathon Foster, Jaehwi Jang, Florian Jourda, Anna LaRue, Eli Leland, Nate Ota, Therese Peffer, Nate Pletcher, Andrew Redfern, Beth Reilly, Dan Steingard, William Watts

Undergraduate Student Researchers: Spencer Ahrens, Vikas Bhargava, Po-kai Chen, Randy Chen, Reman Child, Marc Ramirez, Duncan Wilson, Xin Yang, Yi Yuan

The UC Berkeley team formed an interdisciplinary alliance between the four sub-groups listed after the main title. Weekly interactions among and between the sub-groups enabled high-impact experimentally oriented research mission, while focusing on the common 10x10x10 goal of DR-ETD projects. (Namely 10x cheaper, 10x more capable and >10year life). Over the 2 year period we created early prototypes for the mesh networking of wireless meters, wireless thermostats and wireless temperature nodes. When in final production by commercial entities (in the mid-to-late part of this decade) the OEM costs for the meters and thermostats should be in the "few-dollars" range and the cost for the nodes in the "sub-one-dollar" range.

Table of Contents

Table of Figures

A. BACKGROUND

Introduction

The State of California is moving toward managing electricity use during periods of shortages, as caused by curtailment of *supply* (failures in the power generation or transmission systems, or power market manipulation), or high *usage* (hot weather causing increased air conditioners usage). Measures to reduce the demand for electricity during such shortages are termed 'demand response' (DR). Demand response measures include load reduction, demand bidding, and variable price rates with some mechanism for utility customers to respond to those rates. Variable or dynamic rates are those in which neither time or price are prespecified in the rate. Thus Time-of-use (TOU) rates are not dynamic rates, but critical peak pricing (CPP) and real-time pricing (RTP) are examples of dynamic rates [PG&E 2004]. Demand response measures have the effect of adding elasticity to the electricity market. It has been estimated that a mere 2.5% reduction in demand in response to shortages can reduce the price spikes by 24% [EPRI White Paper 2002].

Need for a New Thermostat

As part of the effort to increase demand responsiveness, the California Energy Commission is currently constructing a new policy to require DR-enabled thermostats for new residential construction in California. This will be part of the State's building energy codes (Title 24 part 6). A number of issues must be addressed before demand-response systems can be effectively deployed on a wide scale in the residential sector. The first is the infrastructure—the meters, communications, and responsive controls, such as a demand response-enabled thermostat. Cost both to purchase and install and usability are other issues. A demand-response thermostat must automatically respond to price signals so that the homeowner is not forced to be a "day trader" in electricity. The demand-response thermostat must be designed so that the homeowner's preferences for cost versus comfort can be easily transferred to the thermostat.

Existing thermostats have very simple functionality. Older electromechanical models contain setpoints plus a deadband, and newer ones are programmable to change setpoints on a predictable hourly schedule, such as setting a furnace at night or when one is away. (Setback thermostats have been required for new residential construction by California building energy codes since 1978). Approximately half of the houses in California that have thermostats have programmable thermostats [CEC, 2004]. However, of the households that have programmable thermostats in California, it is estimated that 35% do not use the programming features, but put the thermostat in hold mode and operate manually [Archacki, 2004]. Adding DR functionality raises the level of complexity beyond the level of the programmable thermostat of today, because now a variable price schedule overlays the occupants' existing patterns of air conditioning and heating use.

Currently, there are a number of programs across the U.S. for encouraging DR in residences and in the small commercial buildings that use residential-scale heating and cooling systems. Most of these programs involve load reduction by a radio-controlled switch on air conditioning units that the utilities control during high demand periods. Very few programs include passing on variable pricing to the customer. In these trial programs, the utility provides participating homeowners a special thermostat equipped with communications to the utility in order to relay prices and to report electricity usage [EEI 2005].

Our system is predicated on the home system receiving a price from the utility that varies over time based on overall demand and supply, and responding by reducing the heating or cooling load or the load of other appliances, as well as informing the occupants of the price and their current electricity consumption. The occupants determine their usage based on their economic, comfort, and convenience preferences. The electricity price and usage is monitored frequently and the accumulated cost transmitted to the utility at least monthly.

Need for New Sensors and Actuators

In addition to controlling air conditioning and heating, there would be further demand responsiveness benefits if our system had a broader scope, managing all significant electrical appliances in the house, and influencing the occupants to manage them in an appropriate manner. For example, pool pumps, electric hot water heaters, and even refrigerators do not run continuously and have some flexibility as to when or how often they come on. Start times could be delayed until the electricity price came down. Similarly, occupants may choose to postpone manually starting a load of laundry if they were aware that the electricity price was high at a particular time.

The broadened scope implies multiple sensors and actuators, more than exist in normal residences today: relays to control on-times of HVAC and appliances, power sensors, temperature and occupancy sensors, and signaling devices to inform occupants about electricity prices and the consequences of decisions. They would be spread about the house, and many would not be where there is convenient access to mains power or communications cabling. It suggests a distributed system.

This system will need to have a **low cost** of purchase and installation and be **simple and convenient to operate,** if it is to achieve widespread market penetration and have a substantial impact on California’s demand responsiveness.

Low cost is important because of social equity: everyone must be able to afford a demand-response thermostat in order for the variable-price rate structure to be socially acceptable. Low cost is also important because, like any new technology, it must pay for itself in order to be successful.

Need for Wireless Network Communication

To achieve low cost, we feel it is necessary to use wireless devices to avoid the substantial cost of running power and communication wires. These devices would need to operate for a long time independently with infrequent battery changes. They should be available from a hardware store, and be installable by a homeowner.

Simplicity of operation is essential for DR to work. Many people find today’s programmable thermostats too complex to program. To be simple enough for most occupants to use, the new DR systems would have to behave autonomously based on effective initial defaults and machine learning; they need to work right out of the box; no programming required in order for it to operate well. The user interface would have to be concise and intuitive for non-technical people. It should help them be effective at managing their home and appliances within a variable-price DR context, which will be a new concept for most people.

Need for Energy Scavenging

Finally, to achieve long life in building applications it is evident that the myriad of networked devices described in this report must operate without replaceable batteries. Apart from battery cost, it would be impractical to expect building owners/users to frequently change batteries in many tiny distributed sensors and actuators. A study of a variety of solar, vibration and flow methods for scavenging is underway as a part of this work

Multidisciplinary DRETD project

UC Berkeley has a project to develop the enabling technology for such a system. The overall UCB Demand Response Enabling Technology Development (DRETD) project addresses the technical issues related to a low-cost, long-life DR system. These include:

- developing low-cost designs for monitoring power in residential circuits using MEMS technology (R. White)
- extending the battery life of radio transmitters by reducing their size and power consumption, and by scavenging power from ambient light and vibration (J. Rabaey, P. Wright)
- developing the open-source wireless network operating system (TinyOS) for this application (D. Culler)
- characterizing the performance of radio networks in building settings (P. Wright)
- developing controls and interfaces to the controls (D. Auslander, E. Arens)

B. THERMOSTAT AND CONTROLS GROUP (Arens and Auslander)

The design of the residential DR system itself — its interfaces, control system, and the non-electricity-metering sensors and actuators, — is being carried out by the 'Thermostat Group'. The system design addresses both system cost and simplicity of use. A prototype was designed, built, and deployed in an occupied house during the 2005 summer season. This paper describes the system design and the results of the deployment test.

Goals of the sub-project on the thermostat and controller

- Design a low-cost demand-responsive electrical appliance manager (DREAM) that exploits wireless technology and a system of learning (both by machine and occupant).
- Develop the hardware and control and communication software of DREAM.
- Test the performance and feasibility of DREAM by deployment in actual occupied house

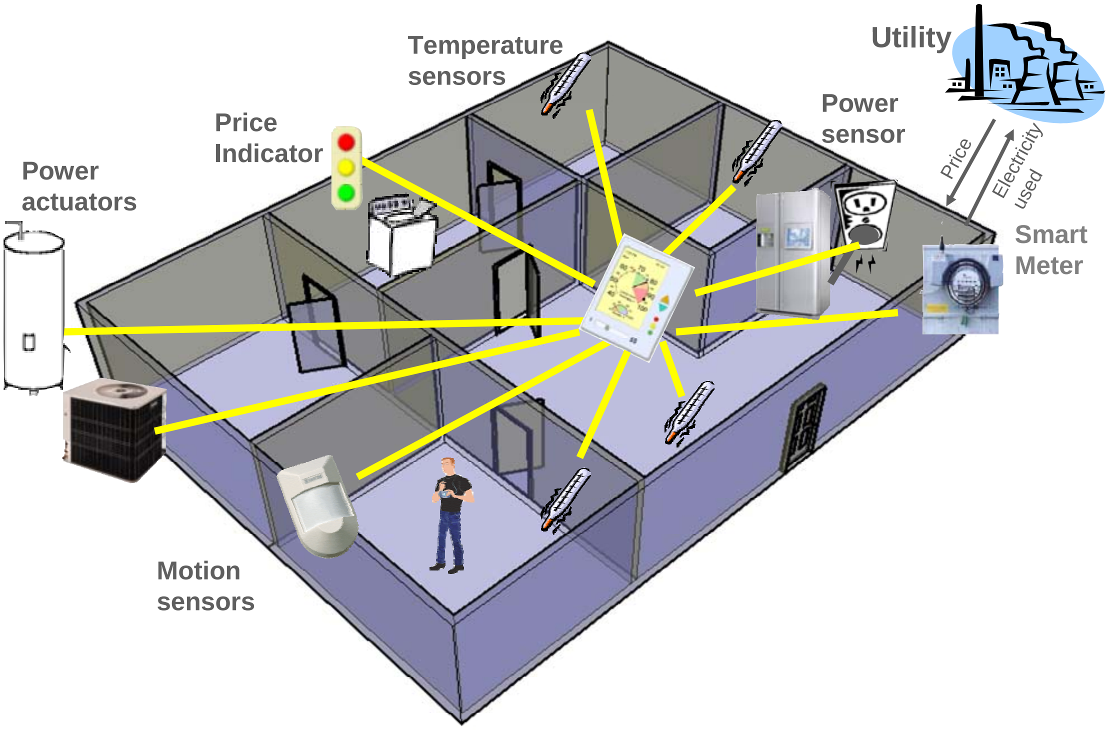

Figure 1: Schematic of the Demand Response Electrical Appliance Manager in a Home.

SYSTEM DESIGN

System Architecture

In order to achieve maximum demand response effectiveness, the system design envisions control or influence over many residential electrical subsystems as well as the ability to get information through sensing throughout the house. If in addition to the control of the HVAC system, as current thermostats do, this system can control electric hot water heaters, refrigerators, pool pumps, etc., then it will be able to do a much better job of shedding electrical load as needed for demand response without undue disturbance to the occupants. Some of these systems, such as pool pumps, could be controlled directly. For others, such as clothes washers and dryers, direct control is probably not practical. The actuation in this case would be occupant-assisted through signaling the occupant via red-yellow-green signals that tell occupants when the time is propitious to run these appliances.

Coupled with the broader control functionality, there is a need for much more information via sensing. It is useful to know temperatures throughout the house, outside weather conditions, occupancy, appliance use, and power consumption. These combine to allow for more targeted control and to be able to deliver predictable behavior and energy cost to the occupants. The system we are designing is thus far more information-rich than current thermostats and has extended command capability.

The system design, then, is driven by the need for distributed sensing and actuation in a system that could be implemented for reasonable cost. Because the cost of wiring is usually the gating factor in systems requiring distributed sensing and actuation, a major enabling technology for this system is low-power, low-cost wireless communication. Each node in this wireless system has a low-power computer or microprocessor, a low-power radio transceiver, and multiple analog or digital input/output channels for sensing and actuation. (These units are called motes; mote: “A very small particle,” *The American Heritage Dictionary*). Power is a major issue because an important design goal is 10 years of operation without any needed scheduled maintenance (such as battery replacement).

Motes are capable of “mesh” networking where each mote can communicate with the motes around it as well as with a central controller, a feature needed for widespread networks in which individual motes are further from the central controller than their transmission range. In the houses we have tested until now, it has not been necessary to use a mesh network to increase communication range or improve reliability. The system architecture as deployed has used a central controller and the wireless equivalent of a “star” network for connectivity to distributed motes; there is a base station connected to the central controller and one repeater strategically located elsewhere in the house. The repeater and the base station are powered from the house’s AC mains.

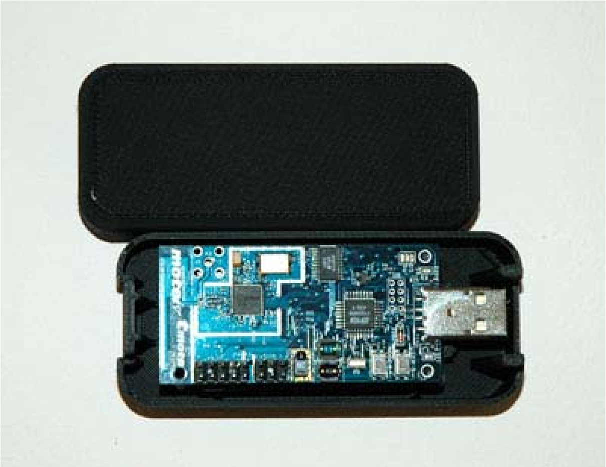

Figure 2: Moteiv ‘T-mote Sky’

We selected a central control design for two reasons: 1) to simplify system deployment in keeping primary control functions in a single software module, and 2) to minimize the power requirements of the computers in the motes. The computing power needed by the central controller is similar to that used by a PDA.

Controller Function

A demand responsive system must be able to operate autonomously in response to price or other demand-related signals received from the electrical grid operator. To do that, the system must be capable of very abstract decision making, such as determining the best cost vs. comfort tradeoff for current conditions, to the very physical, such as turning an air conditioner on or off. At its most basic level, the system must be able to provide HVAC (heat, A/C, fan) control equivalent to current systems. It does that by gathering temperature information from motes equipped with temperature sensors and sending appropriate actuation signals to the mote that is connected to the HVAC system.

The controller's major functions are:

- Receive and process information from sensors
- Send actuation signals
- Control existing HVAC system
- Control other household equipment
- Learn physical characteristics of house from sensor information
- Manage time-of-day profiles (mainly temperature setpoints that follow the adaptive comfort model (deDear and Brager, 2001)
- Display system status to occupants
- Obtain command signals and overrides from occupants
- Learn the preferences and patterns of the occupants
- Receive and display price information from the utility
- Optimize comfort vs. cost based on price and weather information
- Manage power usage based on occupant-provided monthly price cap

While the controller's functions can get quite complex, the controller must operate in an unmanaged environment and be easy and inexpensive to install. This is in contrast to controllers for commercial and industrial buildings, where a substantial amount of effort is spent on installation and tuning, and the system is professionally managed. For this reason, the "learning" items in the function list above are among our key enabling technologies. The controller must operate well in a wide variety of physical environments, large houses, small houses, well-insulated, not insulated and so on, and adjust its operation to the local conditions. This adjustment must be entirely transparent to the occupants.

Likewise, our scheme for demand responsive systems is that price is the mediating factor. Thus, the system must be able to learn occupant preferences with respect to price versus comfort. The history of programmable devices shows that people do not deal well with systems that require them to use a sequence of actions to set up the program. Present-day programmable thermostats are good examples – many are never programmed. However, people will act to correct a situation they do not like, such as being too warm or too cool, as it is clear how to correct the situation. We will use these actions to learn preferences. For example, if an occupant attempts to lower the temperature setpoint at a time when electricity is expensive a confirmation will be required for the action to take effect. The fact that the occupant confirmed that a lower setpoint was desired even though it would be costly to achieve becomes part of the learning process. The measure of success for the learning functionality is that occupants override the system less over time.

Another potential source of information towards better HVAC control and comfort is learning occupancy patterns. The system records the activity pattern of occupants in order to study whether such activity patterns can inform the controller and lead to reduced energy consumption. Most houses have one zone, but multiple sensors may allow for a multi-zone sensing strategy where the HVAC system is only activated if the occupied zone is too hot or cold.

Communications

The wireless network is the communication infrastructure for the system. Despite the very low power of the radio transmitters and the very meager computing capability, it must deliver reliable data to the controller and consistently deliver correct actuation signals. We are using a network infrastructure based on TinyOS, an operating system specifically designed to provide reliable communication in an environment with very limited computing capability. While TinyOS drives the operation of distributed nodes in the system, a central base station connected to the controller receives messages and sends messages which can be intended for all motes, specific groups, or an individual mote. The system is currently configured to communicate in a "star" network with message forwarding used in the repeater mote. Advanced implementation of such a structure allows for a true mesh network, where there are multiple communication paths between motes which are formed ad-hoc.

While the ubiquitous TCP/IP protocol has similar performance goals, its computing requirements far exceed anything that will be available for the residential DR environment in the foreseeable future. The primary driver for these so-called sensor networks is towards lower power for longer lives of self-powered nodes. Thus, the computing capability will at best remain the same as the size and power usage of motes is driven down.

We have constructed a data overlay above TinyOS that treats the component of the system in an object-oriented fashion. We are following the spirit of the IEEE 1451 standard for smart transducers although our system is not able to support the complexity of the full protocol. Each component of the system will be able to register itself with the central controller and give information on what type of sensor or actuator it is, what its calibration characteristics are, and other salient information. See Appendix I. In this way, changing or adding system distributed devices will not require any reprogramming of the central controller.

Sensors

The motes' microprocessors running TinyOS act as intelligent platforms for the sensors as well as handling network operations for communication with the controller. TinyOS allows the unique configuration of parameters, such as sampling frequency and event-based sensing, for each sensor. In addition, the microprocessor allows data processing: averaging or other noise reduction, filtering, sample time control, detection of faults and so on. Intelligent sensing allows for better energy and power management by optimizing data transmission since sending messages is the most power-consuming operation of a typical mote.

Generally, the sensors are connected to the analog or digital input channels by mounting them on an auxiliary circuit board. The ‘Tmote Sky’ from the company Moteiv (previously also called ‘Telos’) can support up to six analog and four digital sensor inputs.

The code to operate the sensors is written in a C- subset language running under TinyOS. Each sensor type requires custom code for its implementation. As noted above, in Communications, each of the sensor types is cast to some degree as an object (in the computing sense) so as to make the interaction with the controller as general as possible. These properties have to be captured in the code written for the motes.

The sensors currently implemented include:

- Temperature – ubiquitous in this system! The actual sensor is normally of thermistor or RTD (resistance temperature detector) type. We measure both air temperature (shielded from radiation) and globe temperature (available to radiative effects). See Appendix A.
- Battery voltage – this is a quantity of internal interest. It provides information for maintenance of self-powered motes.
- Relative humidity – important for comfort estimation.
- Motion – used to determine occupancy of various spaces. Also used to preserve power on the signal light units (see Actuators, below). It uses a passive infrared motion sensor to detect changes in infrared radiation when there is movement by an object with a temperature different than the surroundings (see Appendix B).
- Outside weather – Outside weather conditions are needed for cost estimation and to determine timing for precooling or preconditioning. The weather station includes global and diffuse solar radiation measurements, wind direction and wind speed (see Appendix C).
- Power usage – measurements of power usage are done for the whole house and for individual subsystems or appliances. We are currently using CT metering devices for this. A low-cost, micro-electro-mechanical (MEMS) current meter is being developed. See Appendix D.

Actuators

Actuators connect to the system in the same manner as sensors do, to the I/O channels via an auxiliary circuit board on the mote. In fact, a single mote can contain both sensors and actuators. Where needed, the microprocessors on the motes are powerful enough to perform autonomous control in the event of a communication failure with the central controller.

There are two actuation modules in current use – or maybe it would be better to call that one and a half! The “half” is for the signal light unit used to let people know what the current cost range for electricity is so they can decide whether or not to run selected appliances such as washing machines. The signal light uses the traffic light pattern of red-yellow-green along with an extra light for emergency conditions. We call it a partial actuator because it requires cooperative action on the part of the occupant.

The HVAC actuator (see Appendix E) replaces the connection to the heating and air conditioning units at the conventional thermostat. The HVAC components (furnace, air conditioner, and fan) are actuated by closing 24 volt AC switches, one for each operation. As implemented, all of the operation logic is performed at the controller.

Data Collection

Persistent data collection is important for both operational and experimental reasons. Operationally, the learning functions of the system will have to use historical data that have been collected for algorithms to characterize the system's physical characteristics and the occupant preferences and patterns. Experimentally, we need a complete historical record to verify system operation, track bugs, and to tune and validate our simulation model.

To satisfy these two needs, we developed a database system that collects sensor data and system events. The data is first collected locally via a base mote connected to a laptop computer and then transmitted via Internet to a server in our lab. We thus can review any aspect of the operation and also keep track of current operation of the system .This is crucial for our initial implementations so that problems can be detected quickly and so researchers do not have to travel to implementation sites any more than is necessary.

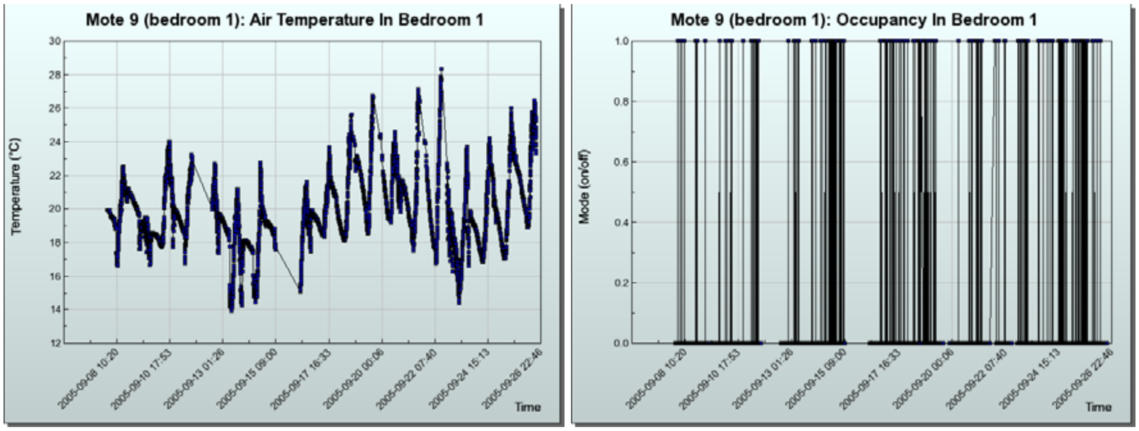

Figure 3: Temperature and Occupancy Data from Mote

The server runs the freely available, open-source MySQL database server (www.mysql.com) to collect data. The database uses an event-based model to store the data generated by the system. A datum sent to the database contains the value and the sensor ID that generated it and is assigned an event ID number. The database contains several tables: one for sensor and actuator information (type and ID), measurement units, measurement values, and mote IDs. This structure allows easy sorting of the data, especially for the human interface.

This database design is flexible, such that different sensors, motes, and measurement units can be added independently of one another. The database can easily keep track of these many-to-many relationships. A change of hardware in the field requires only the modification of the proper ID numbers in the database. See Appendix G.

Controller Implementation

The addition of demand responsiveness and whole house control to basic thermostat functionality leads to a control system with considerable complexity. In order to handle that complexity, we have adopted a layered design for the control system software. In a layered design, each layer (in theory) interacts only with the layers above and below it. This provides for modularization of function and semi-independent design of each layer. This form of layering has been a major factor in the success of the Internet. Networking was theoretically characterized by a seven layer design (Jain and Agrawala 1990). In practice, a four layer design was used to implement TCP/IP (Transmission Control Protocol/ Internet Protocol) – strict adherence to the layered design is why computers from all manufacturers, using network interfaces from many manufacturers, with signals going over wires, wirelessly, over fiber optics, all can connect seamlessly.

We are using the layered hierarchy shown in Figure 4 to implement the control. The lower part of the hierarchy describes basic control functions used to maintain temperature in the house and other functions the controller may be responsible for. The lowest layer, the Mote Interface Layer, maintains communication between the controller and the motes with sensors and actuators. Other than that, the function of the lowest levels is similar to a conventional thermostat – manipulate the HVAC system to maintain temperature in the house. Layers above that, however, fulfill the demand responsiveness needs of the system. Of these, the most interesting is the Goal Seeking Layer. It receives pricing information from above and must make decisions about how to best compromise comfort and cost. In the middle, choices must be made as to how to meet the compromise decided on by the Goal Seeker. In many cases, there are choices as to how to achieve this, whole house fan, air conditioning, ceiling fans, etc.

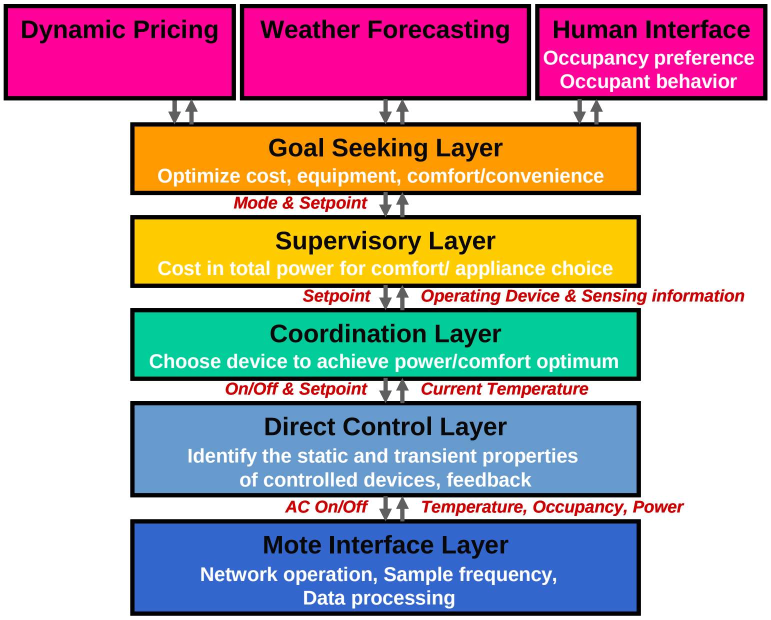
Dynamic Pricing
Weather Forecasting
Human Interface
Occupancy preference
Occupant behavior
Goal Seeking Layer
Optimize cost, equipment, comfort/convenience
Mode & Setpoint
Supervisory Layer
Cost in total power for comfort/ appliance choice
Setpoint
Operating Device & Sensing information
Coordination Layer
Choose device to achieve power/comfort optimum
On/Off & Setpoint
Current Temperature
Direct Control Layer
Identify the static and transient properties
of controlled devices, feedback
AC On/Off
Temperature, Occupancy, Power
Mote Interface Layer
Network operation, Sample frequency,
Data processing

Figure 4: Control Hierarchy Layering

In actually implementing the software, portability has been a primary driver. Portability assures that software does not have to be rewritten when the control has to change context. That context includes different computing platforms and different physical environments. Thus far, we have had to run the software in standard PCs with Windows, Tablet PCs and PDAs. We have used three generations of wireless networks (Mica, Mica2 and T-mote Sky) and we have used them to control simulations of a house, a small model house, a larger segment of a house, and an actual, lived-in residence. In all cases, only the software along the periphery, which actually must interact with the external environment, must change. The core software is insulated by the layered structure from such change.

Our choice of computing environment, Java, has worked well thus far. It has enough complexity to meet our needs and has allowed us to meet all of our experimental conditions very well. The control code is built on base code that implements a task and state transition structure (finite-state machine). This provides a structure for producing software that meets the real-time needs of control well and fits the layered structure also.

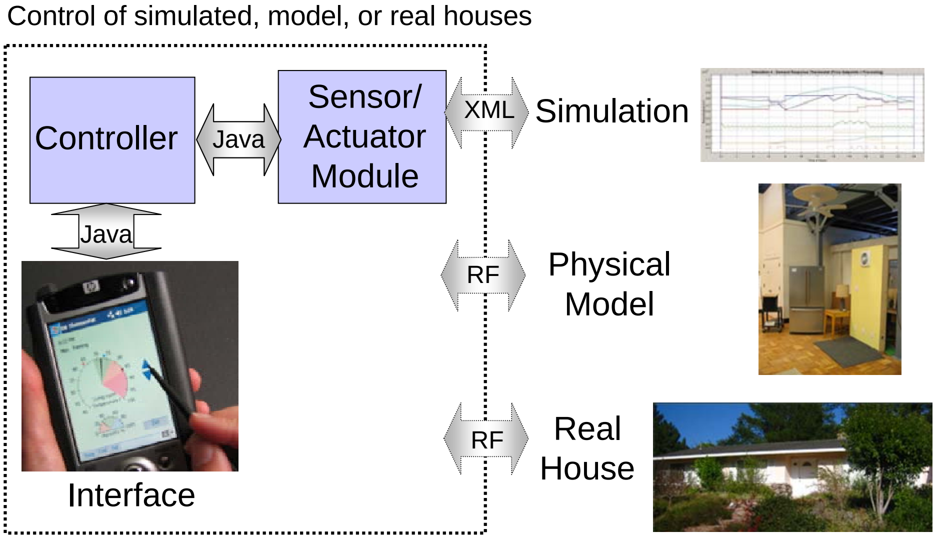

Figure 5: Portability of Java Control Code

EXPERIMENTS BY THERMOSTAT CONTROLS GROUP

Physical description

Over the past two years, we have successfully operated small networks of wireless motes including temperature sensors, actuators (cooler/fan/light), and a controller (Java code run on a PDA or computer) in laboratory settings. We initially demonstrated our network system in a scale model house which had a fully functioning thermoelectric cooling system. It responded to temperature changes and solar loads as imparted by an electric floodlamp, and allowed system performance to be emulated at accelerated timescales. We later built a full-scale wall section with a large fan, electrical outlets, circuit breaker, and standard electrical meter, which allowed our system to operate real appliances such as a refrigerator and room heaters in response to our control code. The system has run on several different mote platforms, which we have sequentially adopted as the mote technology improved. This has helped demonstrate the portability of our sensing and control structure. The next step was to deploy our network outside the laboratory in an actual occupied house, with multiple residents, and test the system over several months.

The house is located southeast of Berkeley, California in a climate that requires both air conditioning in the summer and heating in the winter. The single-story 1825 square foot house has three bedrooms and two bathrooms; the long axis of the house runs north-south. The east-facing windows are protected from solar exposure by trees and the porch roof; however the west-facing windows catch the full brunt of the sun's rays in the afternoon. The house was built in 1968 with an un-insulated floor and walls and single-paned windows; the ceiling has recently been insulated. The packaged HVAC unit sits on the ground outside, and supplies conditioned air via multiple floor vents distributed throughout the house.

Initially, we installed three T-mote Sky motes, and continued adding and relocating motes until we had 13 motes installed in the house. Figure 6 below shows a plan of the house with the final configuration of distributed indoor sensors (motion, air temperature, globe temperature, relative humidity, power sensing) and outdoor weather station. All motes were battery-powered except for one ac-powered repeater mote, and the base mote connected to a Tablet PC. All battery-powered motes transmitted battery voltage data as well as sensor data.

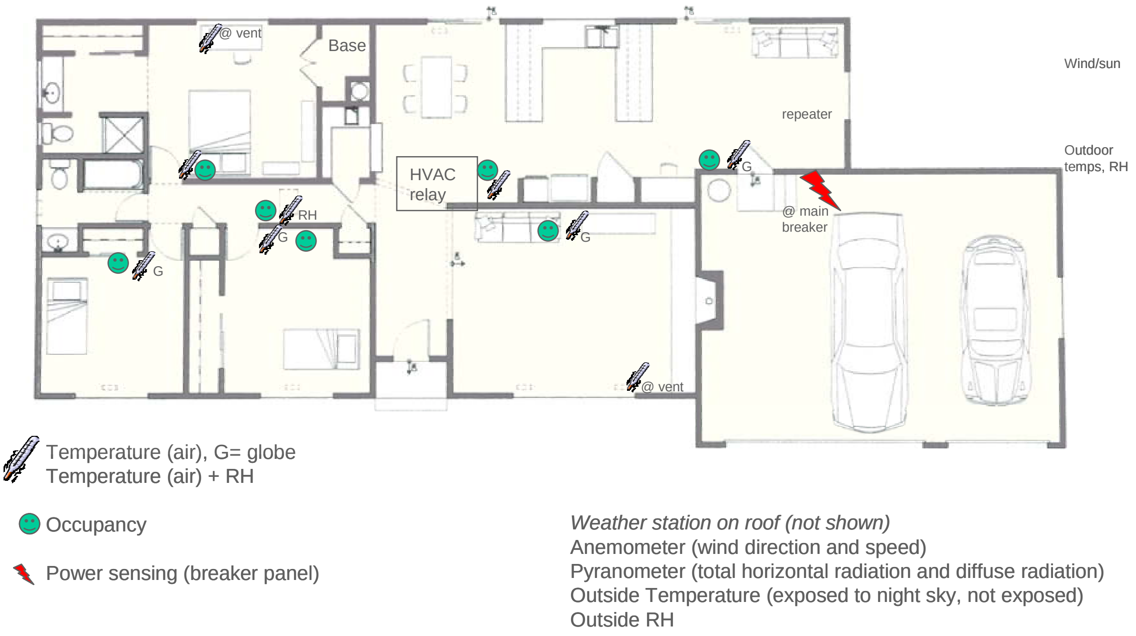
@ vent
Base
Wind/sun
repeater
Outdoor temps, RH
HVAC relay
G
RH
G
G
G
@ main breaker
@ vent
Temperature (air), G= globe
Temperature (air) + RH
Occupancy
Power sensing (breaker panel)
Weather station on roof (not shown)
Anemometer (wind direction and speed)
Pyranometer (total horizontal radiation and diffuse radiation)
Outside Temperature (exposed to night sky, not exposed)
Outside RH

Figure 6: Plan of test house showing location of motes and sensors.

Sensor Deployment

To measure outdoor weather conditions, we installed a mote with four sensors in a weather-tight box on the roof of the house near the chimney. An anemometer and wind vane measured wind speed and direction. Two pyranometers (LI-COR LI-200) measure solar radiation. One measures total horizontal radiation and the other, shielded from direct normal solar radiation by a narrow metal band, measures global diffuse radiation. The difference is the direct radiation on the horizontal. See Appendix C for details on the weather station. Another mote was installed under the eave of the roof, with three sensors: an on-board relative humidity sensor and two temperature sensors. One temperature sensor was located under the eave of the roof and the other exposed to solar and night sky radiation. Combinations of these climate measurements are expected to prove useful in devising future demand-responsive control algorithms.

For most of the indoor motes, we developed a “generic” mote hardware package that can be used to support up to four analog or digital sensors of any kind (see Appendix A). A plastic enclosure was designed to contain the mote powered by two AA batteries and a custom printed circuit (PC) board for the sensor interface to the input/output (I/O) channels on the mote. Four 2.5 mm mono phone jacks were used as the sensor interconnect, since most of our temperature sensors (RTD’s) were prepackaged with mating plugs. On the PC board, voltage divider circuits were set up to connect analog sensors to the Analog to Digital Converter (ADC) ports which could be configured to the specific sensor by installing an appropriate resistor. For digital sensors, no resistor was necessary and the signal would be connected directly to the I/O channel. The I/O lines on the T-mote Sky can be configured as either digital or analog inputs via software, making the electrical design very simple.

As implemented, most generic motes have two temperature sensors (air and globe) and a motion sensor plugged in via the mono phone jacks. One port is available for future sensors, such as light sensor, reed switch to indicate door/window opening, or IR temperature sensor. See Figure 7 below.

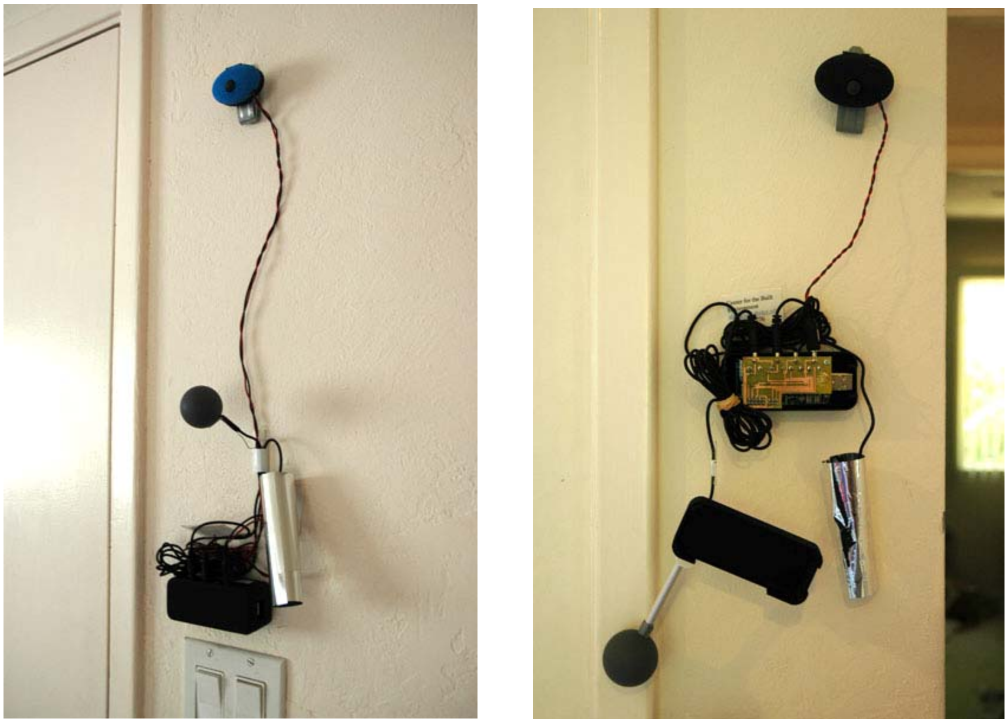

Figure 7: Left- Mote in house with motion sensor "eye", globe temperature sensor (ping pong ball), and air temperature sensor (shielded with low-emissivity Mylar). Right- Mote with cover off, showing sensor board. See Appendix A.

A special package was developed for the power sensor mote. A *Veris* current transducer measured the current in two main circuits as well as the voltage in the main circuit breaker panel in the house. A communication cable transmits this data to a mote via a custom PC board (see Appendix D). Figure 8 below shows the configuration of the CTs in the breaker panel box, and the associated mote (in the grey box with three leads mounted to the right). In this configuration, the mote draws power via the voltage sensor.

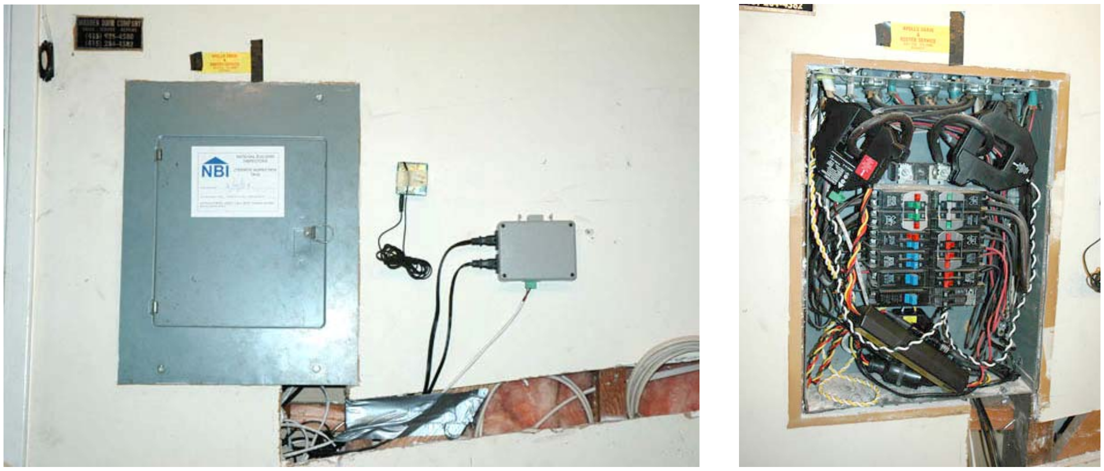

Figure 8: Left: Closed breaker box and mote enclosure. Right: Open breaker box showing CTs and communication cable.

Actuator Deployment

We developed an HVAC actuation mote with four latching relays (24vac hot, heater, ac, fan) to replace the actuation functions of today's thermostat. The HVAC mote was initially designed to include a temperature sensor and LCD display, price signal indicator, and motion sensor; the package was designed around the three C batteries required to operate price signal LEDs running full-time for several weeks. However, for this experiment, only the relay function was tested. See Figure 9 below.

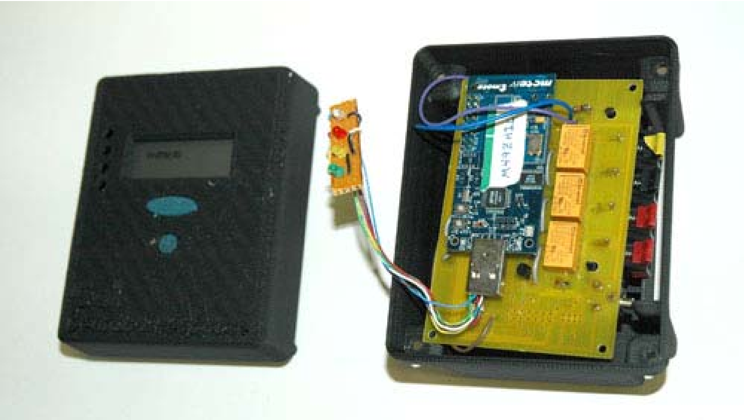

Figure 9: HVAC relay. See Appendix E.

As part of the experimental procedure, we developed a thermostat-switch and sensor mote for safety and testing. This switch allows the user to completely disengage the aforementioned HVAC actuation mote and reconnect the household's original thermostat. In addition this device monitors the operation of the HVAC control wires, the output of both the experimental HVAC mote and extant house thermostat, and sends these feedback signals to the controller to verify operation of the relays. (See Figure 10 below, See Appendix F.)

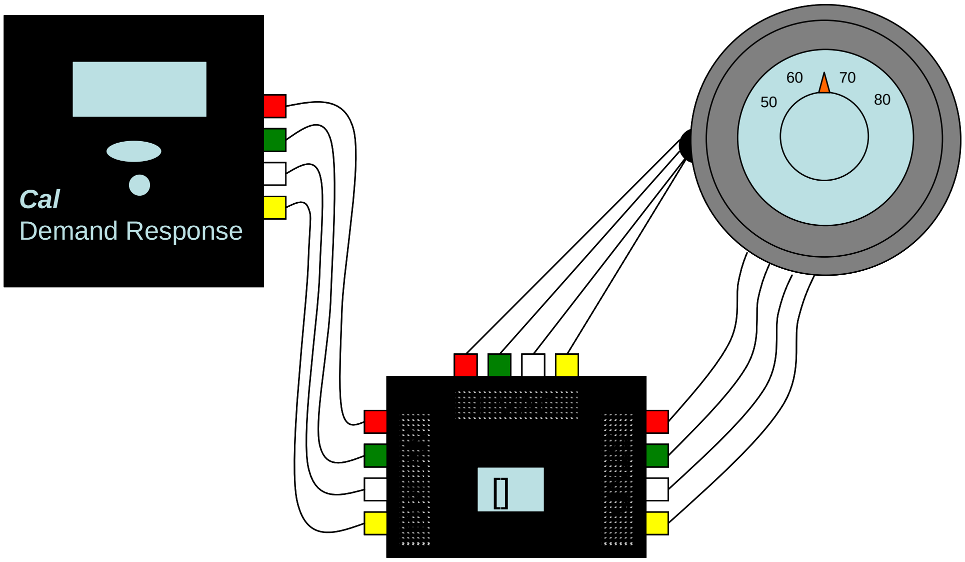

Figure 10: Thermostat switch device (center) changes control of HVAC system from household thermostat (left) to DREAM HVAC relay (right)

The price indicator mote is an example of a signal to an unreliable actuator—the human occupant. While this mote was not tested in the house's occupants in this experiment, we developed the mote as part of the motivational interface to educate occupants and encourage energy conservation behavior during high peak demand periods. See Figure 11 below.

The green/yellow/red stoplight- colored lights operate to indicate three price level ranges. If a light is on continuously, it indicates the current price. If it is flashing, it indicates the future price within a period of, say, ½ hour (this is a variable that we will be testing). So two lights may be on at a time, one continuous and one flashing. The blue diode is the emergency light (similar to a police car's lights) that indicates a crisis event within the electricity supply system It may indicate that critical peak pricing is in effect, or maybe be used just notify occupants to cooperate to avoid a brownout.

The infrared motion-detecting occupancy sensors were developed and packaged for this experiment (see Appendix B).

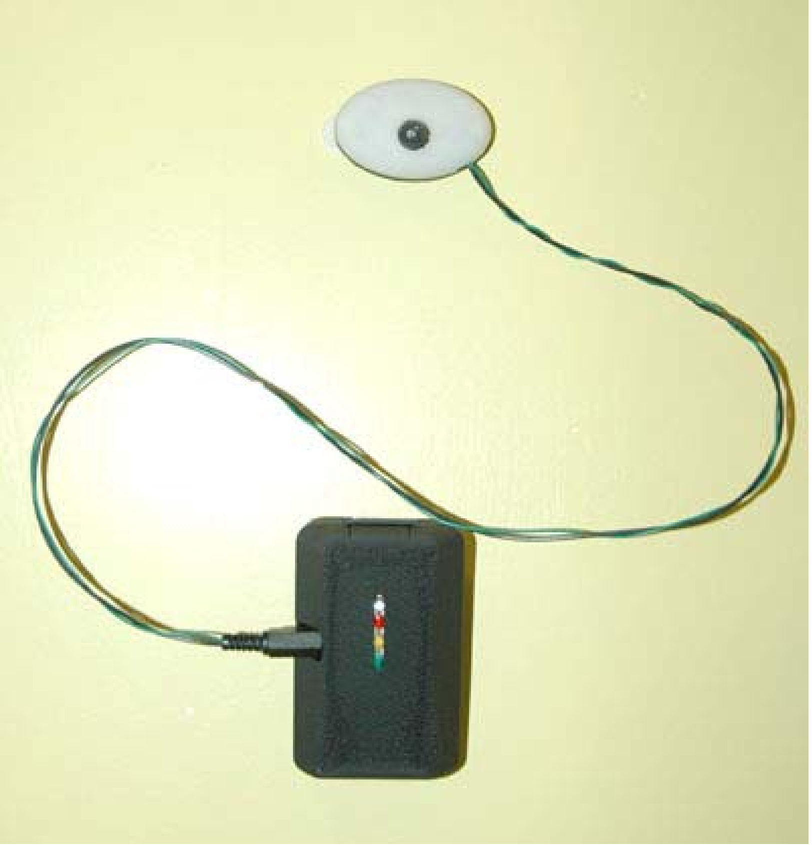

Figure 11: Price indicator mote with red, yellow, green and blue LEDs, and a motion sensor

Procedure

One of the main goals of the house experiment was to test the reliability of the mote network in a real live setting. Using a star network of motes required careful placement of the base mote and Tablet PC with respect to the rest of the motes. We empirically determined that we needed a repeater to relay the signals from the most remote motes. The motes sent scheduled as well as event data. All motes automatically sent sensor data every one to three minutes; in addition, the motes with occupancy sensors sent sensor data whenever the motion sensor detected a change of state.

The control code used for this experiment has been evolving over the past two years. Although we have run the code on a number of desktop and laptop PCs as well as a Windows-based PDA, we had not run the code on a Tablet PC. A Tablet PC was purchased for the experiment, and the graphic user interface code modified to reduce its memory requirements on the tablet.

For experimental purposes, remote monitoring of the system at the house from our laboratory at UC Berkeley was vital. We established a database on a server on campus with an Internet interface. As a backup of the local database in the field, it updates every several hours through the internet. Also, we set up a virtual network computing (VNC) server on the Tablet PC to allow remote access from any client PC anywhere, to troubleshoot problems, and to restart the controller on the Tablet PC. Establishing a reliable connection to the internet was no simple feat due to security concerns and the firewall on the house wireless router.

RESULTS OF THERMOSTAT CONTROL GROUP FIELD TEST

We expected to encounter problems that appear in long-term testing in a real environment, and were not disappointed in this regard! We encountered numerous bugs in the code, problems with the hardware, and issues brought on by the structure and configuration of the house and behavior of its occupants. These were all resolved during the field test, except the most intractable one, which was only identified and corrected in March 2006. While we were sleuthing bugs, the network and sensors were not 100% reliable, and there are hours and sometimes days of data missing from the four-month-long test. However we did collect a large set of data for development and testing of our learning algorithms, and for validating our house simulation model MZEST.

The RTD temperature sensor boards had been used before in other experiments. Of our 14 temperature sensors, one failed before installation and one failed after installation and both were replaced. The motes' on-board battery voltage sensors were reliable and allowed us to change batteries before the motes ran out of power. The on-board relative humidity sensors also functioned reliably.

In general the sensors were more accurate than the motes. The resistors on the mote ADC resulted in a +/-1°C spread prior to calibration. We will address this in our future designs. We rarely saw inconsistent sensor data (temperature and motion). The motion sensors however initially used excessive power, draining a set of AA batteries in 6-8 weeks because of the increased data rate associated with occupancy detection. Changes to the strategy used to detect and communicate occupancy greatly improved power management for these motes.

While the HVAC actuator was extensively tested in the lab, the field-testing of the actuator was not complete. The actuator was completed later than the other devices, and the weather had by then become (prematurely) cool. We successfully performed two short-term closed loop tests with the control software, sensors and HVAC actuator at the house. We plan to perform longer fully realistic tests of HVAC control in early summer 2006. We will also begin to test occupant interaction with our price signaling devices.

The most persistent problem during the 2005 summer tests was a seemingly inexplicable intermittent freezing of individual motes. We did a lot of code and hardware checking to try to find the cause. Initially it was thought that the mote failures were due to unreliable radio hardware, or interference due to packet collisions throughout the wireless network. In March 2006 we finally discovered that the system failure was due to improper radio power management in the TinyOS code. The power management puts the radio to sleep for the majority of the time to conserve battery life.

The initial implementation of the radio code turned the radio on via a radio.start command, and subsequently set a 10 millisecond timer for radio initialization. The radio would not always complete initialization to its send state after the radio.start command was called, and therefore could not respond to subsequent send.message commands from the microprocessor. After the send.message event was flagged, a radio.stop command was called. The radio did not reset state as a result of the stop command, and we are not sure how the radio.stop command interacted with the microprocessor or the radio. The mote would remain in this improper state indefinitely unless a person rebooted the mote by either pressing the onboard reset button or cycling the power.

The solution to the radio initialization problem is to use event-based radio power management. Once the radio.start command is called, no message transmission is attempted until the radio state is set to send ready. Conversely, the radio does not listen for a message until the radio.start command has set the state to receive ready. A network of sensing and actuating motes has not failed once since event-based radio power management was implemented.

DISCUSSION OF THERMOSTAT CONTROLS RESEARCH

Our simple star network deployment was successful in that we were able to achieve our functional wireless sensing and actuation system in an occupied house. We discovered that a star network can work in an occupied house (with cordless phones ringing and microwave ovens in operation), but the base station and motes must be positioned with trial and error to assure that the motes' communication distances are not exceeded. To reduce the trial and error, one can insert a single high sensitivity and/or high power repeater in a star network, or establish a denser configuration in a mesh network.

While we were looking for the cause of our power-management-caused network failures, we tested a watchdog timer, where the lack of mote response for any reason would trigger an automatic reset of the mote. We believe that this feature will increase the reliability of the motes in a network.

The next step with the controller development is to write learning algorithms to optimize performance of the equipment, the thermal performance of the house, and comfort of the occupant. These machine-learning schemes will be developed and tested using a simulation tool we have developed. The data we collected over the summer 2005 experiment have been used to validate and fine-tune this simulation tool, to where the simulated energy performance of a house matches the actual data.

The MultiZone Energy Simulation Tool (MZEST) is built on the California Non-Residential Engine (CNE) found at the heart of many of the simulation tools currently approved for establishing performance compliance with California Title 24 energy code. The tool has been modified to run on a five minute time step with field-collected weather data. See Appendix H.

CONCLUSION OF THERMOSTAT CONTROLS RESEARCH

We successfully developed and deployed a simple star network of sensors in a house for four months, and monitored the controller and data from our lab. We detected and solved a number of hardware, software, and database networking problems. Currently, a small network is set up in our campus laboratory office, where we are focusing on calibrating sensors and testing actuators for deployment in houses in summer 2006.

C. NETWORK COMMUNICATIONS GROUP (Culler and Rabaey)

Overview

The availability of an increasing number of sensor networks platforms has made it possible to start deploying a first generation of DR applications. We are still mostly in the research arena; though slowly but surely progressing into "prototypes in real residencies." The Berkeley motes (made available in larger volumes by Crossbow and Moteiv [Hill, 2002]) have served as the de-facto test bed. Other platforms are also now available from universities (for instance, the Imperial College BSN node) and industry (Ember networks, Infineon, Dust Inc, etc) and could be used in the future. These national and international mote deployments prior to the DR project led to the recognition of the importance of the network lifetime and hence the energy-efficiency of the network operation. This inspired some groups to adopt monolithic software design approaches, breaking the traditional layered model of networking. Alternatively, others resorted to a component-based architecture, which allows for the exposure of implementation layer properties to the network and application layer (e.g. the TinyOS environment [Hill and Culler 2002]).

The Berkeley wireless platform, or "mote", architecture and the associated TinyOS was thus a tremendous success as a prototyping tool and widely used in the DR-ETD project. At the same time the Berkeley "PicoRadio" project was developed in parallel, as a lower-cost radio for the future prototypes (eventually replacing the Chipcon–family of radios on today's motes). The sub-group was led by Professors David Culler (motes) and Rabaey (PicoRadio). Culler's students refined and expanded the TinyOS system by adding new functionality and connections to a database on a base-station (called TinyDB). Rabaey's students reduced the power consumption of the PicoRadio and taped-out prototypes.

TinyOS as a mesh networking tool

We began prototyping with TinyOS in the scaled-down, plastic-model houses, equipping them with mesh-networking that supported inexpensive sensors to measure temperature, light, occupancy, and other quantities - as well as scaled-down actuators for the control of model HVAC and lighting units. In such model houses, and during Year 1 of the project, communications and computation for all system components in Figure 1 were carried out utilizing the MICA2 and MICA2DOT wireless sensor platforms from Crossbow Technology, Inc. These wireless platforms, or "motes", contain an 8-bit Atmel ATmega 128L processor operating at 4MHz, 128 Kb of program memory, 512 Kb of data memory, a 10-bit Analog to Digital Converter (ADC) with 6 to 8 channels, a serial communication channel, and a Chipcon radio operating in the 916 MHz ISM band (Crossbow: *see* www.xbow.com). The motes operated from a 3-Volt power supply and were designed to run applications written for the TinyOS operating system in the NesC programming language, a variant of standard C. This open-source operating system and programming paradigm were developed by Culler, *et al* [see Hill and Culler 2002] for use specifically in wireless sensor networks and other energy efficient, resource-constrained systems.

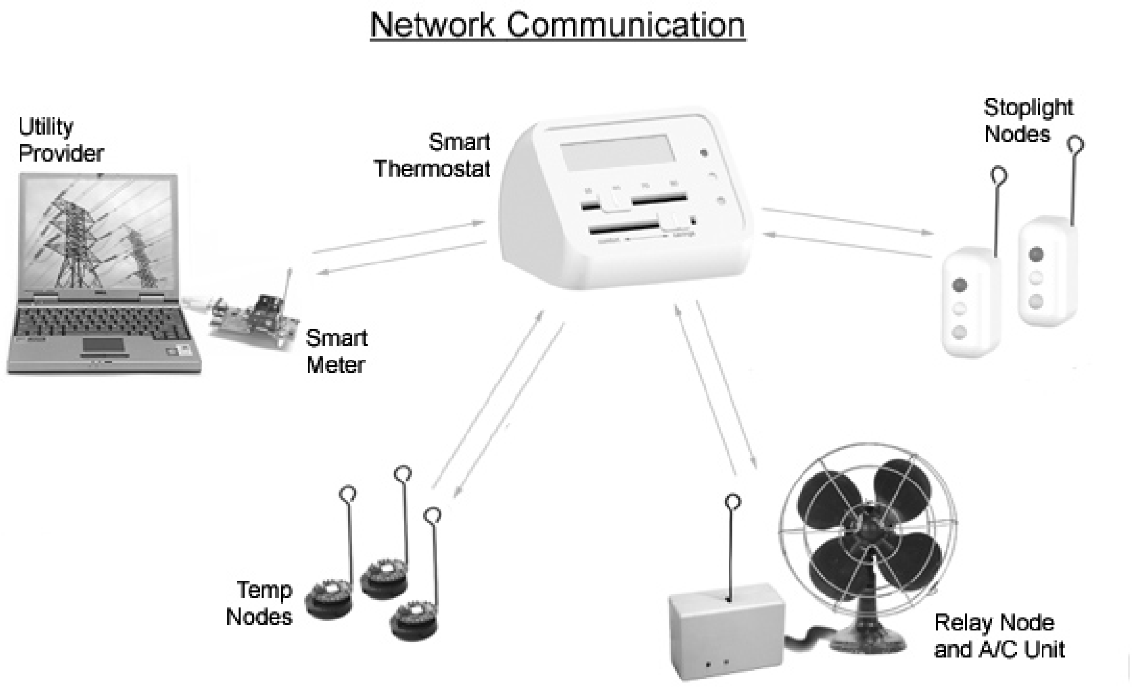

Figure 12: An early prototype using Crossbow MICA motes (Hooks, Ota, & BWRC)

In these early ideas the “smart meter” was simulated on a laptop and tracked power usage. However instead of merely recording a summation of total power used in kWh, the software in Figure 12 supported interval metering, taking data points and recording usage for discrete time periods. This added functionality allowed the simulated meter to be compatible with a variety of dynamic tariff structures. The “smart thermostat” served as the user interface for the system. In addition to the traditional information provided to users via a thermostat, the central device in Figure 12 incorporated a display to indicate the current price of electricity. A stoplight convention was employed to indicate price level, instead of displaying monetary prices in kilowatts per hour (kWh), which we assumed would be largely unfamiliar to the average energy consumer. With the stoplight convention a green light indicated low prices, yellow intermediate, and red high -- alerting users to “adjust their demand” by the slider bar in the unit. Typically this would mean that the user had two comfort settings: one for normal, and one for higher prices.

In the second year the mesh-networking was further evaluated in a 25 node system called Etchnet, installed throughout Etcheverry Hall on the UC Berkeley campus. At that point a strategic decision was made to change hardware to the Moteiv platform (see www.moteiv.com). At the time, this new platform was deemed very robust with a greater wireless range using the 2.4 GHz radio shown in Figure 13. The specific device is ~ 50mm long, 25mm wide with an overall thickness of 5mm. It can be programmed through the standard USB connected shown on the left side of each mote in Figure 13. On the printed circuit board, the16-bit microcontroller has a sub 1mA sleep state and can rapidly wakeup from sleep in fewer than 6ms. This particular platform operates down to 1.8V to extract as much energy as possible from the battery source.

An important point is that the Telos is an open-source platform at the present time and for research reasons we chose that over other competing networking and mote products such as those by Dust Networks. This decision is constantly being re-evaluated. Our experience is that the open-source platforms are overall less reliable for long-life mesh-networking: while the closed-source industrial-hardened platforms and networking software might well be more robust.

Wireless Sensor Networks interact with a residential environment in the form of spatially distributed measurements, diagnosis and possible actuations (Figure 13). The interactions with the environment are accomplished via an array of sensors and actuators.

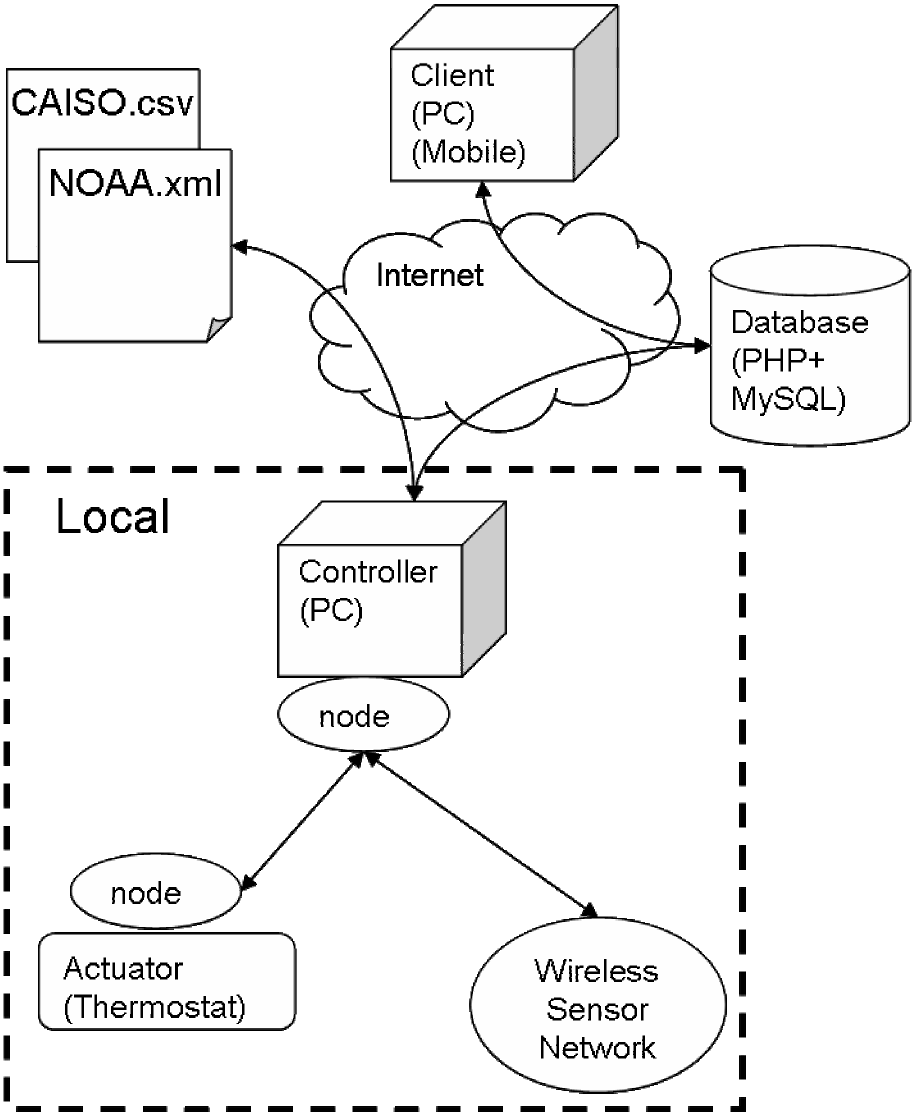

Figure 13 Typical architecture being used by the end of the project

PicoRadio as an advanced low-power device

One of the great challenges of implementing ultra-small sensor nodes is the wireless link. The link must be bi-directional, so passive RFID tag receivers are not applicable. Data traffic in sensor networks is fairly rare, meaning that sensor nodes typically spend substantial time listening to an empty channel. Because of this, the receive power consumption must be minimized. To maintain an efficient link while communicating data, the receiver should provide high sensitivity to reduce the required transmitter power consumption. In addition, the transceiver must be physically small. A traditional implementation with off-chip components and a quartz resonator is prohibitively large and expensive, so an entirely thin-film, batch fabricated solution is necessary.

Therefore, for the PicoRadio work, we first focused on the modeling, design and prototyping of a fully integrated super-regenerative transceiver using bulk acoustic wave (BAW) resonators. The super-regenerative concept, first introduced by Armstrong in the 1920s, has long since been abandoned by the RF community. The goal of this was to show that, through a combination of modern devices, circuit theory, communications theory, and RF MEMS technology, this could be a powerful concept for implementing extremely low power wireless transceivers (Figure 14).

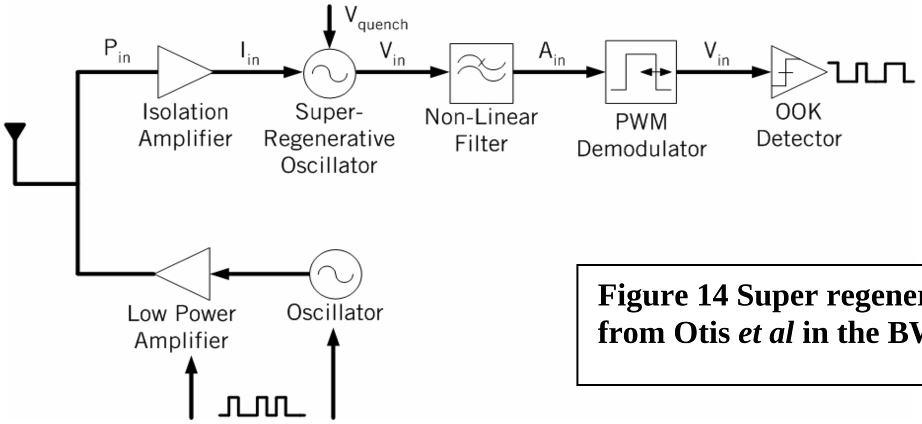

Figure 14 Super regenerative design from Otis *et al* in the BWRC group

The benefits of micromechanical resonators at RF frequencies were utilized in the design of a low-power transceiver [Otis *et al* 2005]. The goal of this first effort was to minimize the implementation area and eliminate all external components, including quartz crystals and surface-mount inductors. A custom (1x2) mm^2 CMOS chip was designed and fabricated. The completed transceiver of the earlier effort is shown below in Figure 15.

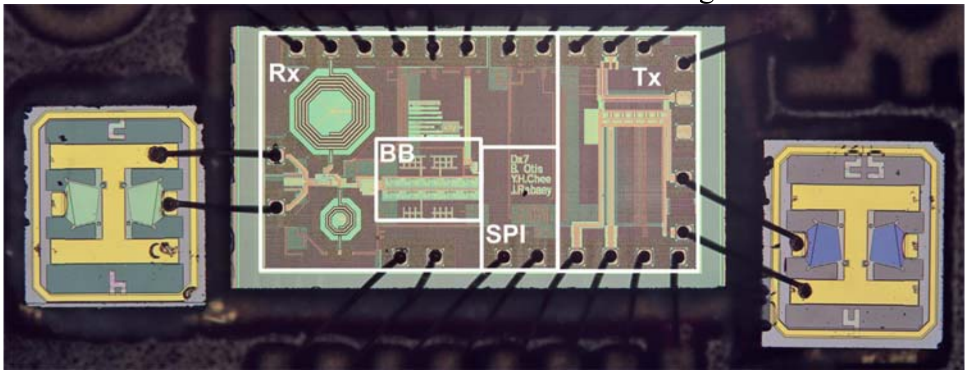

Figure 15 PicoRadio transceiver

The transceiver used no external components except for two bulk acoustic-wave (BAW) resonators, which are wirebonded directly to the CMOS chip. A digital serial programmable interface was implemented on the chip to control all transceiver functionality. This reduced the pad count and allows easy and accurate biasing of all circuitry, eliminating off-chip bias sources and resistors. On chip DACs and current references were used to control circuit bias points. This interface also controlled a binary-weighted capacitor array which tuned the RF frequency of the receiver. Through a 3-bit capacitor array, we demonstrated the stabilization of the receive frequency to within the input bandwidth of the receiver (approximately 500 kHz). The transmitter consisted of an oscillator and a power amplifier. The data was modulated onto the RF carrier by duty-cycling the oscillator between transmitted on-off keyed bits. The transmitter achieved an efficiency of 23% while delivering 480μW. Its efficiency varied less than 3% when the output power changed from 320μW to 600μW. While active, TX power consumed 2.1mW. With on-off keying, assuming equal probability of '1' & '0' the transmitter power was 1.05mW.

This prototype transceiver represented a substantial reduction in receive power consumption and transmitter efficiency over the current state-of-the-art and led us to the next steps of the work, still being investigated as follows. Technology scaling increases the intelligence of extremely small sensor nodes by allowing dense logic. However, it has well-documented negative impacts on analog, digital, and RF circuit blocks. It is necessary to find solutions to the increased leakage, lower supply voltages, and lower breakdown voltages of small devices. As wireless sensor form factors shrink below 1cm^3, the antenna size becomes a limiting factor. In the unlicensed ISM bands of 2.4GHz and 5.6GHz, a quarter-wavelength antenna is 3.13cm and 1.33cm long, respectively. Increasing the carrier frequency, while linearly decreasing the antenna size, dramatically increases the power consumption of many RF circuit blocks. Thus, electrically short, on-chip antennas are necessary for true fully-integrated transceivers.

The next five years will see tremendous changes in active devices and MEMS technologies. Each new technology brings new opportunity for innovation at a circuit and architectural level. For example, FinFETs, resonant body FinFETs, CNT transistors, and integrated MEMS resonators are a new group of technologies that could greatly change the way transceivers are designed. At the end of Year 2 and at the time of writing this report, we are investigating such devices for their integration potential as well as their ultra-low-power characteristics.

D. METERING/SENSORS GROUP (White)

Overview

At the start of this project, the following question was posed: in connection with the need for inexpensive wireless measurements and control of AC voltages and currents in DR-outfitted dwellings, can you make passive proximity sensors for these AC quantities? Passive sensors were sought to minimize (eliminate) the need for power to operate measurement circuits. Proximity sensors were desired in order to permit their installation by untrained occupants of a DR dwelling. These challenges were met with the demonstrations of passive AC voltage and current sensors, and construction of a macro proof-of-concept AC current sensor that could be attached to or built into conventional appliance supply cords (e.g., zipcords) to measure and wirelessly report AC current levels.

As the DR project proceeded, need for other compact electrical measurement and control devices emerged: inexpensive AC outlets under wireless control; wirelessly controlled outlets that also measured and reported the associated currents and voltages, along with power and energy consumed; and wireless current measurements on individual circuits and the whole-house mains. These last were for collecting data on an instrumented, occupied Bay Area house under study.

Passive Proximity AC Voltage Sensor

We built and tested several versions of an electrostatic AC voltage sensor that consisted of a pair of shaped electrodes located adjacent to, typically, a pair of insulated conductors having between them a typical (U. S.) supply voltage – at 60 Hz, either 120 or 240 volts rms (root mean square, the effective steady voltage associated with a sinusoidal AC voltage). A series of tests showed that the AC voltage difference between the two electrodes – the voltage sensor output voltage – was perfectly (within measurement accuracy) proportional to the supply voltage (which ranged in tests from a few volts to 120 V). With the addition of a rectifier diode, the output voltage could be used to charge a capacitor – that is, to scavenge electrical energy from even an open-circuited AC supply line. The output voltages obtained ranged up to about 6 volts when electrodes about five inches long were used. Since the coupling capacitances to the supply wires are relatively small, this method of energy scavenging from open-circuited supply wires appears useful only when very low-power wireless radios become available.

Passive Proximity AC Current Sensor

A chance observation – the discernible vibration of a small handheld permanent magnet that was brought near a pair of insulated AC-current-carrying conductors – led to experiments with a current sensor that employs magnetic and piezoelectric materials and that could be realized with MEMS (micro-electro-mechanical-system) technology.

This current sensor consisted of a flexible member, such as a cantilever, coated with piezoelectric material and connected to an object made of magnetic material. The time-varying magnetic fields produced by the nearby AC currents apply a force upon the magnetic material, and hence the cantilever, which then produces an AC output voltage.

Experiments conducted with cantilevers cut from commercial piezoelectric buzzers to which tiny permanent magnets were attached showed that this piezoelectric output voltage was perfectly (within measurement accuracy) proportional to the AC current. The force is at the powerline frequency (60 Hz) if a permanent magnet is used; with a soft ferromagnetic driving member, one would expect frequency doubling to 120 Hz. The output voltages ranged up to about 0.6 V for an 11.5 A current in a length of conventional zipcord. Note that this current sensor worked well when placed near an unaltered (not separated) zipcord, in contrast with the conventional current transformer (CT) which produced a zero output when clamped around a two-conductor cord in which the two currents flowing in opposite directions caused the magnetic far-fields to cancel.

An as-yet unrealized goal was to employ MEMS technology to these current sensors. Graduate student Jonathan Foster researched certain MEMS cantilever structures, and we hope in the future to evaluate also the use of MEMS cantilevers being made in the power supply sub-group

Wirelessly Controlled Monitoring-Outlets

In the DR house one would like to be able to control individual circuits wirelessly and also perhaps to measure the characteristics of the electrical loads connected to these outlets. We designed and built several prototype devices for these purposes. Student Xin Yang, and earlier engineer Tom Oberheim, was key contributors to this effort.

An early wirelessly controlled outlet was made and tested. The use of a solid-state switch was found to produce overheating at relatively low currents, so an outlet employing a latching electromagnetic relay and a mica2dot (Crossbow, Inc.) wireless mote were found to perform well, being able to control up to 15 A without overheating or damage. Because motes can be programmed to respond only to a particular identifying signal, one could use a single controller to open or close individual circuits selectively (some commercial wireless controlled outlets do not seem to have this important capability). (For details on this outlet see user guide on Manual “Prototype Demand Response Submeter Control Outlet”.)

In many cases, one would like to measure electrical quantities at an outlet, in addition to controlling the outlet. A compact outlet that does this was designed (hardware and software), built, debugged and successfully tested. In it, a latching relay to control the circuit was used (as before), a commercial Hall effect current sensor was employed, and a commercial energy measuring IC (Analog Devices ADE7753) was coupled to the output of the current sensor and to the AC line. Since this device was plugged into a conventional AC outlet, power supply needs for the outlet and the wireless mote are readily met. This device had the advantage of being able to provide information about many electrical quantities – line voltage, current and frequency; power consumption, power factor, energy consumed in a given time. (For details see user’s guide on “Prototype Demand Response Submeter Control Outlet”.)

Wireless Monitoring of a Test House

Need for the ability to monitor wirelessly the currents in a Bay Area test house was identified. Conventional CTs were obtained, modified, fitted with appropriate circuitry, and necessary software for interfacing with wireless motes was written. Two types of devices were made available to the researchers in the Thermostat Control Group. These were: (a) minimal form factor CTs that could (barely) be clipped onto individual circuits originating in the circuit breaker panel, and (b) a larger commercial (Veris Corp.) CT system with 100 amp capacity. An additional modbus interface was written in order to interface the Veris CT system with a TelosB wireless sensor mote. (For details see user guide in Appendix D, "Prototype Demand Response Multi-Purpose House Meter".)

Some final observations for sensors

a) Size matters:

Though the passive proximity AC current sensor described above was not used in the outlets we built, we expect to do so in future studies where the sensor's small size would be an advantage. Examples are in monitoring currents in individual appliance cords in a house, whole-house current monitoring, and monitoring individual circuits in the circuit-breaker box (possibly the current sensors could be built into the circuit breakers themselves). The Telos interface module used to interface with the Veris CT system for whole house monitoring has support for future miniature AC current sensors

b) Conversion to RMS (root-mean-square) Values:

Doing calculations and transmitting data requires energy that may severely reduce battery life in a wireless network. Conversion of sinusoidal sensor outputs to rms values could be done in a mote co-located with a sensor (computation energy cost) or at the control center (transmission energy cost). An alternative is to rectify the sensor's output waveform and send only its DC (rms) value. Of course, calculating power consumption from only rms values of current and voltage is only accurate if the power factor is unity, a condition that is exactly true only for a resistive load.

c) How much data do you need, and how frequently do you need it?

During the first whole-house monitoring, the batteries supplying the wireless motes failed rapidly – within hours. The problem was found to be the high rate of whole-house sensor polling – once every 5 seconds. For most purposes such rapid polling is not needed and a much smaller duty cycle would suffice while greatly extending battery life.

d) ADC (analog-digital converter) resolution: what's needed and what's really available?

In our DR work, we've assumed that an accuracy of about $^{+}/_{-}$ 10% would be adequate for current sensors. (We do not speak of revenue metering, for which $^{+}/_{-}$0.3% is often quoted.) A tacit assumption is also that measuring appliance *current* alone is probably sufficient for estimating power consumption, since the voltage is usually known to be near 120 or 240 volts. These assumptions reduce the power consumed by sensor motes: lower-resolution ADCs operating at lower speeds may suffice, and voltage sensors may not be necessary. Also, one should carefully determine the resolution of commercial ADCs, since experienced engineers often express skepticism about the resolutions claimed by spec sheets for ADCs.

E. ENERGY SCAVENGING GROUP (Wright)

Overview

To power the motes and to especially address the prototyping of a "sub-one-dollar TinyTemp node" that would last longer than 10 years, we focused on energy scavenging opportunities. Our early results of a broad survey of potential energy sources for wireless sensor nodes, both fixed energy sources such as batteries and power scavenging sources, are shown in Appendix J. The data were taken from a combination of published studies, theory, and experiments carried out by the authors. Where applicable, references are listed. The top portion of the table shows sources that have a fixed level of *power* generation. Therefore, the lifetime is potentially infinite. The bottom portion of the table shows sources that contain a fixed amount of *energy*, and therefore the average power generation is a function of lifetime. All power values are normalized to a device size of 1 cm^3. It is assumed that if the entire device size is 1 cm^3, then approximately 0.5 cm^3 will be available for the power system. Therefore, the values in Appendix J are based on 0.5 cm^3 for the power generating, or storage, device. The data show that for short lifetimes, batteries are a reasonable solution. However, another solution is required for long lifetimes. Solar cells offer excellent power density in direct sunlight. However, in dim office lighting, or areas with no light, they are inadequate. Power scavenged from thermal gradients is also substantial enough to be of interest if the necessary thermal gradients are available. It is, however, difficult to find greater than a 10 C° thermal gradient in a volume of 1cm^3. As a final note, the appendix is by no means comprehensive. Many other potential power sources were evaluated, and only those that seemed most applicable have been reported. Of those above the applicable methods for residential DR are more limited and we thus focused on using natural vibrations in a house that would be generated on wooden stairs, moving doors, and near air-conditioning ducts that tend to vibrate. Lead zirconate titanate (PZT) is a material that will generate power from stressing the beam shown below in Figure 16.

TinyTemp Node (mesoscale)

A piezoelectric bimorph from Piezo Systems with the dimensions 31.5x12.7x5.1mm (1.25x0.50x0.02") was used in constructing the generator. This bimorph used a brass center shim and PZT-5A4E, a commercially available piezoelectric material selected for its favorable fatigue characteristics. A 52g tungsten mass was affixed to one end using cyanoacrylate glue, and the device was mounted in a rigid plastic clamp. Figure 16 shows a photograph of the generator.

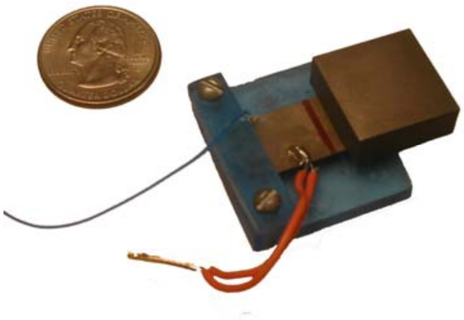

Figure 16: Piezoelectric bimorph generator prototype (Roundy, Leland, Lai)

The AC voltage produced by the generator is inappropriate to power the sensor and radio hardware directly. A circuit was devised to condition the signal from the generator, transforming it into a usable DC voltage. Whereas the generator produced an unsteady, foot traffic dependent AC output with peak-to-peak voltages anywhere from 0–35V, the sensor and radio hardware required 3.3VDC signal for operation. The generator also did not produce enough power for continuous operation of the sensor and radio. The power circuit thus had to perform two tasks: a) Store the generator's output until sufficient energy was collected to take and transmit a temperature measurement; b) Output a steady 3.3VDC current to the sensor and radio hardware. The majority of the power circuitry components were mounted onto a custom-fabricated printed circuit board. The printed circuit board is round in shape and roughly 30mm in diameter to closely match the form factor of the wireless radio hardware. Two 3300μF aluminum electrolytic capacitors were wired in parallel to provide 6600μF of storage. Appropriate storage capacitance was found experimentally to take and transmit a temperature reading for DR. A Crossbow Mica2Dot wireless radio was chosen as the wireless platform for this project. The Mica2Dot provides low power consumption, compact design, computational ability, and programmability. A VSI H10000 thermistor temperature sensor and a 9.83kΩ resistor were used to create a voltage divider. This voltage divider was wired directly to the analog-to-digital converter (ADC) input on the Mica2Dot. In operation, the sensor and radio hardware were turned off while the power circuit collected power from the generator. When a 3.3VDC pulse was released from the power conditioning circuit, the Mica2Dot was programmed to power on, initialize, read the temperature, and broadcast the result. Another Mica2Dot connected to a nearby notebook computer received and displayed the temperature data on screen. A window on the bottom of the casing (made at UCB on a fused deposition modeling machine) allowed the piezoelectric bimorph generator's base clamp to directly contact the source's vibrating surface, thus assuring the most direct mechanical coupling. A small hole allows the thermistor unshielded access to the ambient environment. Figure 17 shows the complete self-powered wireless temperature sensor device in its packaging.

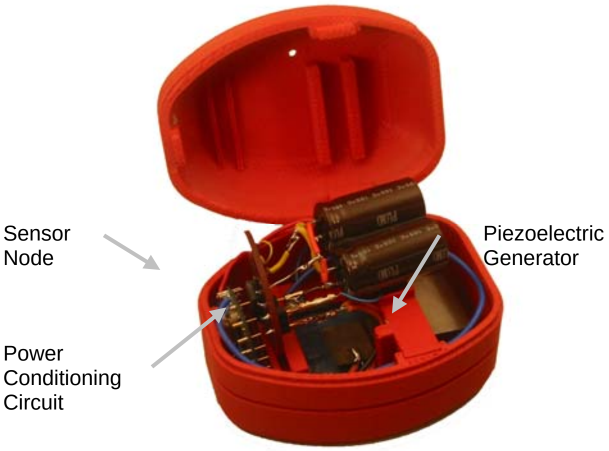

Figure 17: DR "TinyTemp" node (Leland, Lai, Redfern)

The self-powered wireless environmental sensor device was first tested in the laboratory. It was mounted atop a LabWorks ET-126 vibrating actuator driven by an Agilent 3312OA signal generator and a LabWorks pa-138 power amplifier. The vibrating actuator was set to mimic the 27Hz frequency mode of a wooden staircase in a California building. The sensor node was programmed to transmit a temperature reading every 10ms once initialized. With a 816ms pulse of power, only two temperature readings were transmitted. The sensor and radio hardware took nearly 800ms to power on and initialize before transmitting the first temperature reading. The device was then tested in situ. The storage capacitors were pre-charged to 3V using two AA batteries. Fifty minutes of continuous traffic provided by two people walking on the staircase were required to replicate the transmission of temperature readings achieved in the laboratory. Energy collected in the capacitors between pulses was 88mJ. Average power transfer from the piezoelectric generator to the capacitors was 29.3μW. This value closely matches the predicted power output of the piezoelectric generator as described previously. Once the capacitors reached the threshold value of 5V, the capacitors discharged. Power transfer from the capacitors through the remaining portion of the power conditioning circuit was 108mW. Power input to the sensor and radio hardware was found to be 45mW. Therefore, the efficiency through the power circuit is estimated to be 42%.

A brief note on a vibration-powered semi-active RFID tag

Another system design (coined Teeny Temp) comprised the following components: a piezoelectric bimorph generator which converted vibrations to electricity producing an AC signal, power conditioning circuitry which converted the AC signal from the generator to usable DC signal, and RFID Battery-Assisted Passive Tag with onboard temperature sensor.

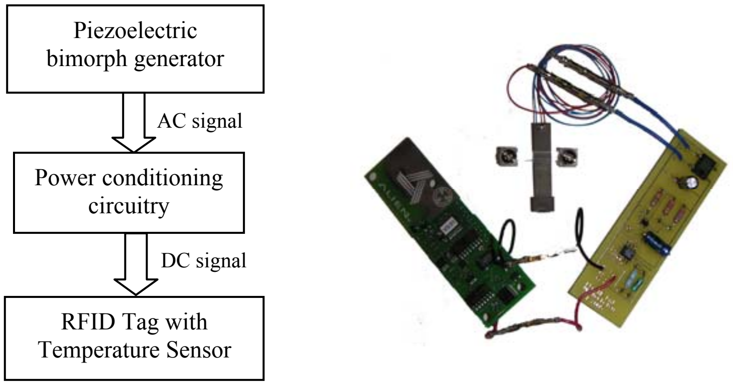
Piezoelectric bimorph generator
AC signal
Power conditioning circuitry
DC signal
RFID Tag with Temperature Sensor

Figure 18. "TeenyTemp" system design (Lai, Redfern)

The goal of the design was to provide enough power to the RFID tag to operate the tag: including powering the onboard sensor, powering the microprocessor, and transmitting useful information to the reader. In order to realize this goal the piezoelectric power generator first generated enough power, then the power conditioning circuit was designed to output a usable supply voltage to the RFID tag while most efficiently making use of the power being generated by the piezoelectric generator. For DR purposes it was thought that TeenyTemp might be an attractive method for family occupancy sensing in relation to turning off/on the critical HVAC system.

Adjusting designs for resonance and maximum output

Current limiting factors in the field of piezoelectric vibration energy scavenging include: coupling coefficients, strain distribution, and frequency matching. This short section addresses these factors with two examples. As a first example, the power output of a cantilevered rectangular piezoelectric beam was limited by its uneven strain distribution under load. An alternative prototype scavenger using a "harmonically matched trapezoidal geometry" solved this problem by evening the strain distribution throughout the beam, increasing by 30% the output power per unit volume. As a second example, the vibration energy scavenging devices developed above operated effectively at a single specific frequency dictated by the device's design. However, for this technology to be commercially viable vibration energy scavengers that generate usable power across a range of frequencies must be developed. Piezoelectric bimorph-based vibration energy scavengers were thus developed whose resonance frequency was adjusted through the application of compressive axial preload. This section describes a new experimental method for examining this effect. It was determined that axial preload can adjust the resonance frequency of a simply-supported bimorph to 24% below its unloaded resonance frequency. Power output to a resistive load was found to be 65-90% of the nominal value at frequencies 19-24% below the unloaded resonance frequency. Prototypes were developed that produced 300–400 microwatts of power at driving frequencies between 200 and 250 Hz. Additionally, piezoelectric coupling coefficient values were increased using this method, with k_{eff} values rising as much as 25% from 0.37 to 0.46. Device damping increased 67% under preload, from 0.0265 to 0.0445, adversely effecting power output at lower frequencies. A theoretical model modified to include the effects of preload on damping predicted power output to within 0-30% of values obtained experimentally. Optimal load resistance deviated significantly from theory, and merits further investigation.

MEMS scale energy scavenging by vibration

The long term goal of energy scavenging devices for DR is the realization of a completely integrated, microfabricated sensor node to mount on walls and surfaces. Thus, we have made progress on MEMS scale piezoelectric cantilevers. To create a ubiquitous device of this nature required careful consideration of a number of materials and processing challenges. In general, the research addressed the need for: 1) sufficient material properties to produce a useable voltage under strain, also exhibiting intimate crystallographic and interfacial contact with the electrodes and underlying substrate; 2) the ability to grow, fabricate, and integrate the power source only with standard microfabrication processes; 3) a geometrical and mechanical design that produce sufficient voltage under vibrations.

We completed early investigations with an exciting wafer-material recently developed by Motorola [18]. It involved the deposition of only one buffer layer, $SrTiO_3$, which was an excellent growth template allowing for the growth of epitaxial PZT thin films. Using SRO as an electrode also allowed the use of typical wet and dry etch fabrication processes, thus permitting a design based completely on standard microfabrication processes. The PZT ($PbZr_{0.47}Ti_{0.53}O_3$) film was grown on a Si/STO substrate via pulsed laser deposition -- chosen for its ability to rapidly produce quality films. The quality of the piezoelectric films was determined through measurement of the PZT coefficient and remnant polarization. Thus we created the arrays in Figure 19 below , showing the side and plan views (left & center) of the arrays, and a small proof-mass on one beam (right).

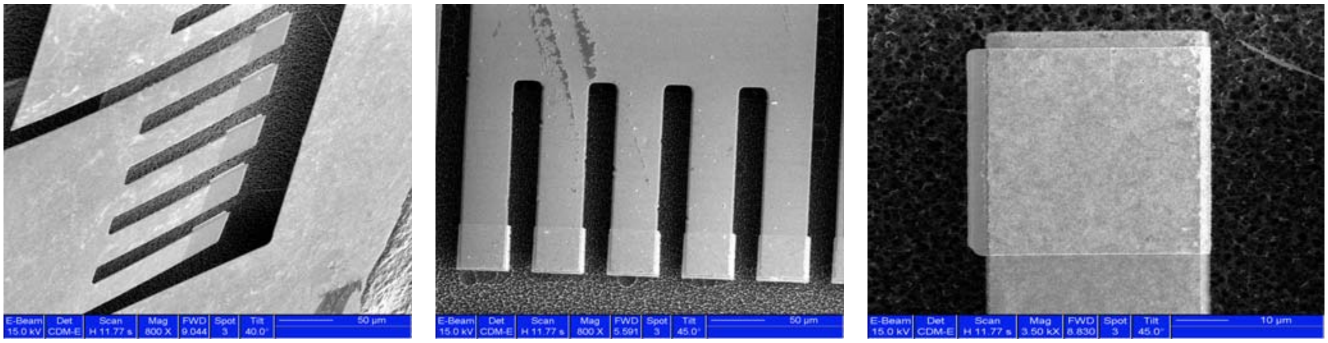
E-Beam 15.0 kV Det CDM-E Scan H 11.77 s Mag 800 X FWD 9.044 Spot 3 Tilt 40.0° 50 µm
E-Beam 15.0 kV Det CDM-E Scan H 11.77 s Mag 800 X FWD 5.591 Spot 3 Tilt 45.0° 50 µm
E-Beam 15.0 kV Det CDM-E Scan H 11.77 s Mag 3.50 kX FWD 8.830 Spot 3 Tilt 45.0° 10 µm

Figure 19 MEMS prototypes (Carleton, Reilly)

The research next needs to build an analytic model for the resonance frequency of the heterogeneous bimorphs (consisting of an elastic layer and a piezoelectric) and couple the results to the house information. In summary, the ongoing work will refine models, investigate the geometry of the beams (especially considering a switch to the trapezoid) and refine the piezoelectric material to increase power output. Integration into a "PicoCube" will be a focus to achieve the 10x10x10 goals. A "sugar cube" size DR mote will be one goal of future work.

F. REFERENCES USED IN THE TEXT (SEE LIST OF PUBLICATIONS IN NEXT SECTION)

Archacki, Raymond 2004. personal correspondence regarding Carrier Thermostat Mode Summary, Summer 2003

Auslander, D.M., J.R. Ridgely, J.D. Ringgenberg. 2002. *Control Software for Mechanical Systems,* Prentice-Hall.

Boisvert, Alex, and Ruben Gonzalez Rubio. 1999. "Architecture for Intelligent Thermostats that Learn From Occupants' Behavior." *ASHRAE Transactions*. 105(1). 124-130.

CEC, 2004, Residential Appliance Saturation Survey. Publication # 400-04-009

de Dear, R.J. and G. S. Brager. 2001. "The Adaptive Model of Thermal Comfort and Energy Conservation in the Built Environment," *International Journal of Biometeorology*, 45(2), 100-108.

EEI, EEI Member and Non-Member Residential/Commercial/Industrial Efficiency and Demand Response Programs for 2005/2006, http://www.eei.org/industry_issues/retail_services_and_delivery/wise_energy_use/programs_and_incentives/progs.pdf

EPRI. 2002. The Western States Power Crisis: Imperatives and Opportunities. http://www.epri.com/WesternStatesPowerCrisisSynthesis.pdf.

Federspiel, C. C. and H. Asada. 1994. "User-Adaptable Comfort Control for HVAC Systems." *Journal of Dynamic Systems, Measurement and Control*. 116(3). 474-486.

Fountain, M., G. Brager, E. Arens, F. Bauman, and C. Benton. 1994. "Comfort Control for Short-Term Occupancy." *Energy and Buildings,* Vol. 21, pp. 1-13.

Hill, J., Culler, D., 2002. "Mica: A Wireless Platform for Deeply Embedded Networks", IEEE Micro. Vol 22(6), Nov/Dec 2002, pp 12-24.

Jain, Bijendra and Ashkok K. Agrawala. 1990. OSI Seven Layer Network architecture, *Open Systems Interconnection: Its Architecture and Protocols*, Elsevier, Amsterdam.

Levy, Roger. 1985. *Customer Value of Service Market Study*. Pacific Gas and Electric Company.

Martin, R. M., C. C. Federspiel, and D. M. Auslander, 2002, "Responding to Thermal Sensation Complaints in Buildings," *ASHRAE Transactions*, 108(1), 407-412.

Martinez, M. 2004. Program Manager, Southern California Edison. Personal communication.

Otis, B., Chee, Y.H., Rabaey, J., "A 400µW Rx, 1.6mW Tx Super-regenerative transceiver for wireless sensor networks", Proceedings of the IEEE ISSCC , Feb 2005.

PG&E. 2004. http://www.pge.com/nots/rates/tariffs/advice/tariffsheets/19882-19901.pdf.

UC. 2004. http://ciee.ucop.edu/dretd/.....

UC Berkeley, DRETD 2005. http://dr.berkeley.edu/dream

PIER DR PUBLICATIONS

1. REFEREED PUBLICATIONS

A. ARCHIVAL JOURNALS

1. S. Roundy, D. Steingart, L. Frechette, P.K. Wright and J. Rabaey, “Power Sources for Wireless Sensor Networks,” *Lecture Notes in Computer Science,* Springer-Verlag, GmbH, ISSN: 0302-9743, Volume 2920, 2004, pp. 1 – 17.

2. S. Roundy, and P.K. Wright, “A Piezoelectric Vibration based Generator for Wireless Electronics,” *Smart Materials and Structures*, Volume 13, 2004, pp. 1131-1142.

3. S. Roundy, M. Strasser and P. K. Wright, “Powering Ambient Intelligent Networks” in “*Ambient Intelligence*” Edited by W. Weber, J.M. Rabaey, and E. Aarts and published by Springer November 2004, paper on pages 271-300.

4. S. Roundy, E. Leland, J. Baker, E. Carleton, E. Reilly, E. Lai, B. Otis, J. Rabaey, V. Sundararajan and P.K. Wright “Improving Power Output for Vibration-Based Energy Scavengers” *IEEE Pervasive Computing Journal on Mobile and Ubiquitous Computing*, Volume 4 , Number 1, January – March 2005, pp. 28-36.

5. F. Zavaliche, H. Zheng, L. Mohaddes-Ardabili, S.Y. Yang, Q. Zhan, P. Shafer, E. Reilly, R. Chopdekar, Y. Jia, P.K. Wright, D.G. Schlom, Y. Suzuki, and R. Ramesh, “Electric Field-Induced Magnetization Switching in Epitaxial Columnar Nanostructures,” Nano Letters, Volume 5, Number 4, 2005, pp. 1793-1796.

B. REFEREED CONFERENCE AND SYMPOSIUM PROCEEDINGS

6. S. Roundy, B. Otis, Y-H. Chee, J.M. Rabaey, and P.K. Wright, 2003. “A 1.9GHz RF Transmit Beacon using Environmentally Scavenged Energy,” *ISPLED* 2003, Seoul Korea, August 25 - 27, 2003. *Winner of a Best Paper Award.*

7. Roundy, S., Steingart, D., Frechette, L., Wright, P. K., Rabaey, J., “Power Sources for Wireless Sensor Networks,” 2004, *The 1st European Workshop on Wireless Sensor Networks (EWSN),* Berlin, Jan. 19-21. http://www.ewsn.org/

8. Y.H. Chee, J. Rabaey, A. M. Niknejad, "A Class A/B Low Power Amplifier for Wireless Sensor Networks", Proceedings of International Symposium on Circuits and Systems 2004 (ISCAS 2004), vol. 4, pp 409-412, Vancouver, Canada, May 2004.

9. B. Otis, Y.H. Chee, R. Lu, N.Pletcher, J. Rabaey, "An Ultra-Low Power MEMS-Based Two-Channel Transceiver for Wireless Sensor Networks", Symposium on VLSI Circuits, Honolulu, HI, June 2004.

10. D. Steingart, C. Ho, J.W. Evans, and P.K. Wright, “Design of an On-Chip Secondary Lithium Ion Polymer Microbattery for Millimeter-Scale Wireless Nodes,” *The Minerals and Materials Society Meeting* Fall 2004

11. V. Sundararajan, A. Redfern, W. Watts and P.K.Wright, “Distributed Monitoring of Steady State System Performance Using Wireless Sensor Networks” *American Society of Mechancial Engineers International Mechanical Engineering Congress*, November 13-19, 2004, Anaheim, California, Paper IMECE2004-59884. Proceedings are on Compact Disc, precluding a page reference.

12. E. S. Leland, E. M. Lai and P.K Wright, “A Self-Powered Wireless Sensor for Indoor Environmental Monitoring” *2004 Wireless Networking Symposium*
October 20 - 22, 2004 The University of Texas at Austin Department of Electrical & Computer Engineering Wireless Networking & Communications Group. Proceedings are on Compact Disc, precluding a page reference.

13. B. Otis, Y.H. Chee, J. Rabaey, "A 400uW Rx, 1.6mW Tx Super-regenerative transceiver for Wireless Sensor Networks", IEEE International Solid-State Circuits Conference (ISSCC), San Francisco, CA, Feb 2005.

14. Kate Hammond, Elaine Lai, Eli Leland, Sue Mellers, Dan Steingart, Eric Carleton, Beth Reilly, Jessy Baker, Brian Otis, Jan Rabaey, David Culler, and Paul Wright. “An integrated node for energy-scavenging, sensing, and data-transmission: applications in medical diagnostics.” *The Second International Workshop on Body Sensor Networks*.” Imperial College London April 11-13th 2005.

15. X. Jiang, J. Polastre, and D. Culler. “Perpetual Environmentally Powered Sensor Networks,” The Fourth International Conference on Information Processing in Sensor Networks: Special track on Platform Tools and Design Methods for Network Embedded Sensors (IPSN/SPOTS), April 25-27, 2005. **Received best paper award**

16. J. Polastre, R. Szewczyk, and D. Culler. “Telos: Enabling Ultra-Low Power Wireless Research,” The Fourth International Conference on Information Processing in Sensor Networks: Special track on Platform Tools and Design Methods for Network Embedded Sensors (IPSN/SPOTS), April 25-27, 2005

17. M. Montero, T. Pering, U. Udaud, P.K. Wright, and R. Want, “Experimental Study on the Effects of Human and Electronic-Mechanical Interaction on RF Signal Strength for a Personal Server,” *Proceedings of the 2005 American Society of Mechanical Engineers Pacific Rim Technical Conference and Exhibition on the Integration and Packaging of MEMS, NEMS and Electronic Systems,* July 17-22, 2005, San Francisco, California Paper Reference Number IPACK2005-73154 – Proceedings are on compact disc, precluding a page reference.

18. N. Pletcher, J. Rabaey, "A 100uW, 1.9GHz Oscillator with Fully Digital Frequency Tuning," Proceedings of the European Solid State Circuits Conference (ESSCIRC), Grenoble, France, September 2005.

19. J. Baker, S. Roundy and P.K. Wright, "Improvements in Vibration Energy Scavenging for Wireless Sensor Networks," *The Third International Energy Conversion Engineering Conference, American Institute of Aeronautics and Astronautics*, San Francisco, California, 15th – 18th August 2005

20. J. Polastre, J. Hui, P. Levis, J. Zhao, D. Culler, S. Shenker, and I. Stoica. "A Unifying Link Abstraction for Wireless Sensor Networks," *The Third ACM Conference on Embedded Networked Sensor Systems (SenSys)*, November 2-4, 2005.

21. G. Tolle, J. Polastre, R. Szewczyk, N. Turner, K. Tu, P. Buonadonna, S. Burgess, D. Gay, W. Hong, T. Dawson, and D. Culler. "A Macroscope in the Redwoods," *The Third ACM Conference on Embedded Networked Sensor Systems (SenSys),* November 2-4, 2005.

22. V. Sundararajan, A. Redfern, M. Schneider, P.K. Wright and J. Evans, "Wireless Sensor Networks for Manufacturing Systems" *American Society of Mechanical Engineers International Mechanical Engineering Congress and Exposition,* November 5th -11th Orlando, Florida, 2005, Paper Reference Number IMECE 2005-82224, Proceedings are on Compact Disc, precluding a page reference.

23. E.M. Lai, A. Redfern, and P.K. Wright, "Vibration Powered Battery-Assisted Passive RFID Tag" EUC Workshops 2005, LNCS 3823, December 6-9, 2005, Nagasaki, Japan, pp. 1058-1068

24. B. W. Cook, A. D. Berny, A. Molnar, S. Lanzisera, and K. S. J. Pister, "An Ultra-low Power 2.4GHz RF Transceiver for Wireless Sensor Networks in 130nm CMOS with 400mV Supply and an Integrated Passive RX Front-end," *International Solid-State Circuits Conference ISSCC* 2006 (To Be Published), San Francisco, CA, Feb. 5-8, 2006.

25. E. Reilly, E. Carleton and P.K. Wright, "Thin Film Piezoelectric Energy Scavenging Systems for Long Term Medical Monitoring," *The Third International Workshop on Body Sensor Networks*." MIT, Boston, 2006.

2. NON-REFEREED PUBLICATIONS

A. TECHNICAL REPORTS

26. Dave Auslander, Ed Arens, Charlie Huizenga, Therese Peffer, Alex Do, Xue Chen, Jaehwi Jang, Anna LaRue, Florian Jourda, Po-kai Chen, Reman Childs, William Watts, Yuan Yi, “Initial deployment of a distributed demand-responsive energy management system” CBE Report in progress and to be published May 2006.

B. NON-REFEREED CONFERENCE PROCEEDINGS

27. E. K. Reilly and P.K. Wright, “Vibrational Energy Scavenging via Thin Film Piezoelectric Nanoceramics”, *2003, TMS Conference Poster/Abstract*

28. N. Ota, D. Hooks, P. Wright, D. Auslander and T. Peffer, “Wireless Sensor Network Characterization – Application to Demand Response Energy Pricing” *SenSys 2003, The First International Conference on Embedded Networked Sensor Systems*, November 5-7th 2003, Los Angeles CA P. 334-335.

29. P. Levis and D. Gay. “Reprogramming Sensor Networks Safely, Quickly, and Efficiently,” *Demo Session of The Third ACM Conference on Embedded Networked Sensor Systems (SenSys),* November 2-4, 2005.

C. ARTICLES IN NON-ARCHIVAL JOURNALS

30. P.K. Wright, “The Market Promise of Wireless Sensor Networks,” *Nikkei Business Publications*, Tokyo, Japan, 2004, NIKKEI BizTech, Number 003, pp.134-139 In Japanese.

3. BOOKS

31. S. Roundy, P.K. Wright and J. Rabaey, *Energy Scavenging for Wireless Sensor Networks with Special Focus on Vibrations*, Kluwer Academic Publishers, published in 2004, 1- 212 pages, ISBN Number 1-4020-7663-0.

32. Arens, E., C.C. Federspiel, D. Wang and C. Huizenga, 2005. “How Ambient Intelligence Will Improve Habitability and Energy Efficiency in Buildings” chapter for Ambient Intelligence, eds. W. Weber, J.M. Rabaey and E. Aarts, Springer, March. pp.63-80.

4. OTHER - PATENT

33. S. Roundy, P.K. Wright, and J. Rabaey, " Piezobenders for Energy Scavenging in Wireless Sensor Nets" Patent pending with the Office of Technology Licensing at UC Berkeley

34. E. Leland and P.K.Wright, "Adjustable Resonance Energy Scavenger Disclosure" Patent pending with the Office of Technology Licensing at UC Berkeley (Case B06-067)

35. J. W. Evans, M. Schneider, D. Steingart, P.K. Wright and D. Ziegler, "Wireless Measurement of Operating Parameters for Hall Cells," Patent pending with the Regents of the University of California, Franklin St. Oakland, Client Reference No. B05-019-1

36. D. Culler, J. Hui, J. Polastre, A. Do, X. Yang, E. Arens, C. Huizenga, R. White, and P. Wright. "An Intelligent Apparatus for AC Appliance Monitoring and Control that is Programmable and Networked," Patent pending with the Office of Technology Licensing at UC Berkeley

37. Elizabeth Reilly, Eric Carleton and Paul Wright, "Thin Film Piezoelectric Energy Scavenging Systems," Patent pending with the Office of Technology Licensing at UC Berkeley

H. APPENDICES

APPENDIX A: GENERIC MOTE DOCUMENTATION

William Watts, Mechanical Engineering, UC Berkeley, wawatts@berkeley.edu

Hardware Functionality

The generic mote board has four mono audio jacks that provide power to a sensor (or actuator), and connection straight to an ADC. Adding a resistor allows for a voltage divider set up that connects to the ADC port. Two of the ADC ports can be changed to digital input/output.

The device is not plug and play. The power and signal pins have to be set according to the specific sensor or actuator that is connected to the input jacks. Important Note: The reference voltage for the ADC input must be set to 2.5 V for proper measurement of battery voltage and temperature in this revision. Please find the InternalVoltage.h file in the Code section (http://dr.berkeley.edu/dream). Place that file in your TinyOS tree under – tinyos-1.x/tos/platforms/msp430/

Signal Input Pins

The ADC input pins for the generic sensor board are ADC1, ADC2, ADC3, and ADC7.
Pins ADC2 and ADC3 can be made into GIO (i.e. exclusive digital input/output) ports by connecting a 0 ohm resistor across R16 and R14 respectively. The T-mote Sky datasheet (http://www.moteiv.com) has more in depth hardware documentation.

For each of the input signal pins, there is a voltage divider capability that can be used, if a sensor requires that circuitry. In that case refer to the eagle layout figure 1, in order to find out how to connect a resistor across the signal input and ground. Resistors R1-R4 can be customized to fit a particular sensor's resolution requirements.

The sensor board design is flexible, because you can set the power pins to be input pins, see below for more explanation.

Power Pins

ADC0, ADC6, GI03, GIO2 are the power pins when the voltage divider circuitry is used.
The power pins supply a voltage equivalent to the T-mote Sky mote's battery voltage.

The code in the drapps folder demonstrates how to set pins to power and how to turn them off for power savings.

Alternative Pin Set up

There are cases when not using the voltage divider set up that one might want to have more flexible usage of the pins. For instance, one might want to set the power pins to input and the former input signal pins to ground.

The appropriate ADC files for changing the pin set up are included in the documentation.
Also see the documentation for the set up of the motion sensor on the generic board for an example.

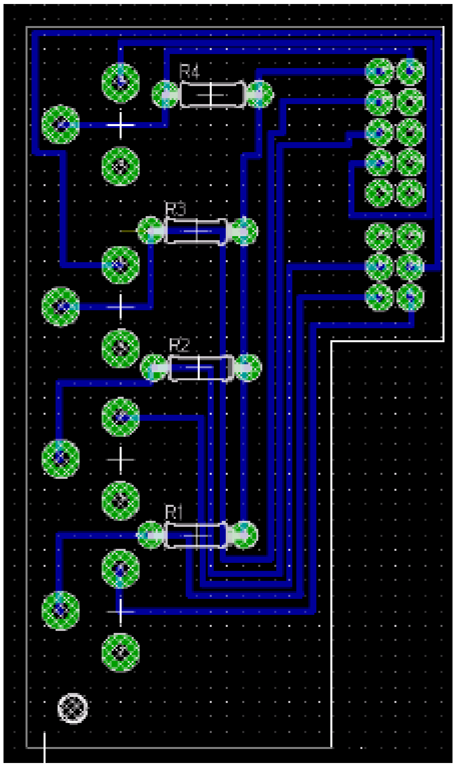

Figure 1: Layout R1-R4 are the resistors for the voltage divider

APPENDIX B: MOTION SENSOR

Po-kai Chen, Electrical Engineering and Computer Science Dept., UC Berkeley

Motion sensor

The motion sensor module is comprised of a Panasonic passive infrared motion sensor (AMN41121) and a 3V watch battery (CR2032). The sensor detects changes infrared radiation which occur when there is movement by a person or object which is different in temperature from the surroundings.

Motion sensor module output

The output of the module can be plugged into a separate T-mote Sky mote using a sub-mini mono jack. The inside conductor is the signal while the outside conductor is ground. The module outputs a digital high of around the battery voltage when motion is detected; otherwise, the output is low (20mV ~ 150mV). When connected to a T-mote Sky mote, the pin stays “not low” for approximately two seconds without additional external capacitances or resistances. This behavior can be adjusted by adding resistors or capacitor to the component board inside this module.

Power

The CR2032 cell contains approximately 230mAh of energy. The motion sensor uses approximately 46uA of current when idle and uses approximately 100uA of current when sensing motion. Assuming the sensor detects motion 10% of the time, the battery will last approximately six months.

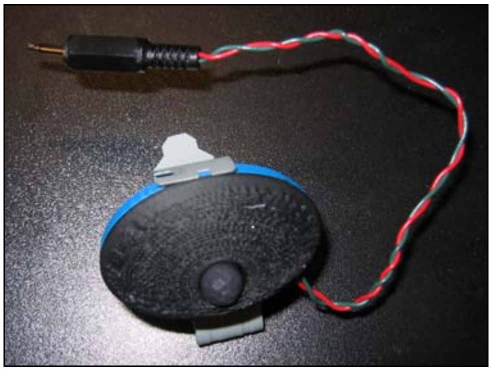

Figure 12 Motion sensor module

APPENDIX C: WEATHER STATION

Po-kai Chen, Electrical Engineering and Computer Science Dept, UC Berkeley

The weather station consists of five main components, a Moteiv T-mote Sky mote for broadcasting weather data wirelessly to a host controller, two pyranometers for measuring global and diffuse radiation, an anemometer and a wind vane. An auxiliary circuit board attached onto the mote provides amplification for the radiation sensors and circuitry for the wind vane.

Sensors
Pyranometers
From the LI-COR instructional manual, “A pyranometer is an instrument for measuring solar radiation received from a whole hemisphere. It is suitable for measuring global sun plus sky radiation”.

A radiation intensity of 1000 Watt / m^2 will drop approximately 16mV across a 200 ohm resistor connected in series with the pyranometer. This voltage is then passed through an amplifier to a range more optimally sensed by the mote’s ADC.

Notes:
The photodiode is not meant to be used under artificial lighting or within plant canopies. Reflected radiation can also provide erroneous results.
The sensor can be mounted at any angle, but it must be level.
The vertical edge of the diffuser must be kept clean.

Anemometer
The anemometer provides a voltage output up to 2.4V that varies linearly with wind speed. This means the output can be connected directly to the mote’s ADC’s for a reading.

Wind vane
The wind vane contains a potentiometer in which the resistive element varies depending on the angular position of the vane. This resistance can be calculated by forming a resistive divider network with another resistor and applying a known voltage.

Power
Several steps were taken to ensure minimal power usage. First, because this mote is not expected to receive any messages, the radio is turned off whenever the mote is not sending a message. This means a longer delay between messages will result in a lower average power usage. When the mote is idling after sending a message and before taking the next reading from the sensors, power is turned off to the amplifier and the resistive divider. Assuming the mote is powered by a pair of 2000mAh AA batteries, the mote should be able to last 46 months. However, this does not take into account the intrinsic battery drain at the fact that there is still energy left if the batteries are replaced at 2.5V.

Issues

Pyranometers

With the default resistors attached at the output of the pyranometers, the output can only go up to 10mV. This is not high enough voltage for T-mote Sky's ADC to get a good resolution. This problem is solved by adding an amplifier to amplify the signal. An appropriate gain must be chosen, in this case, 68, to ensure that the maximum output doesn't exceed the ADC's reference voltage. To save power, the supply pin to the amplifier is turned off whenever the pyranometer's ADCs aren't in use.

Amplifier

The current board contains an amplifier rated for a 3V minimum supply. However, the amplifier appears to be working in this configuration down to at least 2.7 volts.

Wind vane

Since we are measuring the resistance of the potentiometer using a resistive divider, the reading will change as a function of battery voltage. In order to get a more accurate reading, the battery voltage is taken into account when calculating the potentiometer resistance.

Anemometer

The anemometer can output up to 2.4 volts. This means instead of using the 1.5V reference voltage, we need to use the 2.5V voltage reference if we are to be able read up to the maximum voltage output. If we use the 2.5V voltage reference, we must ensure the AA battery supply must not fall below 2.5V.

Battery voltage sensor

We can measure battery voltage between 1.5V and 3.0V using the 1.5V voltage reference and between 2.5V and 5.0V using the 2.5V voltage reference. Since we already need to maintain a 2.5V battery supply (see issues with the Anemometer), and monitoring battery voltage above 3.0V seemed useful, we chose to use the 2.5V voltage reference to measure the battery voltage.

APPENDIX D: POWER SENSING

Xin Yang, Richard White

Electrical Engineering and Computer Science Dept., and the Berkeley Sensor and Actuator Center (BSAC), UC Berkeley

Prototype Demand Response Multi-Purpose House Meter User's Guide

October 2005

Table of Contents

1. Introduction

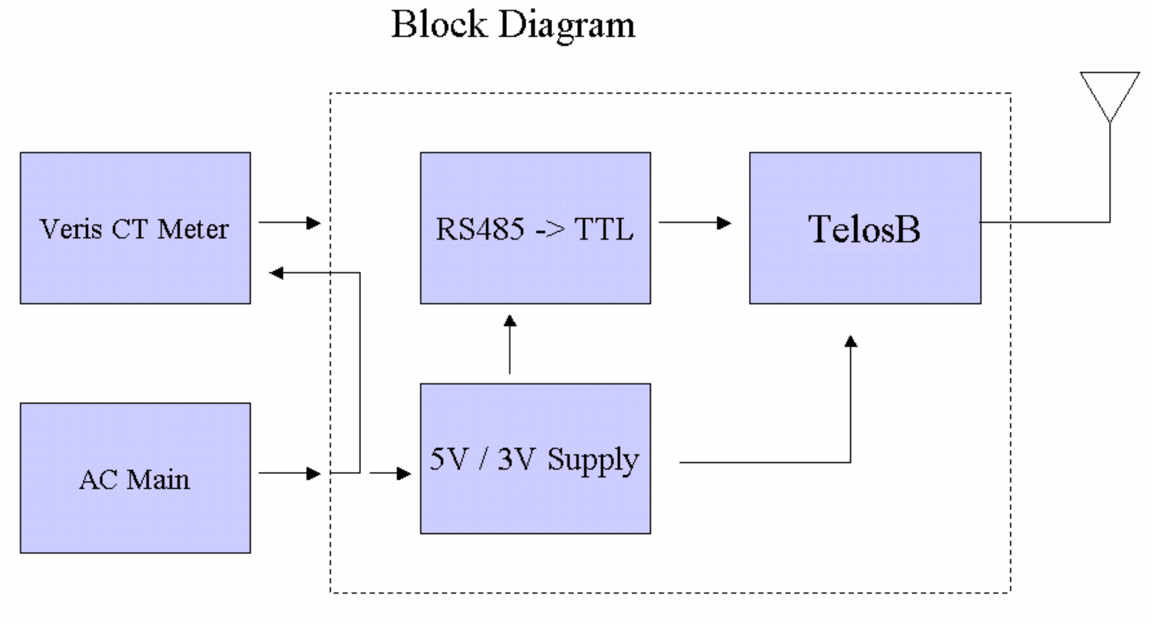

The house meter is composed of two major components. The first component is the Veris H8036 100Amp CT based Meter. It hooks to the AC system via 3 CT's and 3 voltage lines. In a residential environment where there is only a single phase, only 2 CT's and 2 voltage lines are used. The other major component is the interface module, which communicates with the Veris Meter. The interface module consists of a RS485 to TTL converter, a 5V power supply that runs off of 100 – 270 AC, and a TelosB mote, which is responsible for messaging with the Veris CT Meter as well as wireless communication with the home DR monitoring system.

2. Getting Started

2.1 Installing the Veris CT

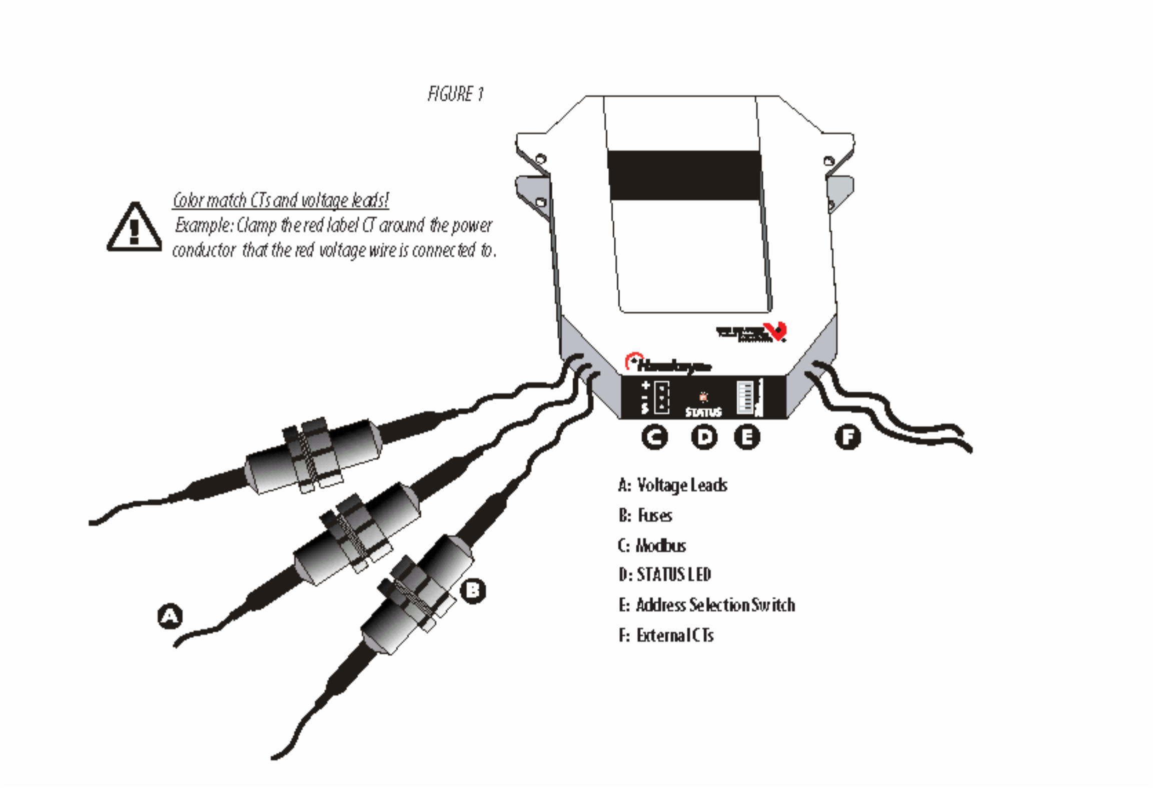
FIGURE 1
Color match CTs and voltage leads!
Example: Clamp the red label CT around the power conductor that the red voltage wire is connected to.
STATUS
A
B
C
D
E
F
A: Voltage Leads
B: Fuses
C: Modbus
D: STATUS LED
E: Address Selection Switch
F: External CTs

2.1.1 Wiring CT Meter to circuit breakers

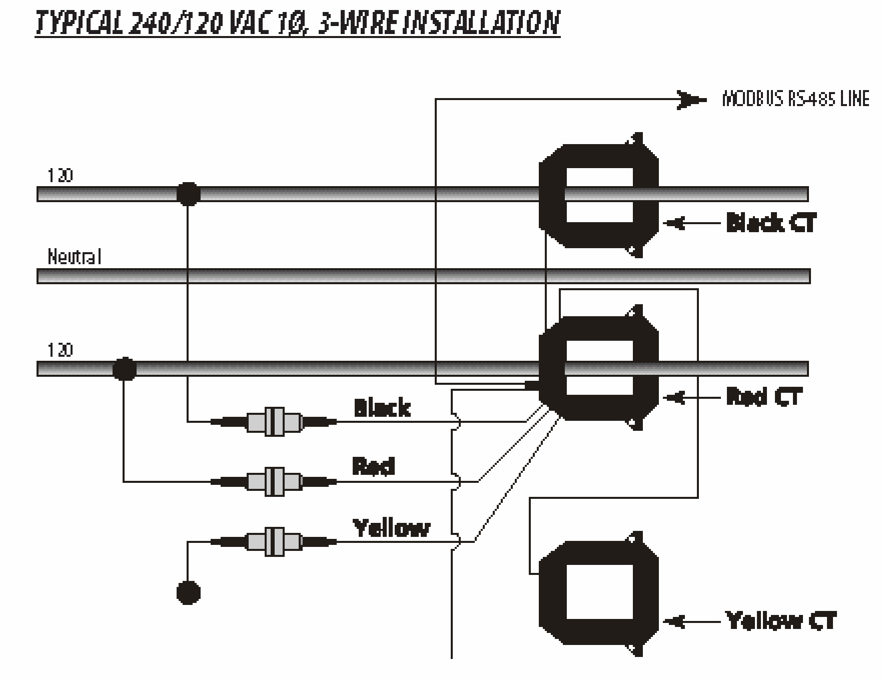

2.1.2 Setting Veris CT device ID

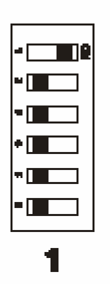

Please make sure the device is set to ID 1.

2.1.3 Connecting the RS485 cable

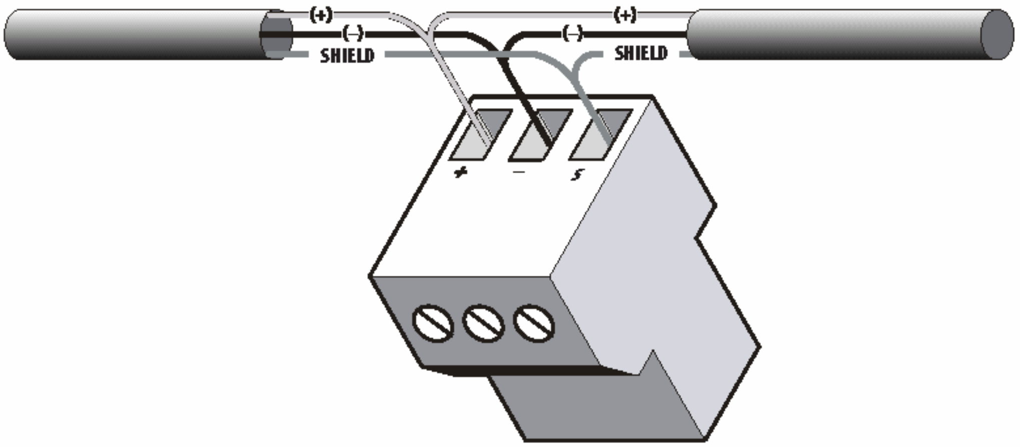

FIGURE 4

NOTES

1. DO NOT GROUND THE SHIELD INSIDE THE ELECTRICAL PANEL.
   All Modbus wires, including the shield should be insulated to prevent accidental contact to high voltage conductors.
2. The Modbus cable should be mechanically secured where it enters the electrical panel.
3. All Modbus devices should be connected together in a daisy-chain fashion.
4. The Modbus cable should be shielded twisted pair wire BELDEN 1120A or similar

⚠ **WARNING: After wiring the Modbus cable, remove all scraps of wire or foil shield from the electrical panel. This could be DANGEROUS if wire scraps come into contact with high voltage wires!**

2.1.4 Unused CT and Unused Voltage Contact

The unused Yellow coded CT will remain unconnected to any lines.

The unused Yellow coded voltage lead is unconnected in the 3-pin receptacle.

2.2 Connecting the Telos interface Module

2.2.1 Connecting RS485 cable

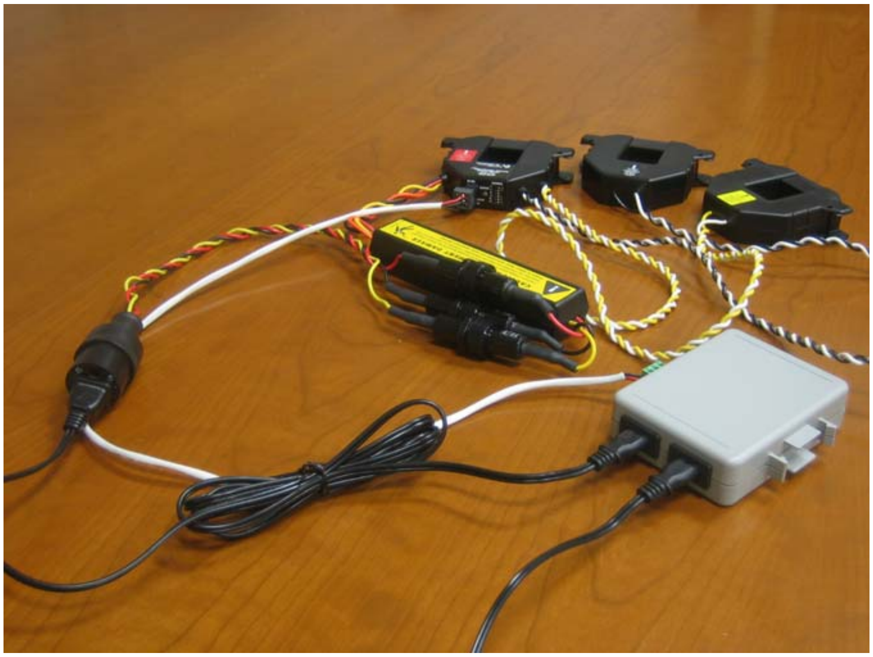

Notice the white RS485 cable connection between the red CT and the telos interface module.

2.2.2 AC voltage pass through

The Veris CT Meter requires contact with the AC voltage. The telos interface module also requires contact with AC voltage to supply power to its circuitry. There are two parallel connectors built into the telos interface module to give 2 different wiring options. These 2 parallel connectors are interchangeable.

The first option involves not using the extra connector in the interface module. The Veris CT meter will directly connect to the AC Mains. The mote interface module will also make a direct connection to AC voltages.

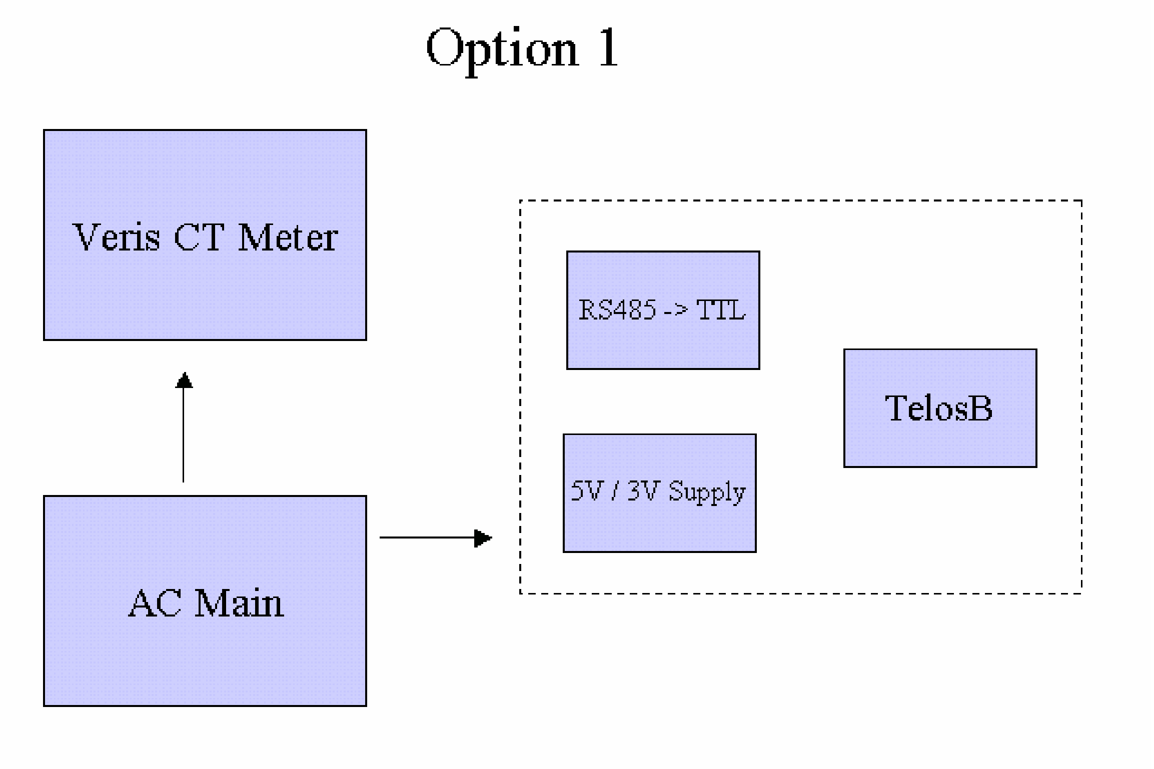

Warning: This option will leave one of the connectors on the interface module exposed. The exposed module will carry dangerously high voltages! Please use the provided end cap in this situation.

The second option is to use the AC voltage pass through connector. The AC mains are connected directly to the Telos interface module. The second parallel connecter on the interface module will then be connected to the Veris CT Meter passing the AC Mains connection with it.

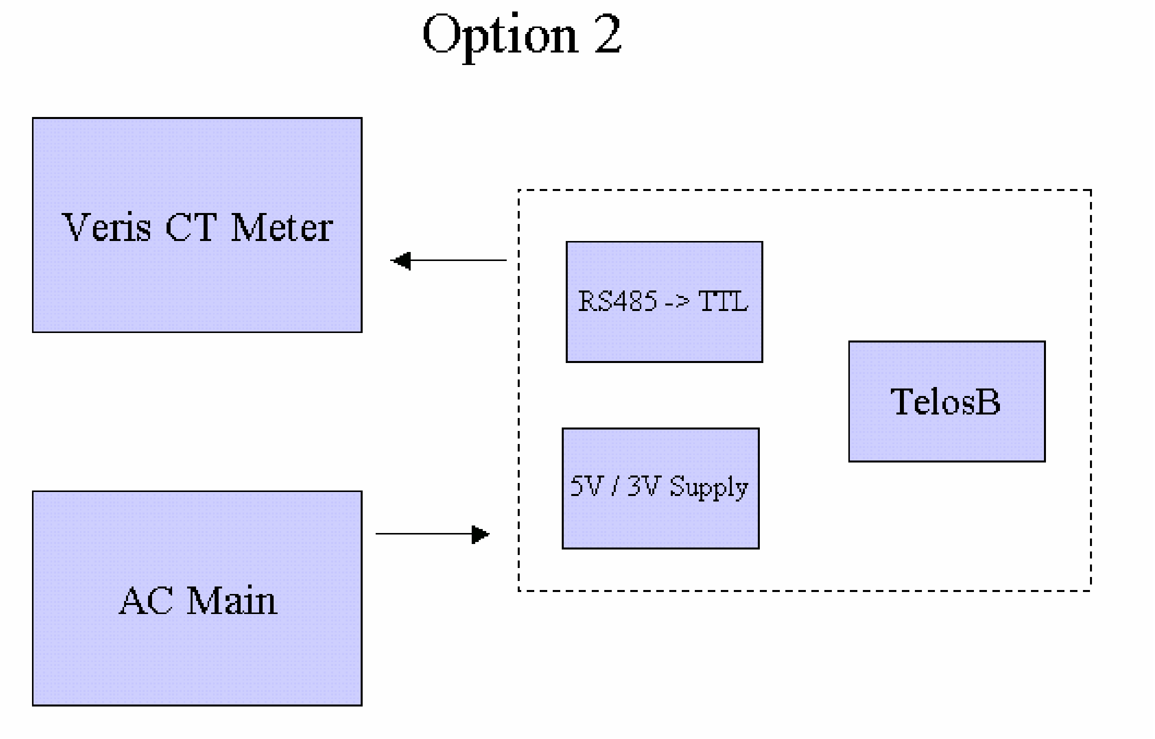

2.2.3 Mounting Brackets

There is a option of using mounting brackets that will allow the interface module to be mounted on a wall.

2.3 Reading the Packet Structure

Recall that in addition to interfacing with the Veris CT Meter, the Telos module also transmits energy data wirelessly. The packet structure is as follows.

HEADER (2)	**LENGTH (1)**	**FCF (2)**	**DSN (1)**	**DESTPAN (2)**	**ADDR (2)**	**TYPE (1)**	**GROUP (1)**	**PAYLOAD (MAX 28)**	**CRC (2)**	**FOOTER (1)**

	Sensor 1		Sensor 2		…
Mote ID (2)	Sensor ID (2)	Raw Data (2)	Sensor ID (2)	Raw Data (2)	…

ADDR: 0xFFFF
TYPE: 0x10
GROUP:0x83

Mote ID: 20

Sensor Description: Current Phase A
Sensor ID: 720

Sensor Description: Current Phase B
Sensor ID: 721

Sensor Description: Power Phase A
Sensor ID: 722

Sensor Description: Power Phase B
Sensor ID: 723

Sensor Description: Voltage AB, RMS
Sensor ID: 724

3. Hardware

3.1 Schematics

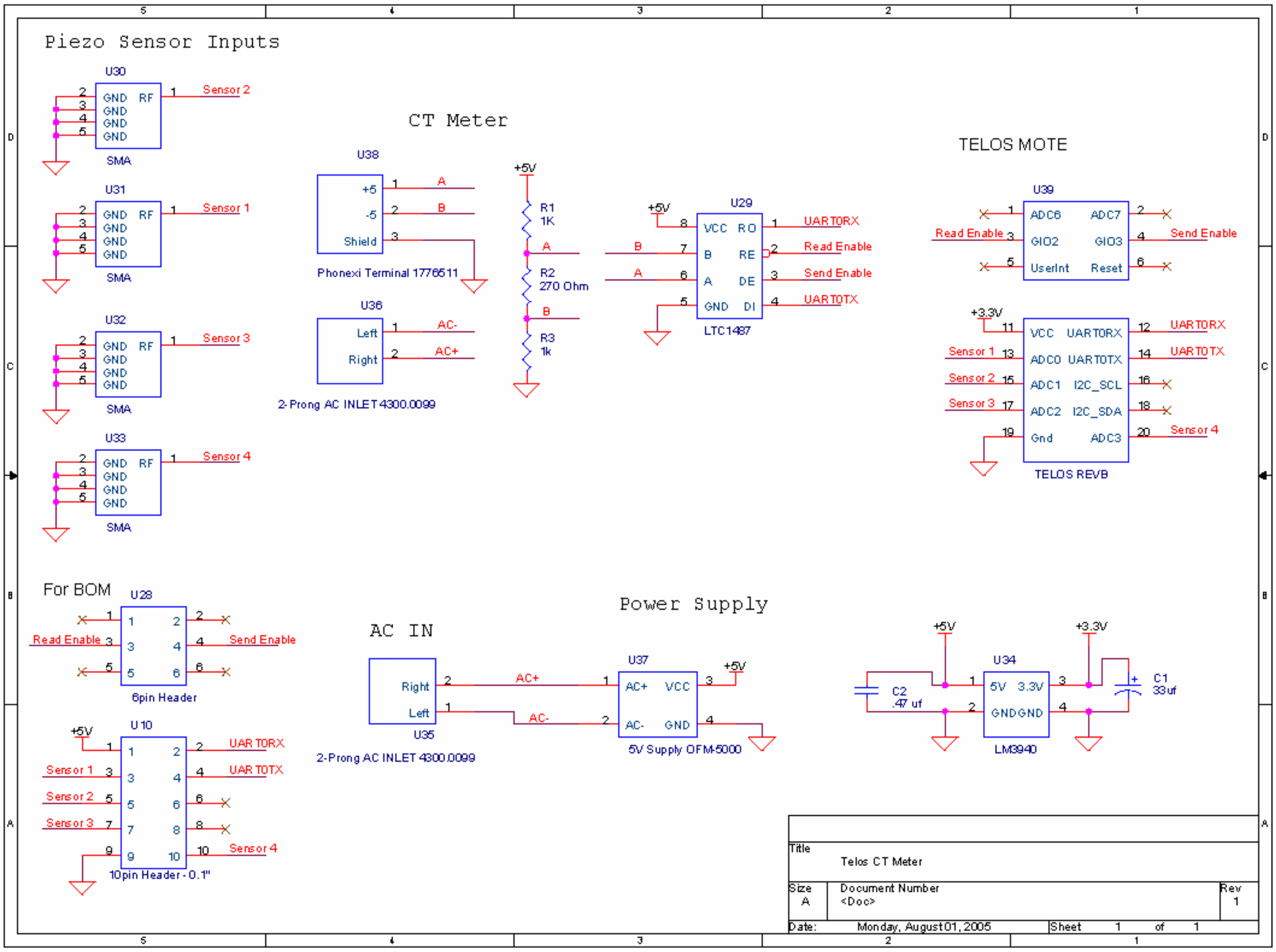

3.2 Layout

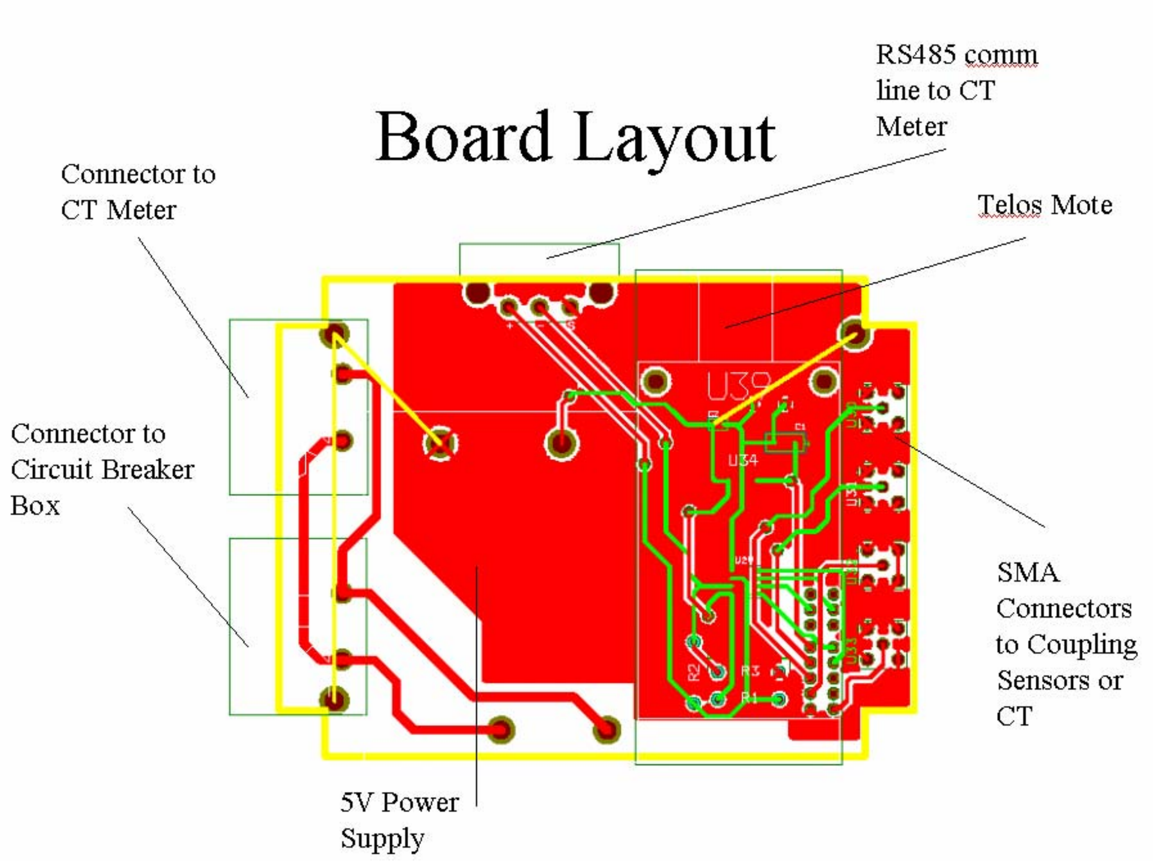
Board Layout
RS485 comm line to CT Meter
Connector to CT Meter
Telos Mote
Connector to Circuit Breaker Box
U39
U34
SMA Connectors to Coupling Sensors or CT
5V Power Supply
R2
R3
R1

3.3 Pictures

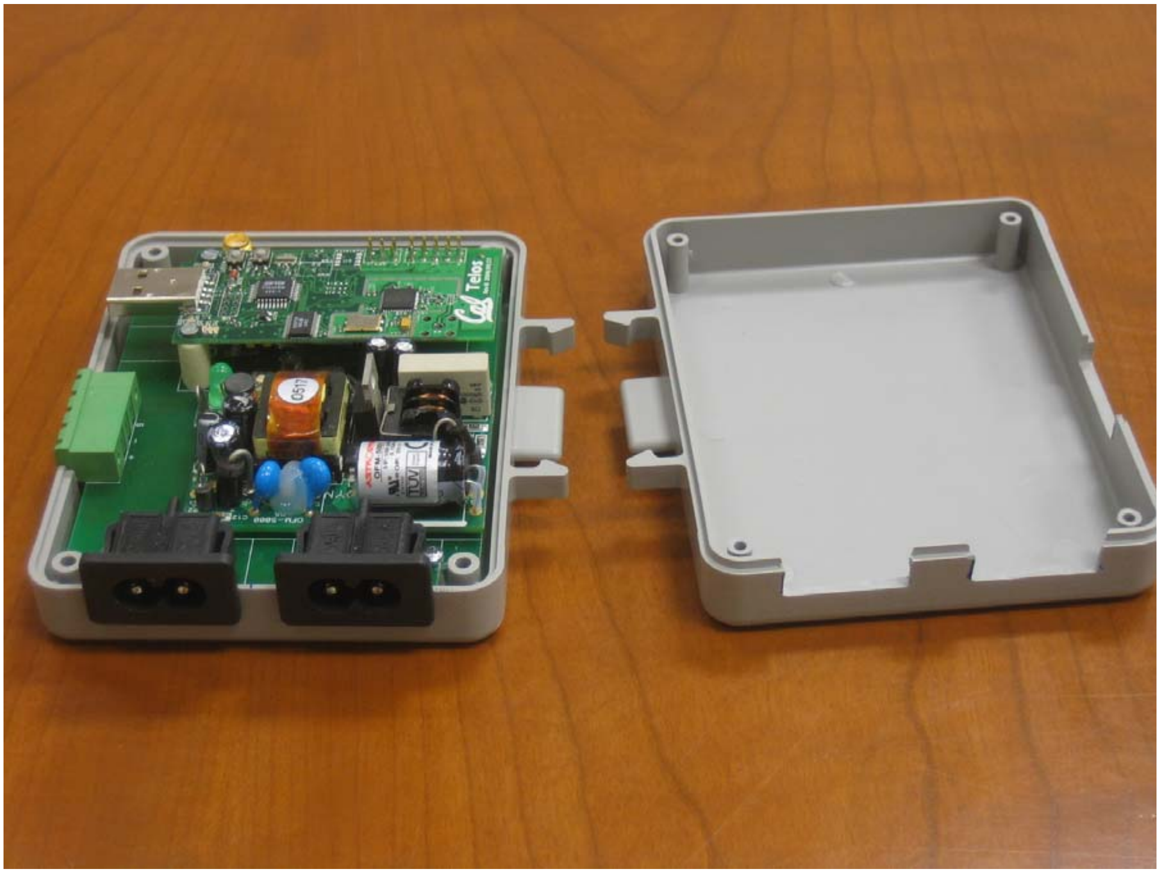

4. Software

4.1 Wiring Diagram

Source Code is located at:
/opt/tinyos-1.modbus/apps/HouseMeter
/opt/tinyos-1.modbus/tools/java/net/tinyos/hscope

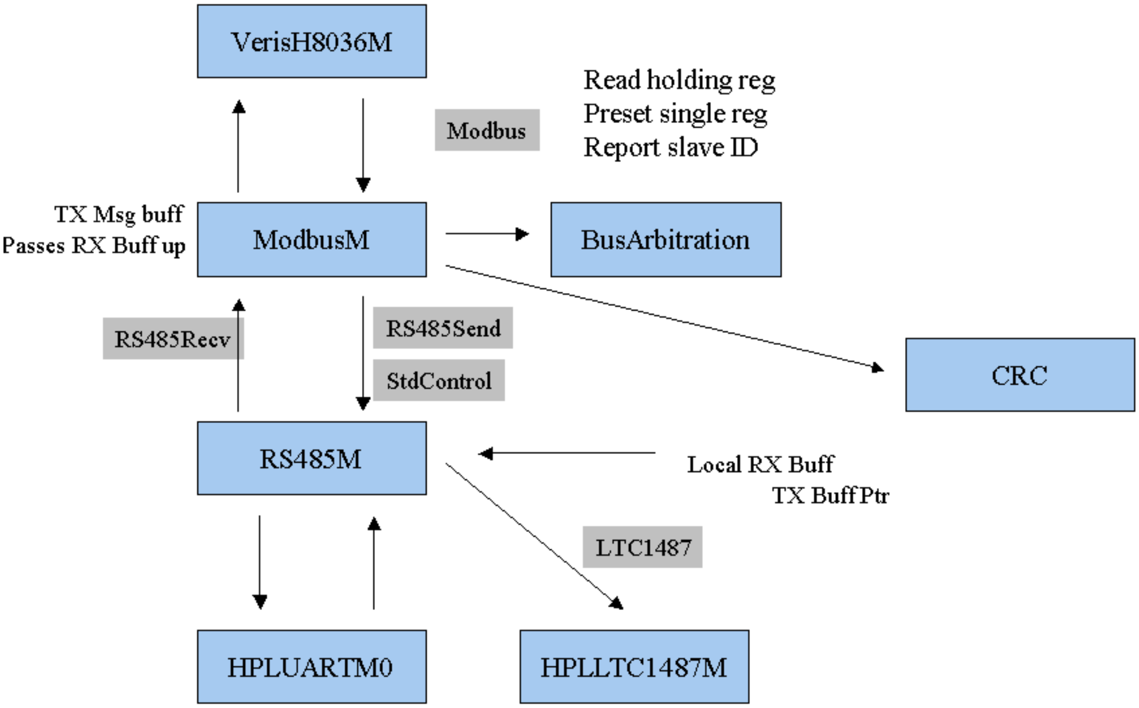

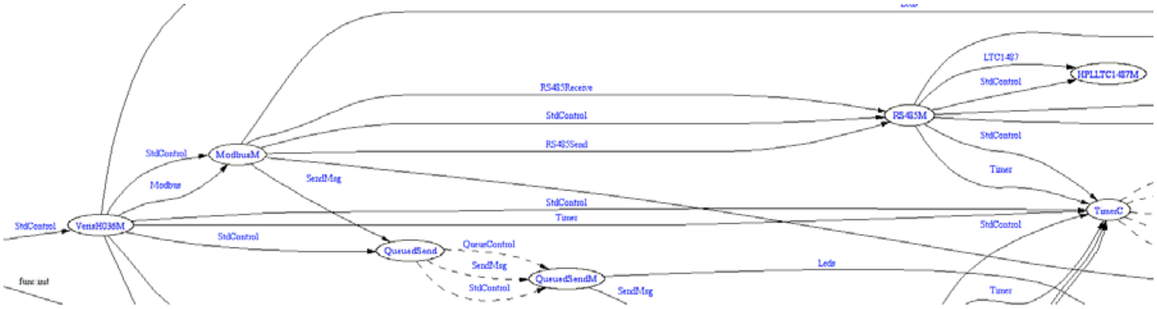

5. System integration:

5.1 Test App

There is a sample java application written to read and graph the sensor readings. It has sample code for doing the unit conversions from engineering units.

Source code location: /opt/tinyos-1.modbus/tools/java/net/tinyos/hscope

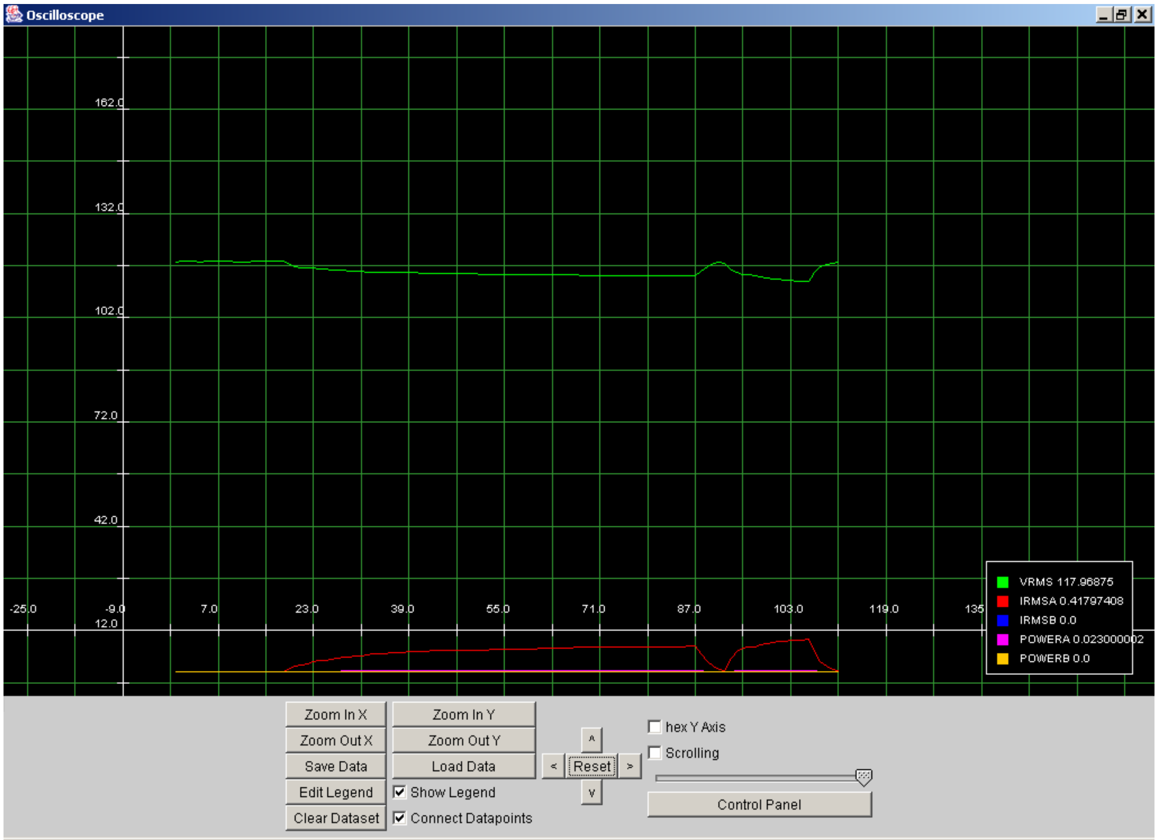

☐ hex Y Axis

☐ Scrolling

☑ Show Legend

☑ Connect Datapoints

5.2 Conversion Table

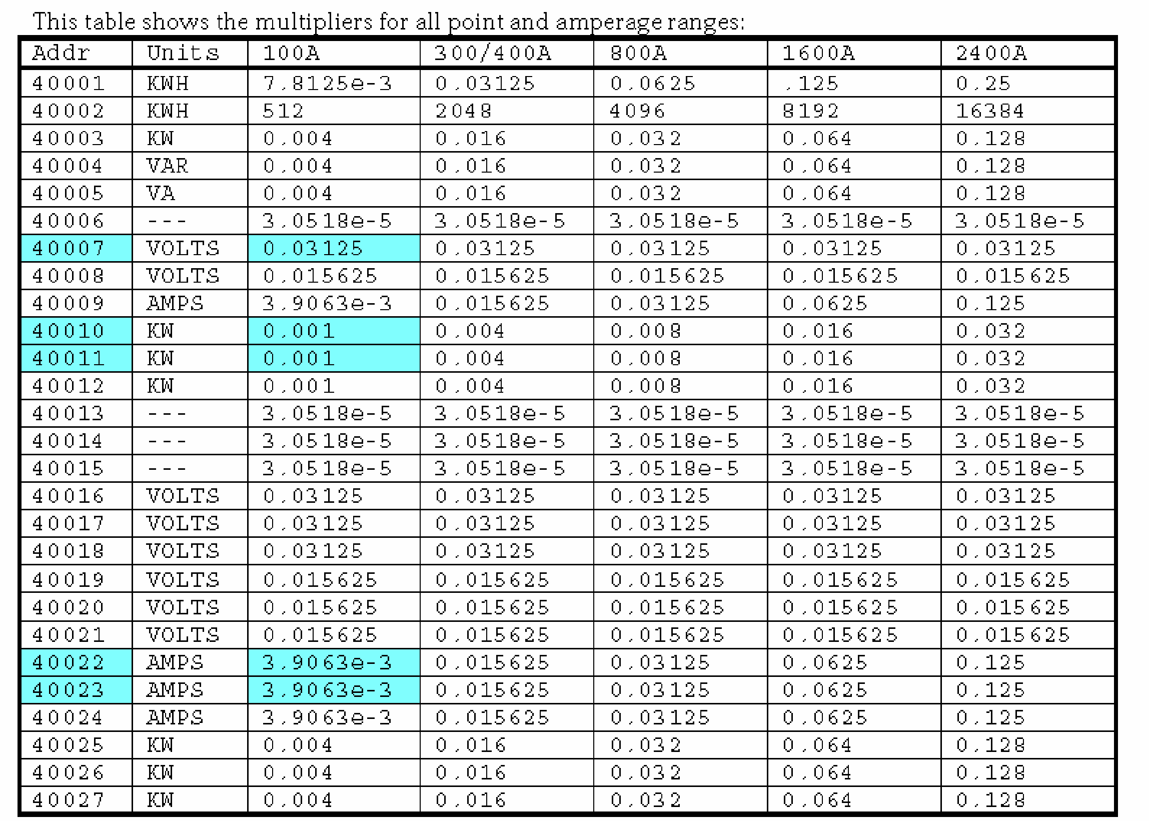

This table shows the multipliers for all point and amperage ranges:

Addr	Units	100A	300/400A	800A	1600A	2400A
40001	KWH	7.8125e-3	0.03125	0.0625	.125	0.25
40002	KWH	512	2048	4096	8192	16384
40003	KW	0.004	0.016	0.032	0.064	0.128
40004	VAR	0.004	0.016	0.032	0.064	0.128
40005	VA	0.004	0.016	0.032	0.064	0.128
40006	---	3.0518e-5	3.0518e-5	3.0518e-5	3.0518e-5	3.0518e-5
40007	VOLTS	0.03125	0.03125	0.03125	0.03125	0.03125
40008	VOLTS	0.015625	0.015625	0.015625	0.015625	0.015625
40009	AMPS	3.9063e-3	0.015625	0.03125	0.0625	0.125
40010	KW	0.001	0.004	0.008	0.016	0.032
40011	KW	0.001	0.004	0.008	0.016	0.032
40012	KW	0.001	0.004	0.008	0.016	0.032
40013	---	3.0518e-5	3.0518e-5	3.0518e-5	3.0518e-5	3.0518e-5
40014	---	3.0518e-5	3.0518e-5	3.0518e-5	3.0518e-5	3.0518e-5
40015	---	3.0518e-5	3.0518e-5	3.0518e-5	3.0518e-5	3.0518e-5
40016	VOLTS	0.03125	0.03125	0.03125	0.03125	0.03125
40017	VOLTS	0.03125	0.03125	0.03125	0.03125	0.03125
40018	VOLTS	0.03125	0.03125	0.03125	0.03125	0.03125
40019	VOLTS	0.015625	0.015625	0.015625	0.015625	0.015625
40020	VOLTS	0.015625	0.015625	0.015625	0.015625	0.015625
40021	VOLTS	0.015625	0.015625	0.015625	0.015625	0.015625
40022	AMPS	3.9063e-3	0.015625	0.03125	0.0625	0.125
40023	AMPS	3.9063e-3	0.015625	0.03125	0.0625	0.125
40024	AMPS	3.9063e-3	0.015625	0.03125	0.0625	0.125
40025	KW	0.004	0.016	0.032	0.064	0.128
40026	KW	0.004	0.016	0.032	0.064	0.128
40027	KW	0.004	0.016	0.032	0.064	0.128

6. Unused Features

6.1 SMA connectors wired to 4 ADC Channels

There are four SMA connectors on the left side of the following picture that is unpopulated. These footprints are connected to 4 ADC lines of the telos mote. This allows easy future integration of any analog sensor onto the line powered telos platform.

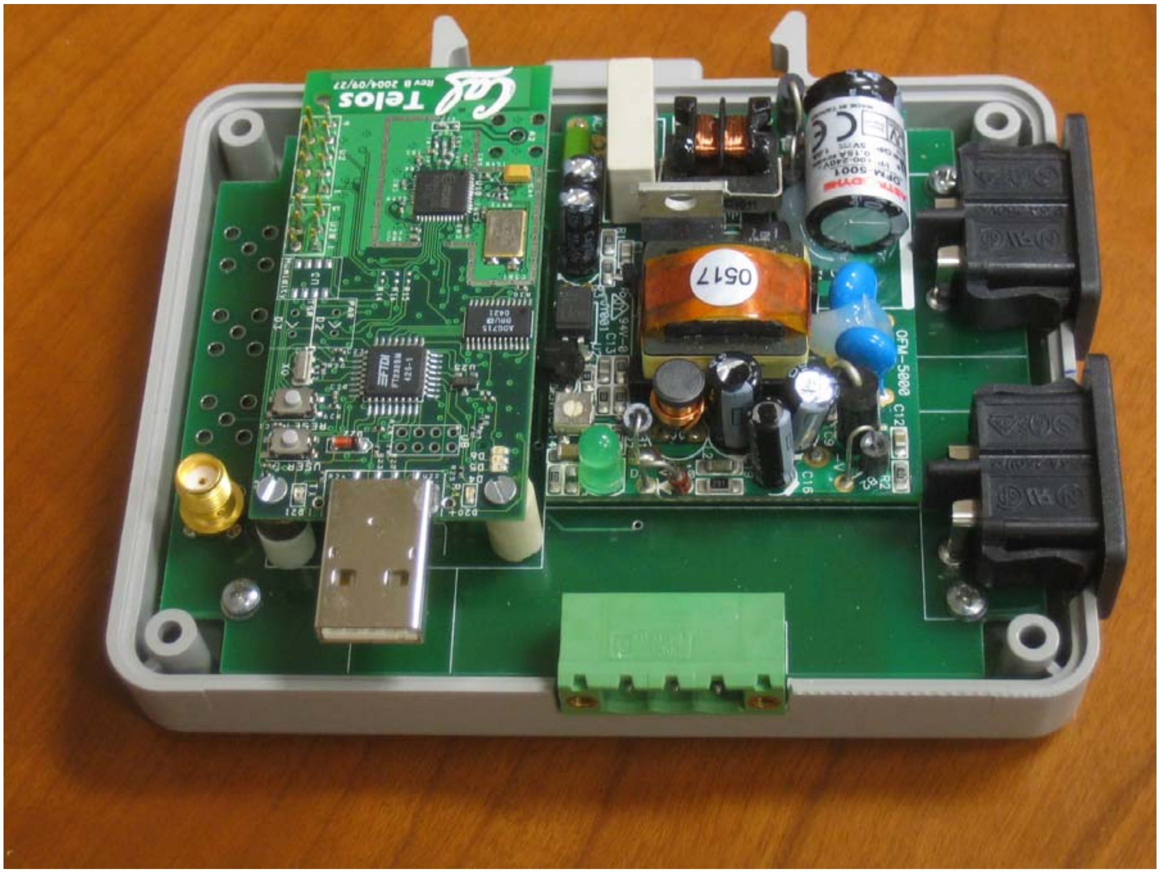

APPENDIX E: HVAC RELAY

Reman Child, Electrical Engineering and Computer Science Dept., UC Berkeley
July 7, 2005

Description

The HVAC (Heating Ventilation and Air Conditioning) relay mote serves three primary purposes: relay control, temperature sensing, and power price indication as per the Demand Response Electrical Appliance Manager (DREAM) framework. Circuitry also exists for quick hardware installation of an optional UI board (found in the receptacle mote), which adds an LCD screen for temperature and other user information displays.

Relay control

Residential HVAC at the thermostat level works by shorting the 24vac line to the heat (heating), compressor (cooling), or fan line, usually in response to some predetermined change in temperature. (For our purposes, only a 4-wire system was implemented). The HVAC mote implements this functionality with three latching relays tied to the 24vac hot and respective heat, compressor, and fan lines. When the T-mote Sky mote receives a relay command from the controller, it sets its expansion pins (see Table 1) to turn the corresponding relay on or off.

Since the relays are latched, power is saved by only setting/resetting the relay for the amount of time necessary to switch - about 5 ms. Unlatched relays, in comparison, must be continuously powered in the ON state.

012	Relay command
000	Compressor ON
001	Compressor OFF
010	Fan ON
011	Fan OFF
100	Heat ON
101	Heat OFF

Table 1: Relay commands - in this case, 0 refers to ADC0, 1 to ADC1, and 2 to ADC2.

Price indication

Price indication occurs with four LEDs and their respective colors: blue (critical), red (high), yellow (medium), green (low/normal). The LEDs are controlled by an I2C chip which operates off the I2C Clock and I2C data expansion pins on the T-mote Sky. Refer to Table 2 for an LED pin mapping to the I2C pins. For low power consumption, the LEDs operate off 3mA in the default setup. If this is not sufficient, the 1K and 1.5K resistors tied to the LEDs can be switched to lower resistive values.

I2C pin	LED Color
4 (I/O 0)	Blue
5 (I/O 1)	Red
6 (I/O 2)	Yellow
7 (I/O 3)	Green

Table 2 I2C pin mapping

Temperature sensing

Temperature sensing is achieved by connecting an RTD to the mono jack located next to the compression terminals. Because the RTD is powered straight off the battery, there is no voltage regulation. This means that when calibrating the RTD, the current battery level must be accounted for and used to find the correct calibration curve.

On the T-mote Sky, the RTD voltage is read off the ADC3 expansion pin.

User interface board

Pins for JTag and a 14 pin header have been added to the circuit board for future implementation of the receptacle mote UI board.

Installation

Installation is relatively simple. The HVAC mote is designed to be used in the four wire HVAC configuration common to a large number of residential buildings. The four wires are colored red, white, green, and yellow, for the 24vac hot side of transformer, heat, fan, and air compressor respectively. To install the HVAC mote, simply connect the wires coming out of the wall (or previously connected to the house thermostat) to the color-coded compression terminals on the side of the HVAC mote.

Now, connect the RTD temperature sensor to the mono jack located on the same side as the compression terminals.
Finally, make sure the on/off switch is in the on position. Installation complete.

Notes

General

In the event of hardware or battery failure, the HVAC mote can be manually overridden by the switch located at the top of the unit. This breaks the connection between the 24vac and the rest of the circuit, effectively switching off any relay that might be set ON.

Programming

Pin mappings have been outlined in previous sections. For efficient power consumption, the HVAC mote should be programmed to turn the radio on at 10 or 30 second intervals. This assumes that the controller will then send any price/relay change commands for at least 10 or 30 seconds (respectively).

Also, relays should be set/reset for the minimum time necessary to switch (about 5 ms). The relays draw about 55mA when powered, so savings here can be very significant.

Eagle

In the Eagle board file, layer 100 (yellow wire) denotes the jumper wires. Since the HVAC mote was created on a single-sided PCB, these wires must be manually soldered in. Also, the fingerprint for the transistors in the board file and the physical transistors differ, so the transistors must be positioned opposite to how they appear in the board file.

APPENDIX F: THERMOSTAT SWITCH

Po-kai Chen, Electrical Engineering and Computer Science Dept., UC Berkeley

The thermostat switch contains a physical switch that physically shorts the four wires from the wall with two thermostats also attached to it. The second function of this device is to determine if the heater, fan, or AC is on. With two sets of sensors, the mote is able to determine which thermostat is shorting which signal, regardless of which position the switch is in.

The switch together with the sensors enables us to perform three tasks:
(1) Monitor the actual electrical connection of the HVAC relay mote before it is hooked up to the house's HVAC system for testing purposes.
(2) Monitor the usage pattern of the existing thermostat.
(3) Once the testing phase is over, we can still monitor which signal the HVAC relay mote is sending to the HVAC system. The switch enables a fallback to the existing house thermostat in case something goes wrong.

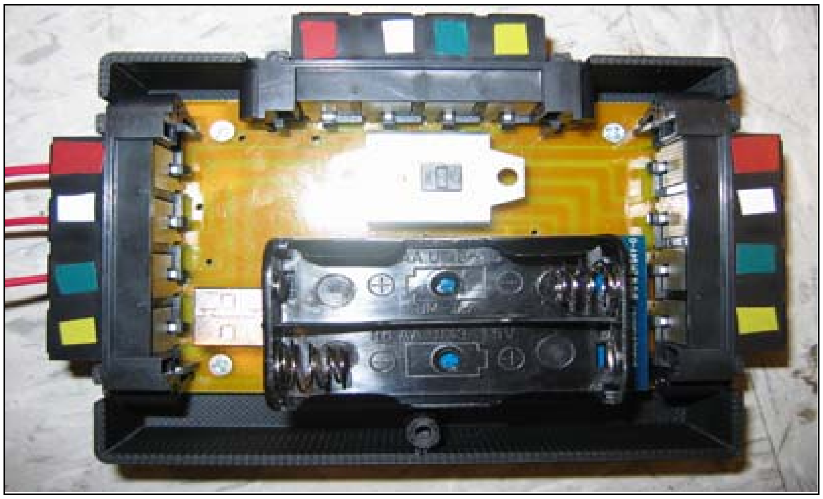

Figure 13 HVAC Switch

The HVAC switch contains three sets of four-jack compression terminals. The terminal in the center is to be connected directly to the HVAC system through the four wires coming through the wall. The terminal that's pointed by the USB connector (pictured on the left in Figure 1) is to be connected to the HVAC relay mote. The last terminal (pictured on the right in Figure 1) is to be connected to the original thermostat. The switch located in the center top of Figure 1 is a standard four pole / double throw switch. If the switch is switched to the left (called position 1 from now on), the HVAC system will be controlled by the thermostat on the left; if the switch is switched to the right (called position 2 from now on), the system will be controlled by the thermostat connected by the terminal to the right.

Device Input / Output

The main IO, as described above, consists of the two thermostats and the switch as inputs, and the terminal going out to the wall as the output. In addition to these physical IO connections, the device also outputs the HVAC status through the T-mote Sky mote using radio. As the raw sensor data can vary from system to system for the same state, it is difficult to determine the system state for a system based just on raw sensor data. Therefore, instead of calculating and sending the system state, this device sends the raw data from the six sensors and lets the receiving side do the conversions.

Table 1

	LOW	HIGH	4095	FLOAT
711.value	Heater On	-	Heater Off	-
712.value	Fan On	-	Fan Off	-
713.value	AC On	-	AC Off	-
714.value	Heater Relay On *	Heater Relay Off *	Heater Relay On **	Heater Relay Off **
715.value	Fan Relay On *	Fan Relay Off *	Fan Relay On **	Fan Relay Off **
716.value	AC Relay On *	AC Relay Off *	AC Relay On **	Fan Relay Off **

*** Indicates the switch is in position 1**

**** Indicates the switch is in position 2**

The T-mote Sky mote is sampling six points on the circuit, with sensors IDs of [711,716]. The table above summarizes the possible outputs from the device. Depending on the particular HVAC system, a different LOW / HIGH threshold may be required. From the initial device testing, a LOW range of < 100 and a HIGH range of > 3000 seem to work. The message structure of the data packet that this mote sends out follows the standard DR structure for seven sensors, the six listed above and one for reporting the internal battery voltage.

NOTE:

This device does not control the thermoelectric air conditioner on the plastic model house. It is not able to handle the 14 amps of current pulled by the air conditioner.

APPENDIX G: DATABASE STRUCTURE

Florian Jourda, Mechanical Engineering, UC Berkeley

Database issues and solutions for the test during the summer in Moraga House

Requirements

We want to save sets of data during the real-time test of the DR system in Summer 05 in order to analyze them later. These data will be stored in a database located on a server of UC Berkeley. They will be stored in the laptop in the house, thus the controller should rely on access to them for processing (even for learning).

The data we want to save are:

- Input from real sensors:
  - **Temperature** measurement of all the different areas
  - **On/Off** status of all the appliances
  - **Consumption** of all the appliances
  - **Occupancy** of all the areas
  - **Weather** station: anemometer, pyranometer (both global and diffuse radiation)

- Output to real actuators:
  - **Price indicator lights** on non-controllable appliances
  - **On/Off** order of the controllable appliances, especially Heat and Cooling
  - **LCD screen** to display information

- Input or output of simulated components:
  - **Price** information from the price generator

Solution

We can use a MySQL database located on a server at UC Berkeley to store the data. All the required software is free and familiar for many of us.

We have to:

- define the **database organization** (see next pages)
- write the **PHP code** to operate the database.
- and incorporate a **"recorder"** in the laptop that will send the collected data to the database at regular intervals (e.g. 1 hour). The recorder should be integrated in the Java code of the controller in order to have access to all data (thus it should be programmed in Java). The first job of the recorder could be to store on the laptop, in temporary files such as text or XML files, the last set of data used by the controller, and a second function could be to communicate the data of theses files to the database before erasing them. Or if the laptop has enough resources, the recorder could keep the data in RAM.

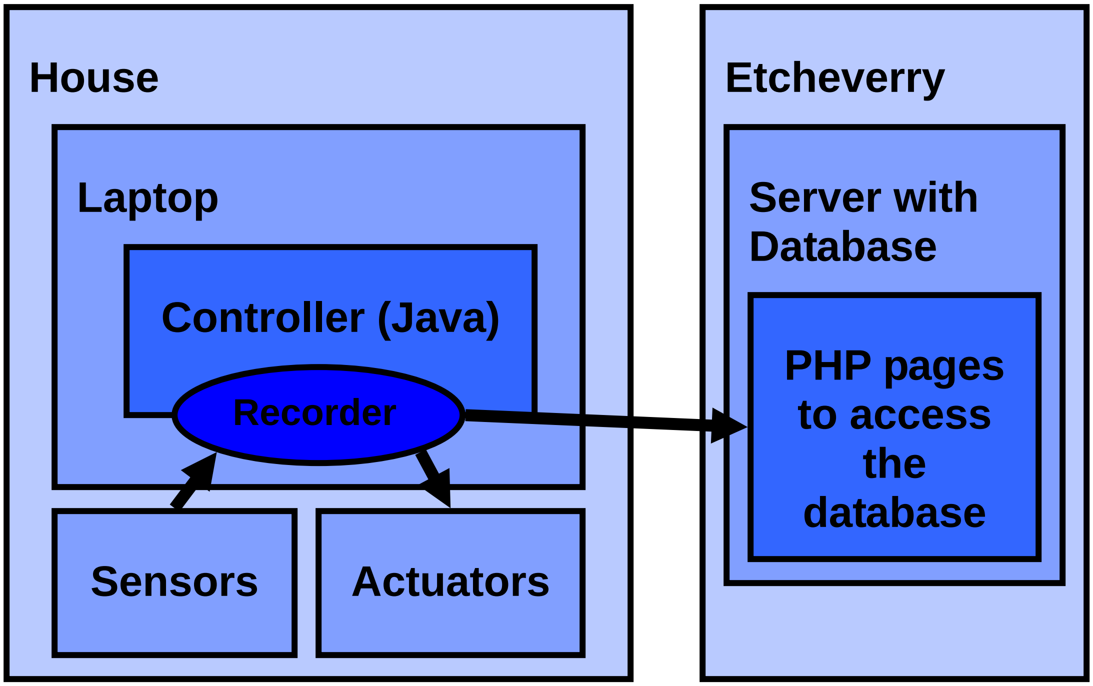

Figure 1: Global Scheme

Database organization

All the input/output data (temperature changing, actuation of appliances…) we want to record can be considered as event. We can then store all the data in only one table in the MySQL database using this concept of "event". This makes the organization very simple. The following array shows an example of fields we can use:

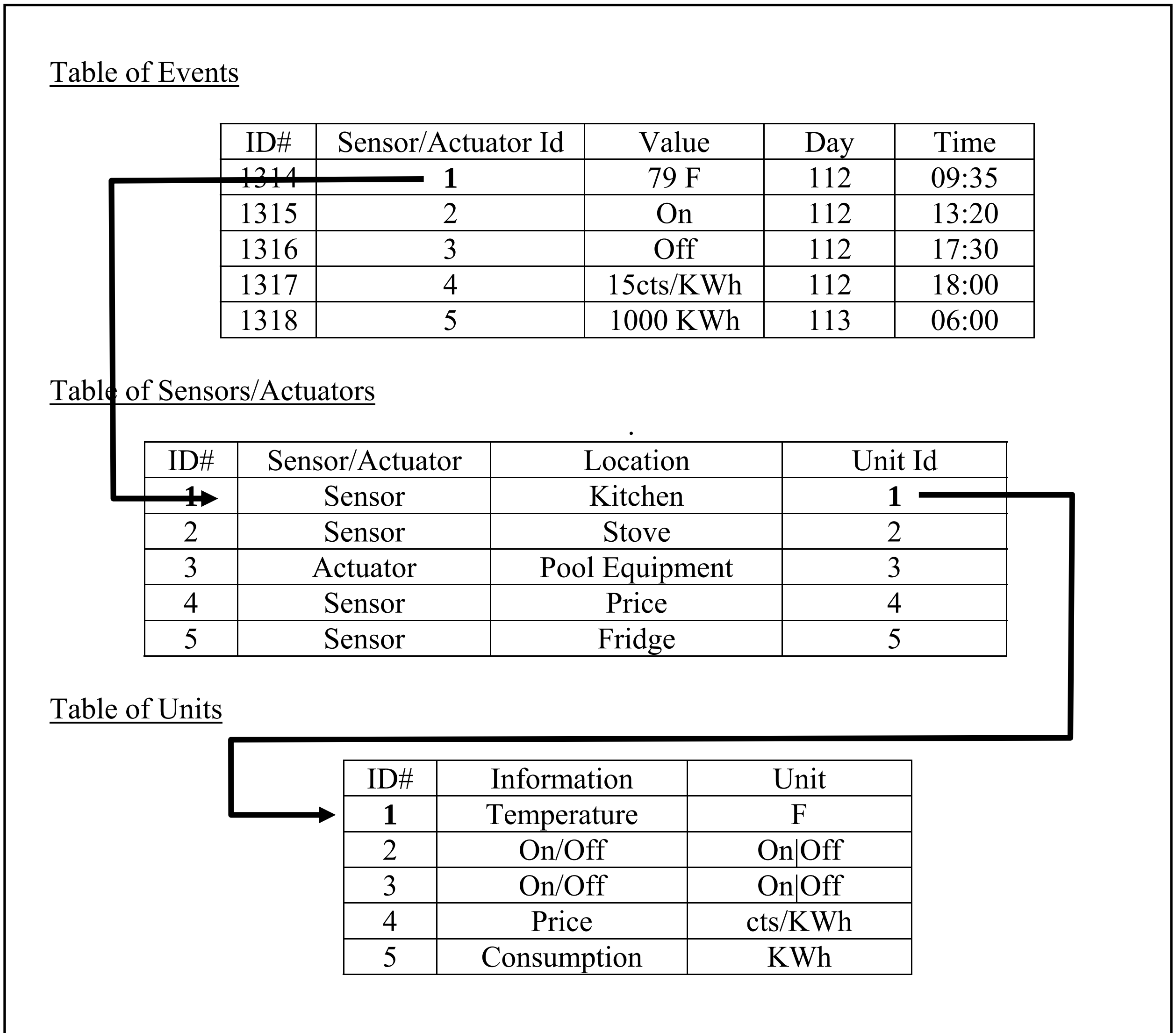

Table of Events

ID#	Sensor/Actuator Id	Value	Day	Time
1314	**1**	79 F	112	09:35
1315	2	On	112	13:20
1316	3	Off	112	17:30
1317	4	15cts/KWh	112	18:00
1318	5	1000 KWh	113	06:00

Table of Sensors/Actuators

ID#	Sensor/Actuator	Location	Unit Id
1	Sensor	Kitchen	**1**
2	Sensor	Stove	2
3	Actuator	Pool Equipment	3
4	Sensor	Price	4
5	Sensor	Fridge	5

Table of Units

ID#	Information	Unit
1	Temperature	F
2	On/Off	On|Off
3	On/Off	On|Off
4	Price	cts/KWh
5	Consumption	KWh

Figure 2: Data organization in the database

Filtering

The quantity of data stored in the database can become rapidly very large if we store all the events. Thus, we will have to eliminate useless or redundant information.

One example is temperature measurement. If the temperature in the living room does not change significantly for two hours, and if the sample time for measurement is one minute, we will not save 120 events "Temperature Living Room=78 F", whereas only one is enough. Thus we can decide to save a new event of temperature only if the difference of temperature with the last value is bigger than a certain threshold of tolerance as shown in the following figure:

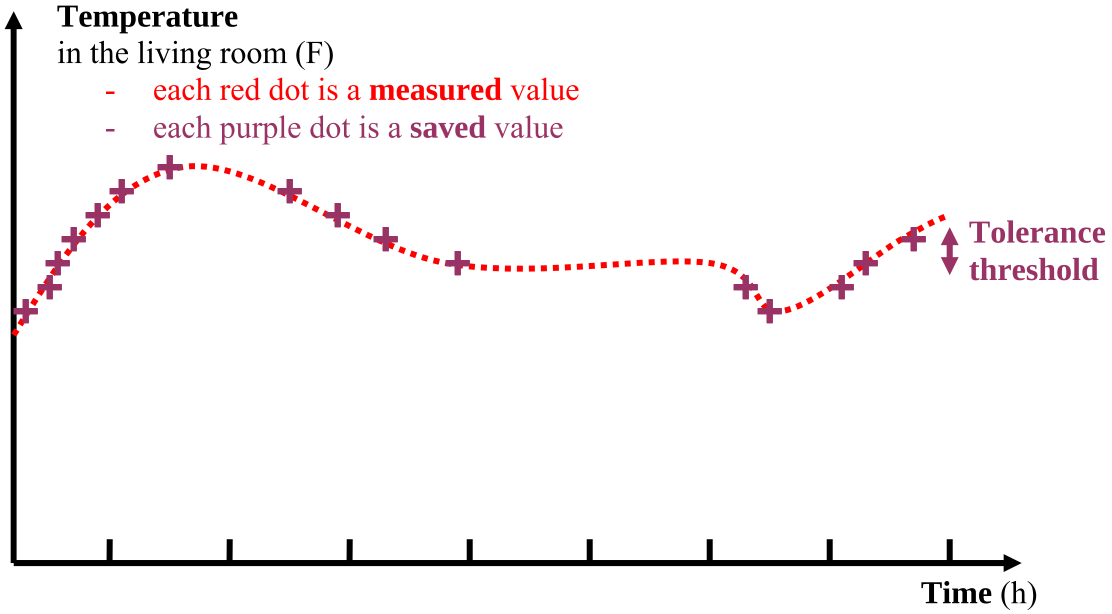

Figure 3: Filtering of temperature events

Next step

The next step will be to think about how we can save data to allow the controller to access information needed for learning.

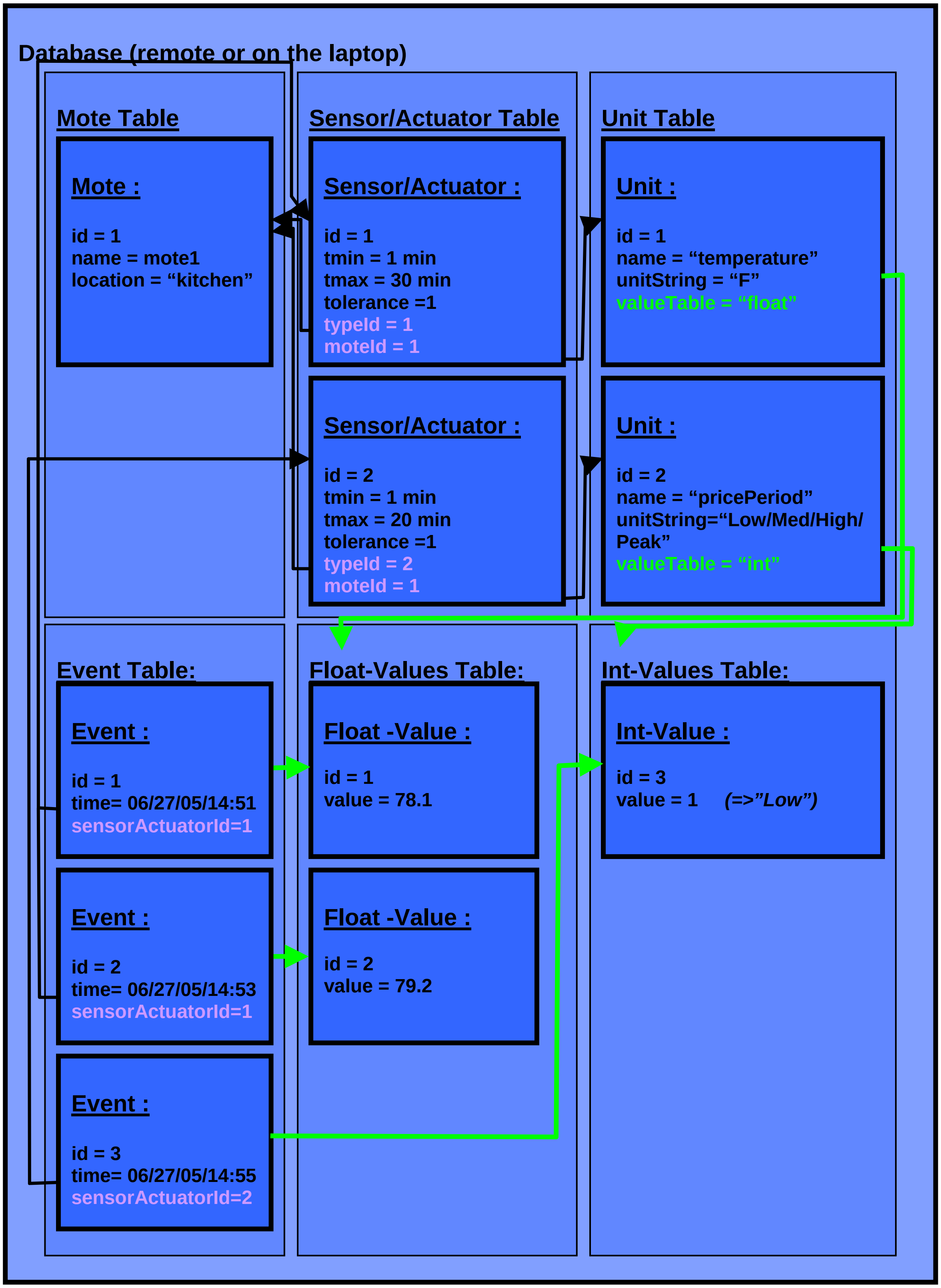

Figure 1 : Database organization (object oriented)

APPENDIX H: MZEST

Anna LaRue, Architecture, UC Berkeley

As we develop a demand response-enabled thermostat, we must also develop an environment in which to test it. Before testing the thermostat, control strategies, and other infrastructure in a physical house, we are testing the control strategies in a simulated house environment. For this, we use the Multi-Zone Energy Simulation Tool (MZEST) to simulate the energy use and thermal responses of houses under different control strategies. MZEST is a multizone extension of the simulation code (California Non-Residential Engine or CNE) used by CALRES, the energy simulation software distributed by the California Energy Commission used for demonstrating compliance with state residential Title 24 energy standards. We chose MZEST because it can predict the temperature in several different thermal zones and because we had access to the source code. The tool currently uses 5-minute time steps, which allows us to use our external controller to control MZEST in the same manner that the controller would control a real house.

MZEST requires certain input parameters, including the specification of a weather file and designated house construction information. The weather file is hourly climate data in the form of a TMY2 (Typical Meteorological Year) file, but may be composed of weather data collected on site. The house construction parameters are specified in input files, and include construction material properties, wall and roof constructions, window specifications, infiltration rates, and adjacencies of walls, rooms, and zones. To tune the simulated house to a physical house, the shading coefficient of each window may be specified as an hourly variable. Internal gains, the results of specific equipment use and occupant schedules, can also be specified hourly. The size and efficiency of the physical house's HVAC equipment must also be specified.

In the same way a standard thermostat controls a real house, MZEST currently conditions the simulated house to meet the needs of only one zone. In a real house, that zone is the one in which the thermostat is located; in MZEST, a "control zone" must be designated. The other zones are also conditioned but, as in a physical house, will generally not exactly meet the control zone setpoint, since solar gains, occupancy, and other internal gains differ from zone to zone.

The output of MZEST includes several types of information such as report spreadsheets and graphs depicting annual energy use, cost, and so on. For this project, one of the most important reports is the temperature of each thermal zone at each time step. MZEST also reports the energy use of the HVAC system and the energy balance of each zone at each time step.

The Demand Response Electrical Appliance Manager (DREAM, our Java control engine for all air conditioning and electrical loads controller) can run MZEST the same way it will operate in a house. To test the DREAM on a real house requires the installation of sensors, actuators, a communications network, and the replacement of the original thermostat with the new controller. However, testing DREAM with a simulated house merely requires the simulation of these sensors and actuators. We interface the simulation directly with DREAM via an XML data transfer. MZEST writes outdoor temperature and zone temperatures to a file. DREAM then reads those temperatures as if they came from sensors and, using its control strategies and our price simulation, determines how to condition the house. DREAM then dictates to MZEST, through the same file, whether to heat or cool. MZEST heat or cools and calculates the house's thermal response.

DREAM controlling MZEST:

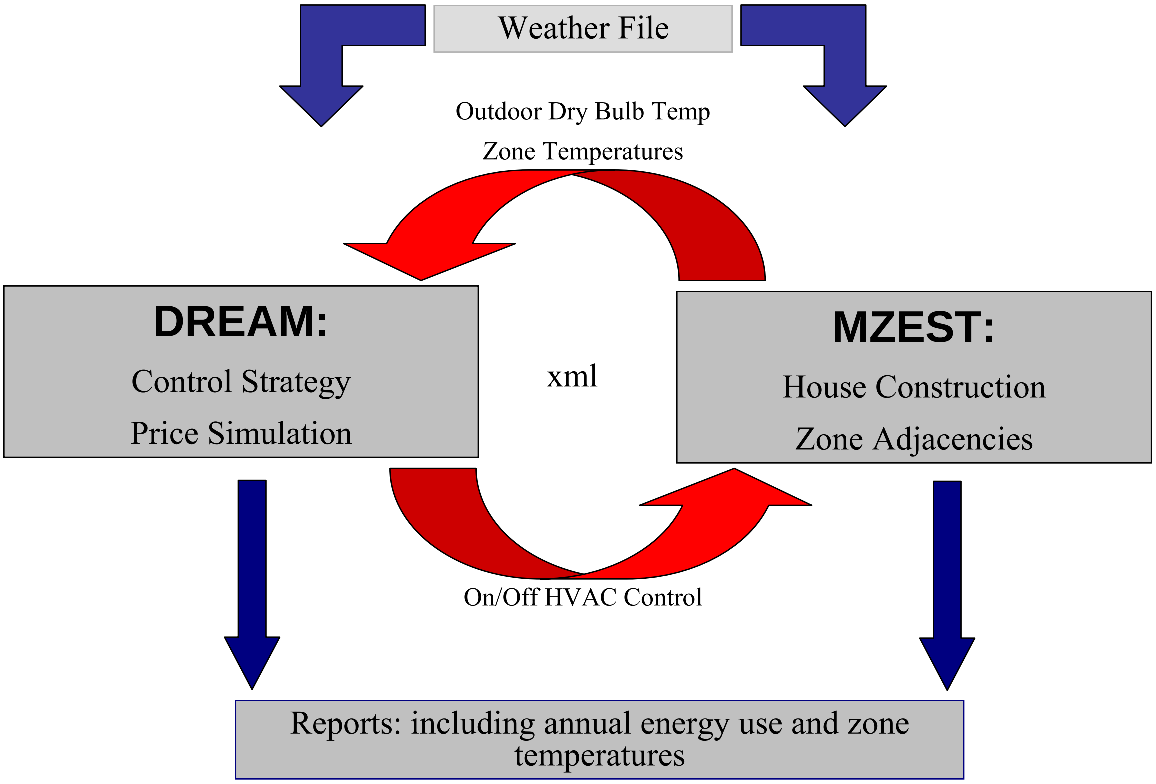

Because we can simulate many different kinds of houses, we will be able to predict the effect of our demand response control strategies on the energy use profile of a range of house types located in any California climate zone. We can then train the controller to learn the behavior of the house and the simulated preferences of the occupants and optimize its control strategies to each individual house and its occupant accordingly.

APPENDIX I: COMMUNICATIONS DATA STRUCTURE

Xue Chen, Mechanical Engineering, UC Berkeley

For the 2005 test house, we used Moteiv T-mote Sky motes. The final implementation at the house included two motes with just temperature sensors, six motes with temperature and occupancy sensors (one included relative humidity), one mote with whole house power sensing at the breaker box, one mote outside with temperature and relative humidity sensors, one mote with solar radiation and wind speed and direction sensors, one repeater mote, and one base mote. We also tested the HVAC actuation mote and Thermostat switch mote.

These motes communicated via an onboard radio using the TinyOS operating system. We created a structure for the messages passed by these motes, which is described below.

1. Message Structure:
   We decided to just transmit raw data at this point and do the conversion to data with the proper units and precision at the controller/laptop side for now.

Moteiv T-mote Sky Message Structure:

HEADER (2)	**LENGTH (1)**	**FCF (2)**	**DSN (1)**	**DESTPAN (2)**	**ADDR (2)**	**TYPE (1)**	**GROUP (1)**	**PAYLOAD (undeter-mined)**	**CRC (2)**	**FOOTER (1)**

(Unit: byte)

a. The length of the Payload (mote ID, sensor ID, and Raw Data) s flexible; length is indicated at byte "LENGTH"
b. DESTPAN and ADDR are set to 0xFFFF, for broadcasting purpose.
c. TYPE is the handler ID in TinyOS. We use this to identify different types of messages. Motes will drop messages with wrong handler ID automatically.

TYPE (handler ID) 1 byte	Description
0x10	Message sent from sensor motes
0x21	Message sent to relay motes
0x22	Message sent to LED motes
…	…

d. GROUP is group ID. It is set to 0x83 for all the motes in the 2005 test.

e. PAYLOAD

	Sensor 1		Sensor 2		…
Mote ID (2)	Sensor ID (2)	Raw Data (2)	Sensor ID (2)	Raw Data (2)	…

- Mote ID is a unique number assigned to each mote for identification purposes.

- Sensor ID is the unique number assigned to each sensor. It is assigned in the way shown in the following table, so we can easy detect what type of sensor it is.

Sensor ID Table:

ID Number	Description
100 ~ 199	Air Temperature
200 ~ 299	Relative Humidity
300 ~ 399	Infrared
400 ~ 499	Occupancy
500 ~ 599	Light
600 ~ 699	Aperture reed switch
700 ~ 799	Power (outlet + breaker panel)
800 ~ 899	Radiation (diffuse, global)
900~999	Wind direction, wind speed
1000+moteID	Battery voltage for moteID
…	…

- Raw data sample:

7E 42 04 01 08 1F FF FF FF FF 0A 33 01 00 26 0B 84 6F 7E

2. IEEE 1451 Standard: We followed the spirit but not the letter of this standard.

3. Conversion layer

We had several choices and much discussion over where the conversion of raw data to usable data might occur. The choices are listed below, and will be reviewed at a later date.
#1: Do conversion at controller with a calibration table. (Current method)
#2: Do conversion at controller and receive calibration coefficients from motes. Can we use TEDS of IEEE 1451?
#3: Do conversion at motes and send an integer and a coefficient to controller. On controller, divide the integer by the coefficient. How to do the conversion with fast speed and little energy consumption by the mote? Consider the speed and power.

4. Things to Test:

Q1: How many cycles does the Moteiv T-mote Sky microprocessor use to do calibration? For both linear and nonlinear calibration formula.
Q2: Does the Moteiv T-mote Sky have hardware to do multiplication and division?

Moteiv T-mote Sky message structure field description:

Variable		*Length (bit)*	*Definition*
Header		16	7E 42
Length		8	To-send/receive data bytes
FCFHI		8	Frame Control Field High Byte
FCFLO		8	Frame Control Field Low Byte
DSN		8	Data Sequence Number (for acks)
DESTPAN		16	Destination PAN Identifier (like group id)
ADDR		16	Destination address (0xFFFF)
TYPE		8	AM type, Handler ID
GROUP		8	Group ID
Data (data body)	MOTE ID	16	Mote local address
	SENSOR ID	16	"Bit on" represents the sensor type.
	RAW DATA	16	Sensing data
STRENGTH		8	RSSI
LQI CRC ACK		8	Link Quality Indicator
TIME		16	(Reserved) Time stamp of transmit/receive
FOOTER		8	7E

Note:

- In raw data, except for Header and Footer, code 7D 5E substitutes 7E, and 7D 5D substitutes 7D.
- The following fields *Strength, LQI CRC ACK*, *Time* are not actually transmitted or received on the radio! They are used for internal accounting only. The reason they are in this structure is that the AM interface requires them to be part of the TOS_Msg that is passed to send/receive operations.
- Both devices have source address, destination address and PAN (Personal Area Network) identifier set to 0xFFFF. In this mode, the receiver will accept any data packets from any node, regardless of the PAN to which it belongs or the source or destination address of the node. It is possible to establish a private PAN in which the receiver only receives packets which are destined for the PAN to which the receiver belongs.

Reference:

1. 802.15.4 specification for information about relevant fields (FCF, DSN, Destpan), http://standards.ieee.org/getieee802/802.15.html
2. the CC2420 datasheet for others (Strength, LQI)
3. the TinyOS tutorial for a discussion on AM types

APPENDIX J: TABLE OF POWER SCAVENGING ENERGY SOURCES

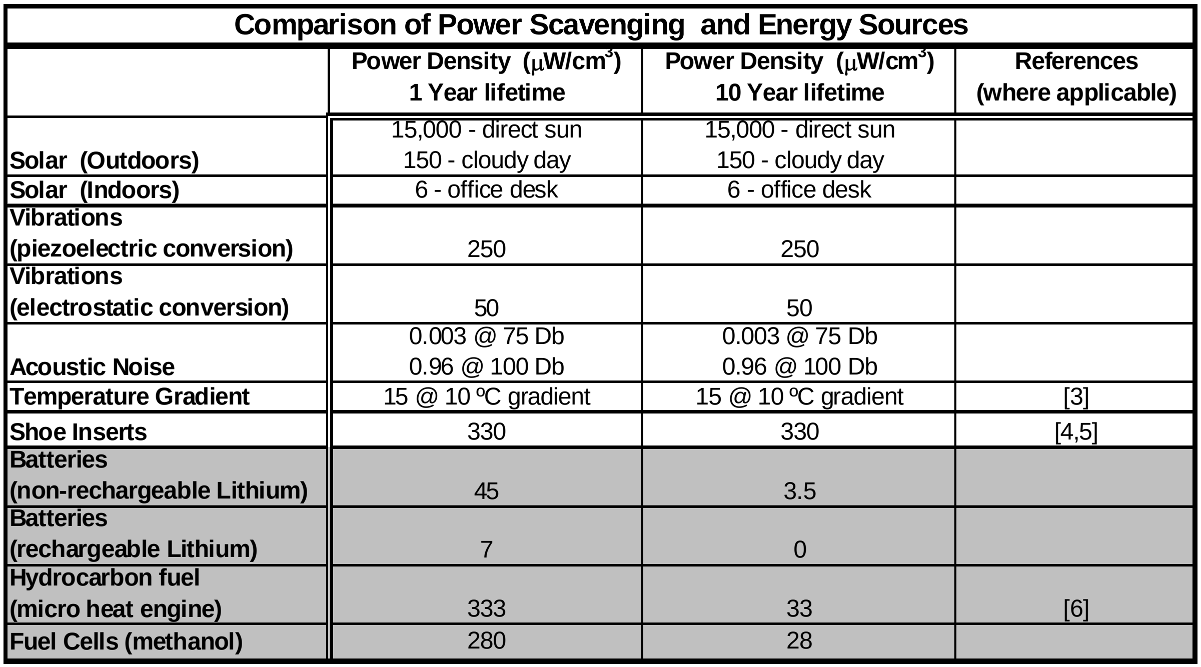

Comparison of Power Scavenging and Energy Sources			
	Power Density (μW/cm^3) 1 Year lifetime	**Power Density (μW/cm^3) 10 Year lifetime**	**References (where applicable)**
Solar (Outdoors)	15,000 - direct sun 150 - cloudy day	15,000 - direct sun 150 - cloudy day	
Solar (Indoors)	6 - office desk	6 - office desk	
Vibrations (piezoelectric conversion)	250	250	
Vibrations (electrostatic conversion)	50	50	
Acoustic Noise	0.003 @ 75 Db 0.96 @ 100 Db	0.003 @ 75 Db 0.96 @ 100 Db	
Temperature Gradient	15 @ 10 ºC gradient	15 @ 10 ºC gradient	[3]
Shoe Inserts	330	330	[4,5]
Batteries (non-rechargeable Lithium)	45	3.5	
Batteries (rechargeable Lithium)	7	0	
Hydrocarbon fuel (micro heat engine)	333	33	[6]
Fuel Cells (methanol)	280	28	

Table 1: Comparison of Power Scavenging and Energy Sources
The top part of the table contains source with a fixed level of power generation;
the bottom part of the table contains sources with a fixed amount of energy storage.

APPENDIX K: PRICE SIGNAL SIMULATION – PRICE GENERATOR

\

Xue Chen

Motivation:

In order to evaluate the performance of thermostat control strategy, which responses electrical price signals, we have done lots of computer simulation. The simulation simulates the whole process of demand-response-enabled thermostat control, which includes the simulation of the house, the residents, the weather and the utility price signals. Price Generator is such a tool to simulate the price signals sent by a utility company, such as PG&E and South California Edison. It simulates two types of price signals: time-of-use rate with critical-peak price, dynamic four-level rate. Controller's responses to these two price policies are evaluated by simulation.

Let me give two definitions first. These two rates are the outputs of price generator.

Static Time-of-Use Rate with Dynamic Critical-Peak-Price (TOU with CPP)

Fixed rate that changes seasonally for low, medium and high time periods with an additional "Critical Peak" price (CPP), which is dispatched during medium and high periods, with several hours advance notice for a maximum of 50 hours per year.

Dynamic Four-Level Rate

Non-fixed low, medium, high and critical peak time periods, with several hours advance notice.

Procedures:

Price generator develops a model to generate price signals, which based on meteorology, in particular, temperature, and some randomly-generated events. By statistical data, we found temperature and electricity usage and electricity price have some relationship. Therefore, a model is developed to simulate price signals given temperature information with random events. Randomly-generated events simulate the emergency cases of short-of-energy, such as equipments failure. To be noticed that we are not attempting to replicate utility pricing procedures. In reality, utility pricing procedures is much more complex. Our goal is to use a simple model to simulate these complex procedures and to produce a reasonable-looking price pattern for us to evaluate thermostat control strategy.

Price generator generates price signals in four procedures. First, simulate the nonlinear relationship between temperature and electricity loads. Statistical data of California power exchange wholesale electrical power prices (Figure 1) is used as references. Second, generate some random events to simulate the shortage of electricity supply. Third, define different policies to generate retail price. At last, set the parameters of time ahead when price arrives.

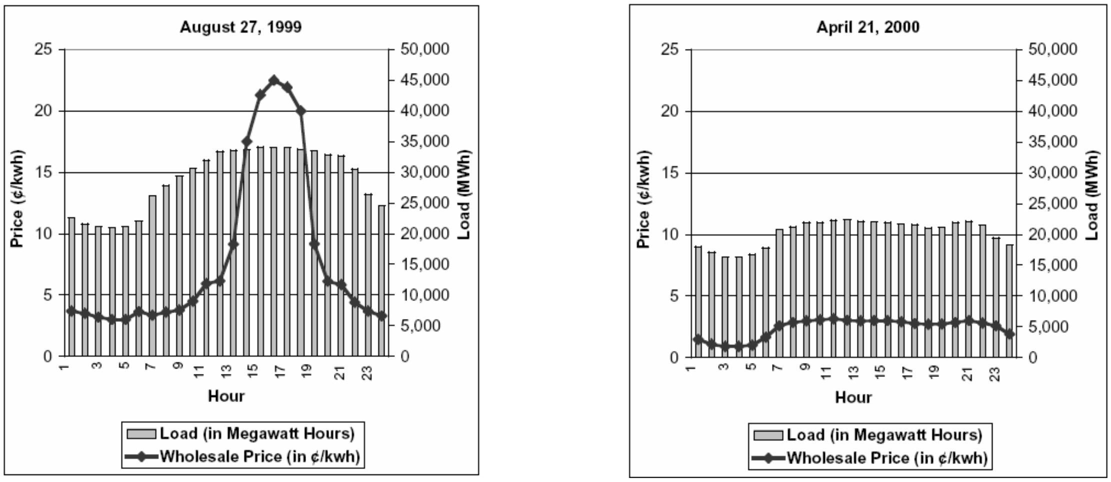

Figure 1: California power exchange wholesale electrical power prices

The following is the details of price generator simulation.

1. Simulate the nonlinear relationship between temperature and electricity loads. Because electricity load varies across season, different models are set for different seasons. The following plots are relations of temperature and load. I set two simple models for summer and spring/autumn/winter.

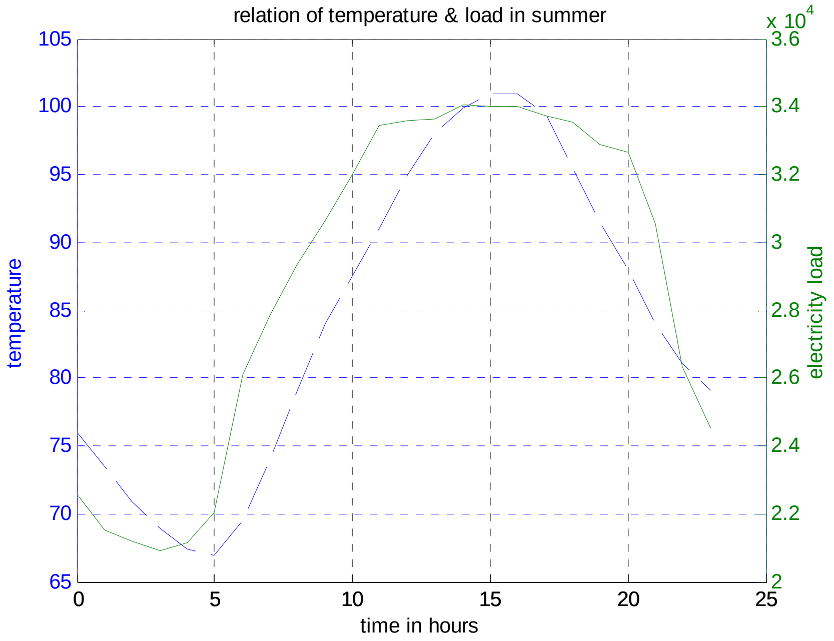

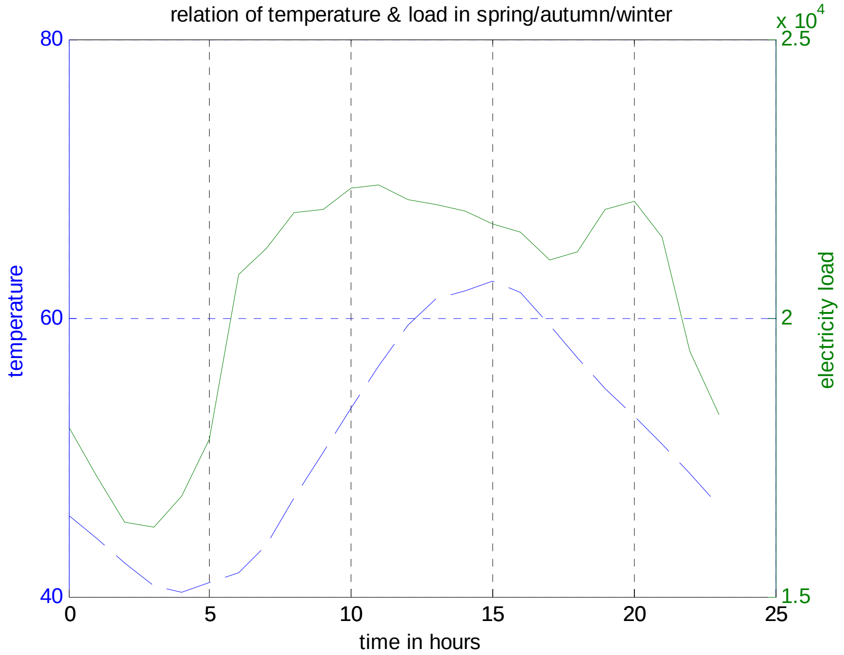

2. Generate electricity supply signals. The percentage of power capacity is used to demonstrate the actual supply. The randomly-generated negative impulses represent the electricity shortage because of equipment maintenance, malfunction or other situations that interrupt the supply. These interruptions might happen on schedule or unexpectedly. The supply signal changes every 30 minutes.

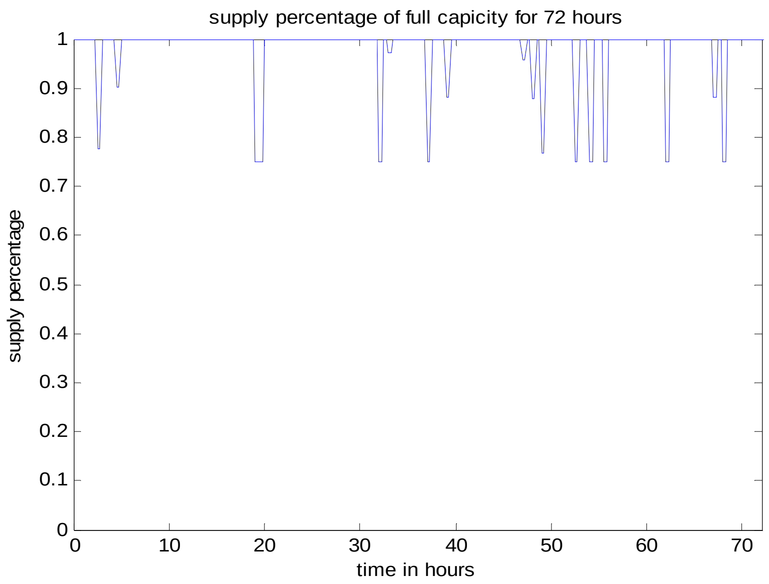

3. Generate wholesale spot price of electricity. From the ratio of electricity demand and supply, the wholesale price can be generated. The following plot shows a five day simulation. The light blue line is supply, the deep blue line is load and the black line is the wholesale price.

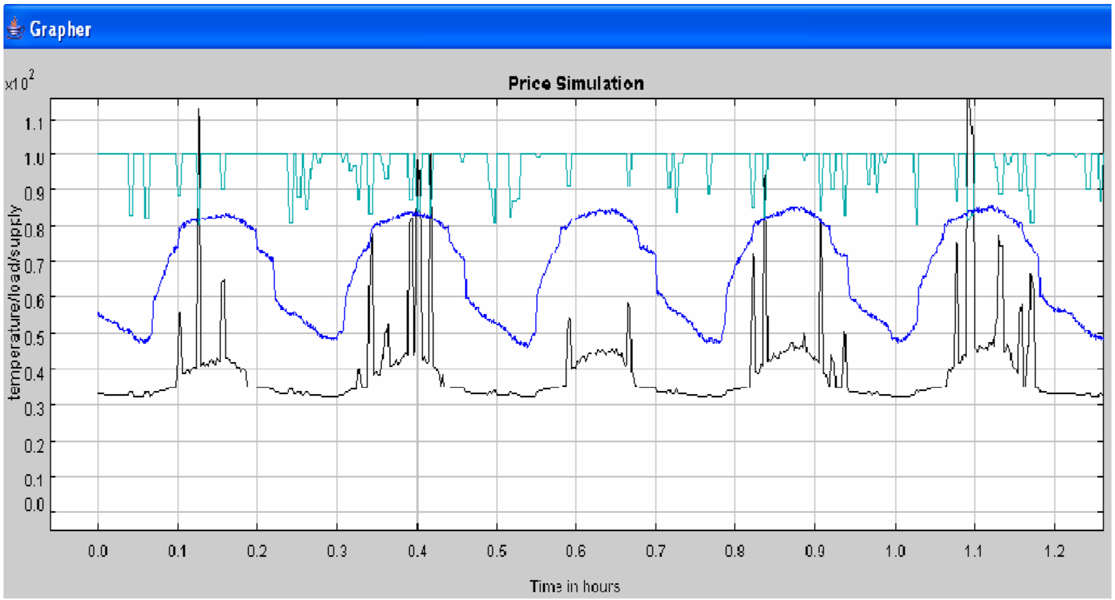

4. Define retail price policies and generate retail price signals. From this wholesale electrical power price, we can set any kind of policy to generate the retail price.

Dynamic four-level rate: set different thresholds for low, medium, high and critical price and generate discrete prices. (Below figure, green line)

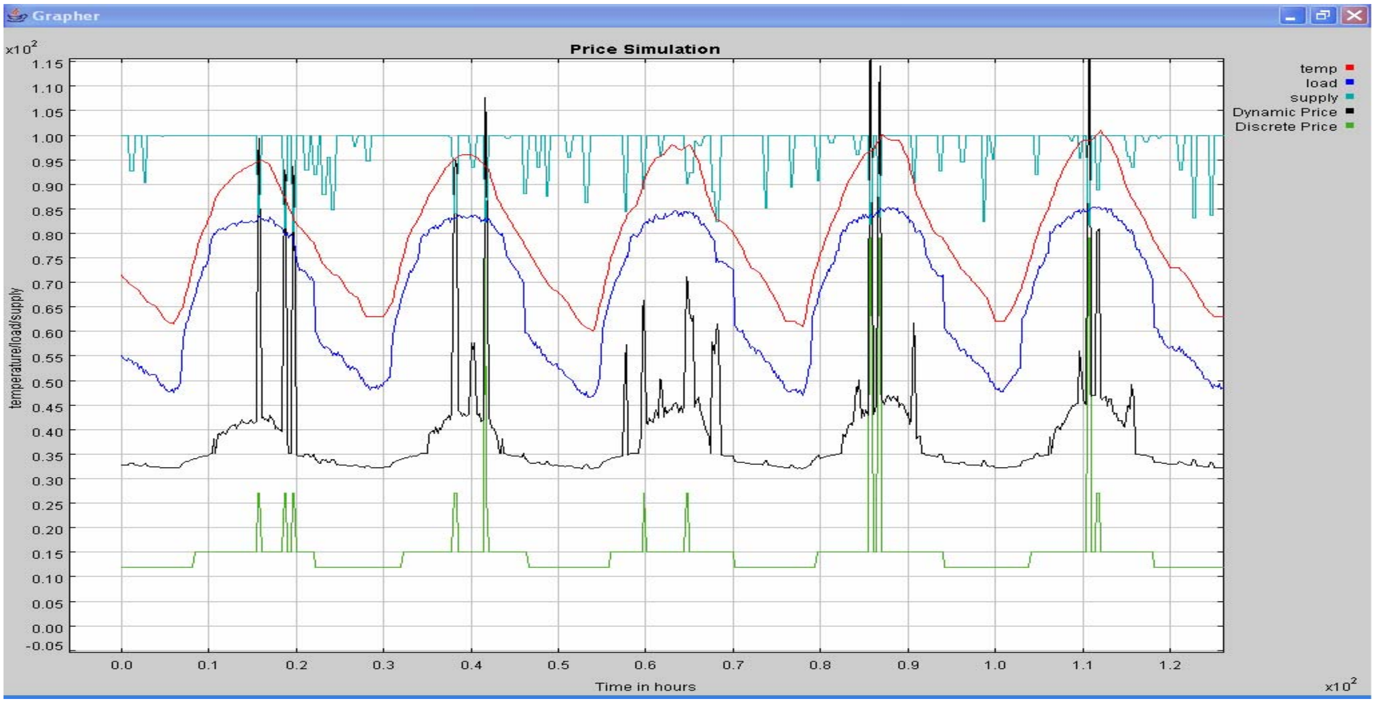

Time-of-use rate with critical-peak price: Based on time of use (TOU) schedule, additional critical peak price is generated from the wholesale dynamic prices. Set fixed rate that changes seasonally for low, medium and high time periods; when the wholesale dynamic price is bigger than a threshold, "Critical Peak" price happens.

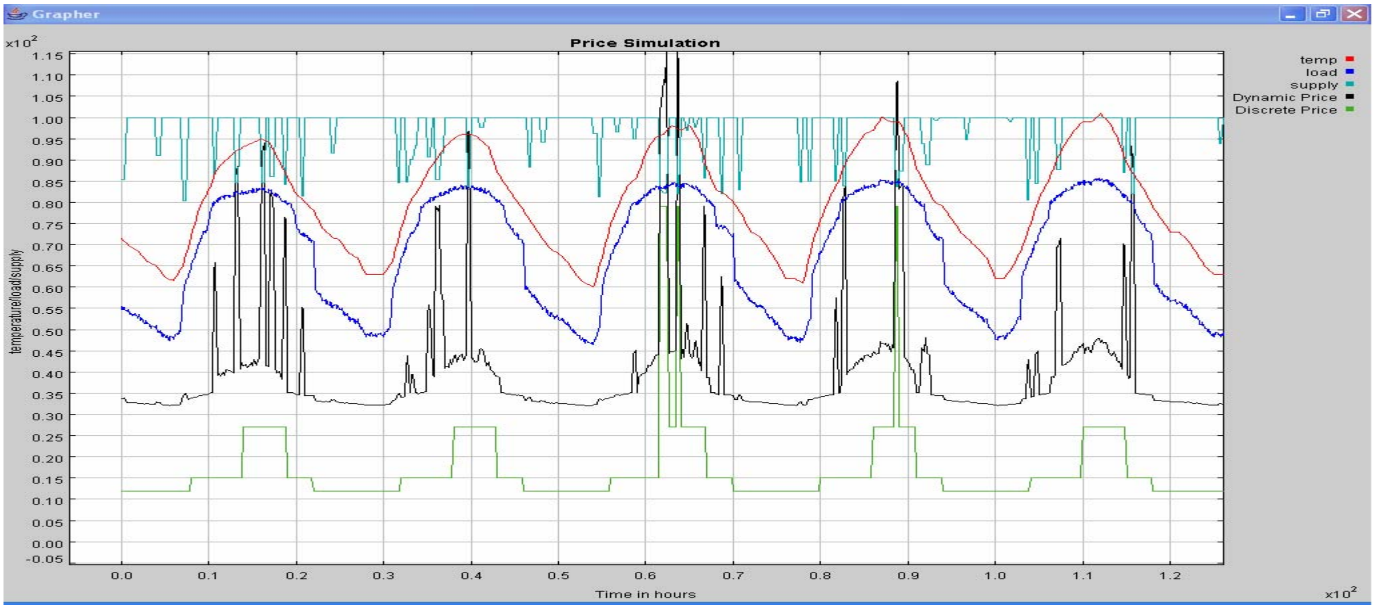

5. Flexible notification time for price. The notification time (ranging from one hour ahead to one day ahead) can set and the control strategy tested for different settings

Application:

Price generator has been used from last spring. It has been tested with both a house model MZEST and the on-site testing (at a real house). It generates reasonable electricity price signals successfully.

For simulation with house model MZEST, in order to compare different control strategies, an identical weather and price time sequence should be used. Price generator is able to generate identical time sequences given identical weather inputs without losing randomly-generate-events functions. (With the same weather inputs, price generator generates the same random sequences.)

Last summer, we fed price sequences generated by price generator into the test house to examine the response of the real house. The price is based on hourly weather data forecasted one-day-ahead by weather station.

APPENDIX L: EXPERIENCES WITH WIRELESS SENSOR NETWORK PERFORMANCE IN RESIDENTIAL ENVIRONMENTS

Nathan Ota Paul Wright

Center for Information Technology Research in the Interest of Society

Department of Mechanical Engineering
University of California, Berkeley
Berkeley, CA 94720
{nota,pwright}@kingkong.me.berkeley.edu

ABSTRACT

This Appendix reports on packet-level performance of 2.4GHz Telos wireless sensor nodes in residential environments. The objective is to characterize the packet loss to determine the necessity of mesh networking for residential wireless sensor networks. The results describe two experiments consisting of deployments in four residential houses. The data show the majority of links in a residential house have no loss. The minority of lossy links typically exhibit short bursts of loss lasting from a few seconds to a few minutes. Asymmetrical links exist in all houses and account for 17% of lossy links. Multiple link loss account for approximately one-quarter of all losses and typically extend across multiple rooms. Lastly, this paper discusses the relevance of the data to application engineers and experiential lessons in performing long-term deployments for network characterization.

General Terms

Measurement, Performance, Reliability, Experimentation.

INTRODUCTION

The application of wireless sensor networks to residential environments is an area of significant research and commercial interest. Application domains include energy management [5], health care [1], productivity [2], and safety [4]. Application engineers require knowledge about the capabilities and weakness of any component in a system, including a wireless sensor network. However, a lack of understanding exists about actual wireless sensor network performance in residential environments.

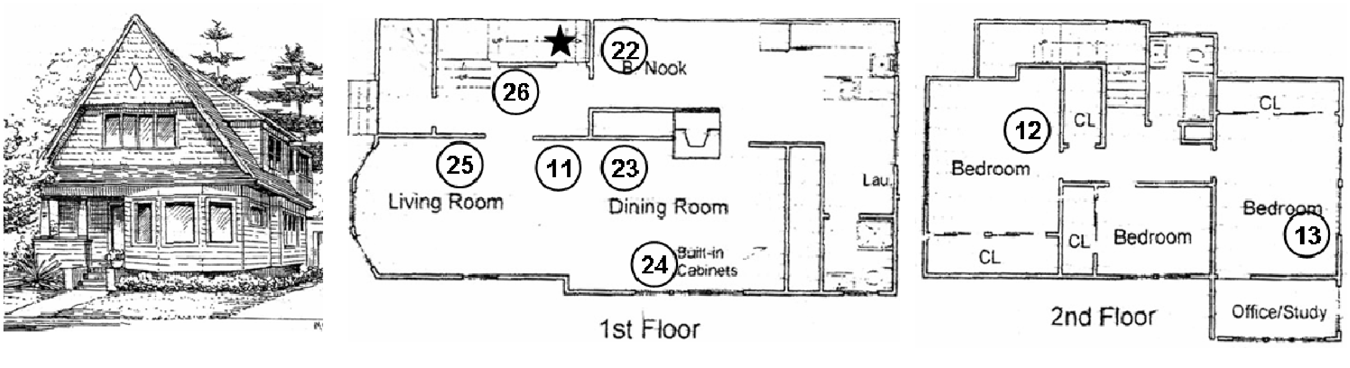

Figure 14: 1500 sq. ft. 1910's two-story house with wood frame construction and dry wall interiors. First floor contains no doors between rooms. Bedrooms have hollow wood doors. Node ID numbers are shown in circles. The star represents the base station.

Packet-level communication performance is an accepted metric for characterizing the performance of a wireless sensor network. Packet-level performance impacts many aspects of wireless sensor network and system. Each application requires a level of reliability and connectivity from the wireless sensor network to achieve a desired application performance. Medium access protocols may require retransmissions to overcome packet corruption. Mesh routing protocols endure retransmissions transmissions to handle unreliable links. Undesirable consequences include excessive latency, inefficient bandwidth consumption, and unneeded energy consumption by a node.

Previous research has shown the environmental specific characteristics of various low-power radios implemented by wireless sensor networks. [7] provides evidence of short range signal attenuation by showing a transitional zone as a function of distance from a transmitter in an outdoor controlled experiment. This attenuation creates inequality in packet transmission success among links equidistant from a common node. A second experiment of thirty nodes confirms the irregularity in an indoor academic setting. The authors propose a routing mechanism to handle the link differences, which is founded on a packet-level link quality estimator [8]. [10] provides corroborating evidence of this transitional zone effect in an office building and outdoor environments. The authors conclude the causes of these packet loss characteristics are difficult to identify although systematic methods can easily characterize the behavior. While these and other analyses [9] show general characteristics, performance in residential environments is not well documented. The application engineer is left to make high level assumptions about packet-level performance for a residential wireless sensor network.

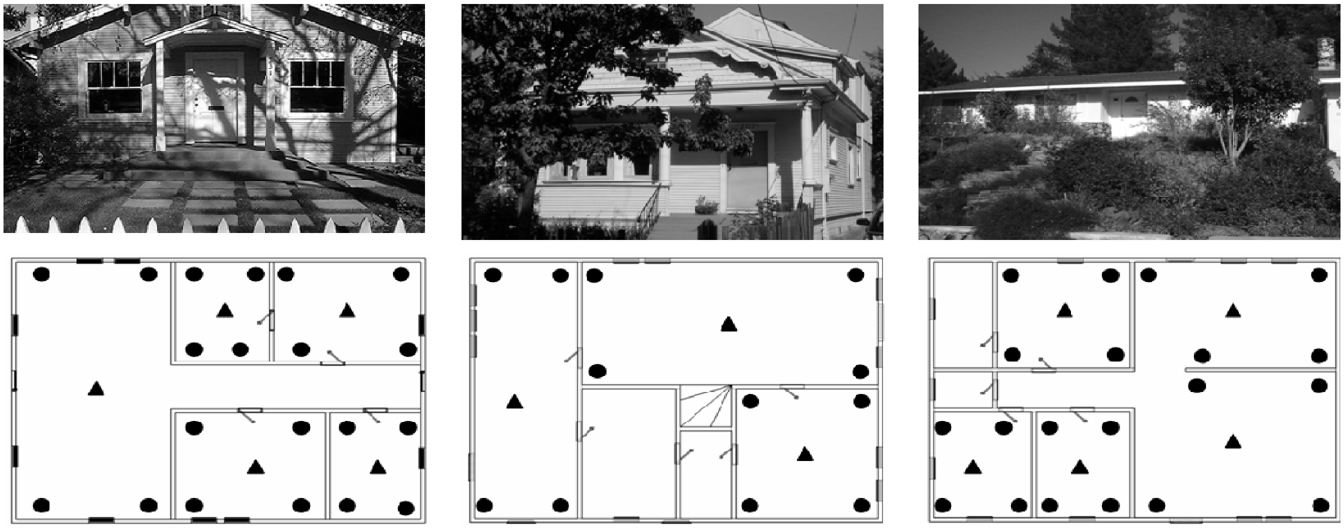

Figure 15: (Left) 1000 sq. ft. 1920's bungalow house has plastered interior walls and solid wood doors. (Middle) 1300 sq. ft. 1920's two-story house has dry wall interior walls and hollow wood doors. Second floor (not shown) is a 20'x20' bedroom. (Right) 1800 sq. ft. 1960's Ranch-style house has dry wall interior walls and hollow wood doors. All houses are wood frame construction. Floors plans are not to scale. Approximate locations are shown for beacon nodes (triangles) and listener nodes (circles).

In this paper, we report on two field experiments of 2.4 GHz Telos motes in four different houses. The objective was to characterize the packet loss characteristics to determine the the necessity of multi-hop and mesh networking. Section 2 describes the experimental procedures, setup, and test houses. Section 3 presents the data from the experiments and analysis of aggregate packet loss, symmetry, packet loss events. Section 4 discusses the relevance of the packet-level analysis to application engineers. Lastly, Section 5 concludes with a summary of findings.

EXPERIMENTAL PROCEEDURE

Two experiments were conducted to examine packet losses in a network of 2.4 GHz Telos motes [6] with the standard printed circuit board antenna. We used TinyOS (release 1.1.x) [3] with 0dBm transmit power. No casings were used. All nodes were located at approximately waist level and in-plane with the floor with the circuit board facing up.

The first experiment examined controlled environments in three different houses: a bungalow, a two-story, and a Ranch-style house (see Figure 15). Each room contained one node near the center of the room and a node in each room corner. Each node that was located in the center of a room was tested as a beacon. In round-robin fashion, one beacon node at a time transmitted 1800 sequentially numbered packets at 10 packets per second. All other nodes, including the other beacons, recorded the sequence number of each packet and then recorded missing sequence numbers. After each beacon node transmitted 1800 packets, the log of missing packets was downloaded from each node using generally available TinyOS tools. Houses were tested with all the doors open and then with all the doors closed. Only three test personnel were present inside the houses during testing.

The second experiment examined an uncontrolled and occupied two-story house for approximately two weeks. Eight nodes were placed throughout the house (see Figure 14). The nodes transmitted sensor readings once per minute and implemented a CSMA medium access protocol without multi-hopping. The base station node connected to an internet-connected personal computer that was located in a closet below the staircase. A Java application, that utilized SerialForwarder, logged data to a remote database in real-time. The Java application time stamped each incoming packet upon reception of the message event, prior to uploading the message to the database.

RESULTS

The experiments produced results for aggregate packet loss, contiguous packet loss events, separation between contiguous packet loss events, spatial loss characteristics, multiple link loss characteristics, and link symmetry. A*ggregate packet loss* is the percentage of total transmitted packets that are not received. *Contiguous packet loss events* and separation between events are measured as the count of consecutively numbered packets. *Spatial packet loss* is the number of rooms in which at least one node fails to receive a transmission. *Multiple link loss* is the number of links that fail to receive a transmission. *Link symmetry* is the ratio of aggregate packet loss between each direction of a bi-directional link.

Data from the first experiment provides high resolution, short duration "snapshots" of packet level communication performance. Figure 16 shows the raw packet losses on each link in the bungalow house for both open and closed door conditions. Note the data is normalized from actual time to packet time since multiple round-robin transmission sessions are shown. High-loss links appear as solid vertical lines, while patterns of multiple link loss are visible as horizontal sections. Sporadic short losses are visible as sparsely dotted vertical lines and are common to several links. Qualitatively, however, a link does not always appear to become more lossy under closed door conditions.

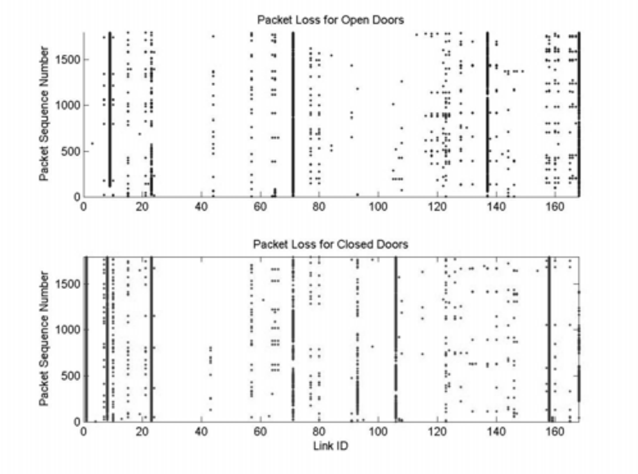

Figure 16: Packet losses for individual links in the bungalow house during open door (top) and close door (bottom) conditions. A dot represents a missing packet.

In the first experiment, aggregate packet loss per link ranges from zero to nearly 100%. Figure 17 shows cumulative distribution of overall aggregate packet loss for each house. The majority of links, ranging between 75% and 92% of all links per house, have no packet loss. A significant number of links, between 3.5% and 21% of all links per house, have packet loss less than ten percent. Relatively few links, ranging between 2% and 5% of all links per house, have packet loss greater than 10%. Aggregate packet loss in closed door conditions is greater than that with open door conditions for each house. Aggregate packet loss in the bungalow, two-story, and ranch house increases by 11%, 45%, and 61%, respectively, under closed door conditions. The data also show that intra-room links have no loss. The majority of loss occurs in the corner of each room. At least one beacon node in each house has zero-loss communication to and from all other beacon nodes.

The average size of a contiguous packet loss event is 5.6 packets in open door conditions and 6.9 packets in closed door conditions. And although the mean standard deviation is 11% greater with closed door conditions, the coefficients of variance are 0.21 and 0.23 for open and closed door conditions, respectively. The data also show insignificant difference between hollow door and solid door environments. The separation between contiguous loss events ranged from 1 to 1800 packets in length. Figure 5 shows for each link the number of packet loss events, the mean magnitude of packet loss events in packets per event, and the mean separation between packet loss events measured in packets. The majority of lossy links appear near the origin; these links have a few short packet loss events occurring over a short period of time. The time span for an average packet loss event is approximately 0.5 seconds. However, the data show packet loss events up to approximately 200 packets in length or 20 seconds. The correlation between increasing overall packet loss across a link and the magnitude of the packet loss event is positive in all houses regardless of door position. This suggests that greater aggregate packet loss results from larger events rather than more short events. However, the correlation coefficients range from +0.08 to +0.23 suggesting a weak

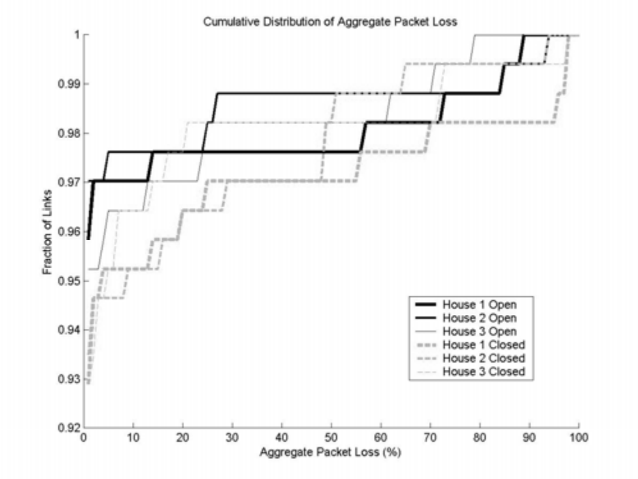

Figure 17: Cumulative distribution of aggregate packet loss per link for each house. Black lines represent open door conditions. Gray lines represent closed door conditions.

correlation. Conversely, the correlation between packet loss across a link and the separation between packet loss events is negative in all houses regardless of door position. This suggests that aggregate packet loss results from sporadic losses rather than short periods of high loss. The correlation coefficients range from -0.39 to -0.26 suggesting a weak to moderate correlation.

Multiple link losses account for 22% of all losses (see Table 1). The data do not contain a packet loss that extends across all links. These losses are typically one packet in length, except for three instances of contiguous packet loss that are two packets long.

Table 2: Statistics for link and room extent data from the first experiment. Link extent measures the number of links. Room extent measures the number of rooms.

	Mean	Max	Std
Link Extent	2.43	8	0.18
Room Extent	1.47	3	0.17

Symmetry results describe only links between sender nodes since those are the only bidirectional links. Asymmetric links cumulatively account for 17% of links throughout all houses and environments. Figure 20 shows the cumulative distribution of the degree of symmetry for all links.

In the second experiment, the data show aggregate packet loss between 1% and 20% per link (see Figure 19). Nodes 11, 23, 24, and 25 have two walls of separation from the base station, in comparison to on wall of separation for nodes 22 and 26. Node 12 is directly above the base station, and has one physical floor of separation from the base station. Node 13 has one floor and several walls of separation. This data clearly show distance with walls of separation increase packet loss. In addition, the overall average length of a packet loss event is 2.5 packets in length with a standard deviation of 12.7 packets. The actual time in minutes is equivalent to the packet length since the transmission frequency was once per minute. However, the average packet loss event magnitude, standard deviation and coefficient of variance for an individual link correlate with the aggregate packet loss for a link. Nodes 13 and 24 average 4.8 and 2.1 packets per packet loss event, respectively. In contrast, the remaining nodes average approximately one packet per event.

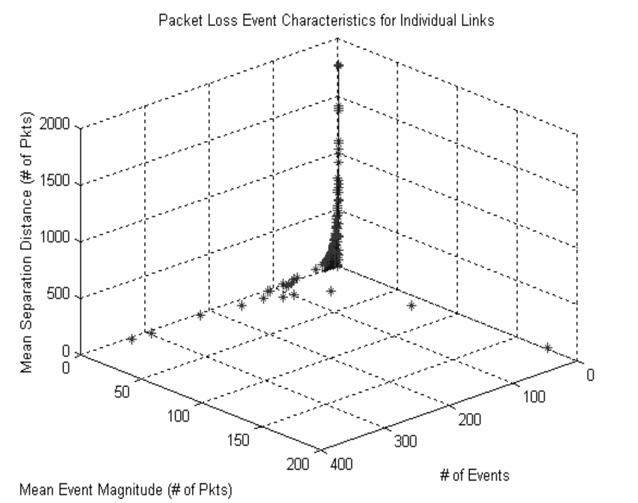

Figure 18: Packet loss event magnitude, separation between events, and total number of events for each individual link.

In the second experiment, data is serially received by the base station. Therefore, the data is aligned into one minute segments to analyze the spatial packet loss characteristics (see

Figure 21). Since the transmission rate of one packet per minute is much less than the saturation bandwidth of the channel as well as the back-off time periods for the CSMA implementation, we assume that losses are a result of reception failure. In deed, the data show a transmission pattern among the nodes supporting little to no contention for channel access.

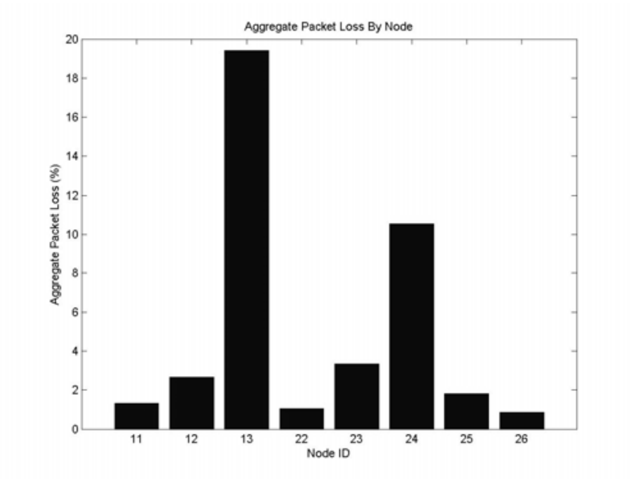

Figure 19: Aggregate packet loss for each node in the second experiment.

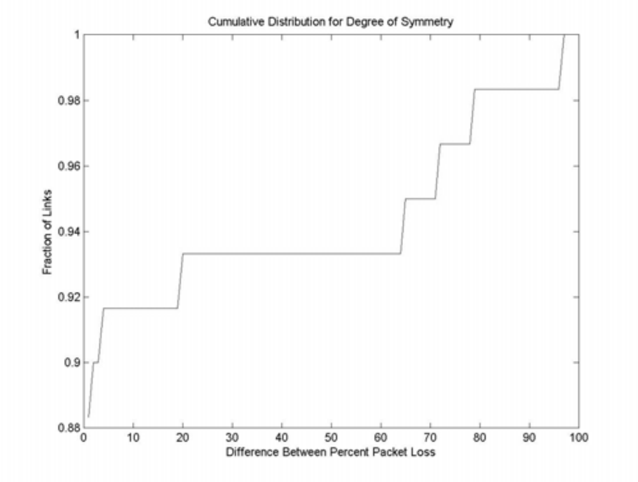

Figure 20: Cumulative distribution of the degree of symmetry. Note the range is abridged for clarity.

The base station fails to receive one or more packets in 29% of the one-minute time intervals during the deployment. Note, this loss percentage is the union of all loss events and therefore is greater than any single link. The average link extent for a packet loss is 1.1 links. Single-link losses account for 90.5% of loss events. The remaining losses occur on multiple links, where 9% are two-link loss events. Only four losses affect more than three links. In addition, approximately 8% of the multiple link losses are part of a larger contiguous single-link loss event. However, the multiple links losses are not typically contiguous. Nodes 13, 23, and 24 are present in the majority of multiple link losses.

DISCUSSION

The data present several insights for the application engineer, beyond characterization of the specific performance metrics. This section contributes a summary of the relevance of these insights. Experiential lessons supplement the quantitative metrics and conclude the discussion.

The aggregate packet loss statistics show that a single hop network is unrealistic for complete coverage in a residential setting. The data supports the necessity of multi-hop networking. However, the data is not conclusive regarding the necessity of mesh networking. A cluster-based tree architecture is one alternative to mesh networking where every node is a router. In fact, the first experiment tests this scenario in that each receiving node is a potential cluster head. The data does support clusters as an option because no loss occurs on intra-room links and at least one sender has no loss to a sender in each of the other rooms.

The correlations between aggregate packet loss of a link and packet loss event characteristics describe the "burstiness" of packet loss. Often times the latency is more directly applicable to application design, such as those in the introduction. Relating the time span of a packet event bridges this information gap. In summary, the time span of a packet loss event ranges approximately 0.5 seconds to several minutes. In this perspective, the application engineer can better understand the implications on system performance where the wireless sensor network is simply, and appropriately, a component.

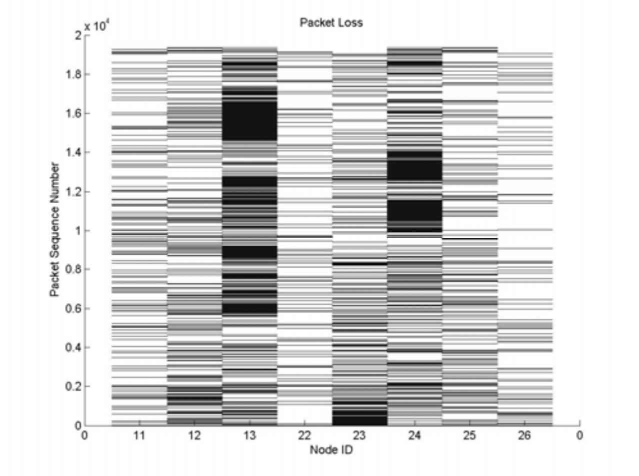

Figure 21: Packet loss events for time-aligned data from the second experiment. Each short horizontal black line represents a missing packet.

Packet loss extends across links and rooms. For the application engineer, this will create voids in a house-wide "snapshot" without acknowledgement-based measures. But, contiguous multiple link and room losses are atypical. As such, correlation with similar current and historical data may be sufficient to estimate missing data and eliminate the need for energy-intensive packet retransmissions. As well, the prominence of asymmetric links requires the application engineer to head latency and energy consumption imbalances.

In obtaining the data through field deployments, rather than simulations, several lessons emerge in retrospect. First, power management is necessary for long-term unattended deployments. The second experiment was preceded by a trial deployment without power management in which batteries were depleted within a week. Radio transmission requires sufficient power resources, without which results in transmission failure. Second, remote system recovery capability is necessary to handle non-network related faults. Error handling should include recovery from power loss and managing multi-user scenarios. Specifically, the local Java application shutdowns when a different user accesses the host personal computer. As well, the generally available SerialForwarder terminates all clients when an exception occurs, resulting in a single point of failure for third party applications. Third, local appliances and devices may have an effect on transmission. In the first experiment, a small sub-experiment confirmed cordless phones significantly impair packet-level communication when the operating frequencies are the same. During the first experiment, the cordless phones were disabled. However, during the longer second experiment, interference from a cordless phone is a systematic challenge and is difficult to identify. Typical loss appears as heavy packet loss when the phone rings and moderate loss during the conversation. Lastly, long-term testing applications should implement a buffer, although the generally available TinyOS distribution (specifically TOSBase) does include a small buffer. In our experience, an unmanaged flow of incoming packets may be blocked by lengthy internet communication to the remote database.

CONCLUSION

In conclusion, experimental data from deployments in four residential houses show the following:

- Aggregate packet loss is typically less than 10%.
- Packet loss is greater when all doors are closed.
- Packet loss events last seconds to minutes in duration.
- Packet loss events are mainly single-link, but infrequently do extend to multiple links and rooms.
- Multiple link losses are typically non-contiguous, but often occur within a continuous single-link loss event
- Asymmetry is present in 17 % of all lossy links.

ACKNOWLEDGMENTS

We gratefully acknowledge the funding (Award DR-03-01) from the California Energy Commission, CITRIS at UC Berkeley, and the Ford Lab at UC Berkeley. The authors thank Will Watts.

REFERENCES

[1] Das, S. and Cook J., Health Monitoring in an Agent-Based Smart Home, Proceedings of the International Conference on Smart Homes and Health Telematics, September, 2004.

[2] Hanssens, N., Kulkarni, A., Tuchinda, R. and Horton, T. Building Agent-Based Intelligent Workspaces. ABA, 2002.

[3] Hill, J., R.Szewczyk, A.Woo, S.Hollar, D.Culler,and K.Pister, "System architecture directions for networked sensors", 9th International Conf. on Architectural Support for Programming Languages and Operating Systems, 2000.

[4] Kottapalli, V. A., et al., "Two-Tiered Wireless Sensor Network Architecture for Structural Health Monitoring", SPIE 10th Annual International Symposium on Smart Structures and Materials, San Diego, CA, March 2003.

[5] Mozer, M., Jordan, M., Petsche, T., "The Neurothermostat: Predicitive Optimal Control of Residential Heating Systems". Adv. In Neural Info. Proc. Systems 9, 1997.

[6] Polastre, J., Szewczyk, R., Sharp, C., Culler, D., "The Mote Revolution: Low Power Wireless Sensor Network Devices". Proceedings of Hot Chips 16: August 22-24, 2004.

[7] Woo, A., T. Tong, and D. Culler, "Taming the Underlying Challenges of Reliable Multihop Routing in Sensor Networks", SensSys 2003 , CA, November 2003.

[8] Woo, A. and D. Culler, Evaluation of Efficient Link Reliability Estimators for Low-Power Wireless Networks. Technical Report, University of California, 2003.

[9] Yarvis, M. D., W. S. Connor, L. Krishnamurthy, J. Chhabra, B. Elliott., and A. Mainwairing, "Real-World Experiences with an Interactive Ad Hoc Sensor Network", Intrn'l Workshop on Ad Hoc Networking. Vancouver, B.C., 2002.

[10] Zhao, J. and R. Govindan, "Understanding Packet Delivery Performance in Dense Wireless Sensor Networks", SensSys 2003 , CA, November 200

APPENDIX M: DEMAND RESPONSE SUBMETER CONTROL OUTLET

Prototype Demand Response Submeter Control Outlet User's Guide

Xin Yang, Richard White

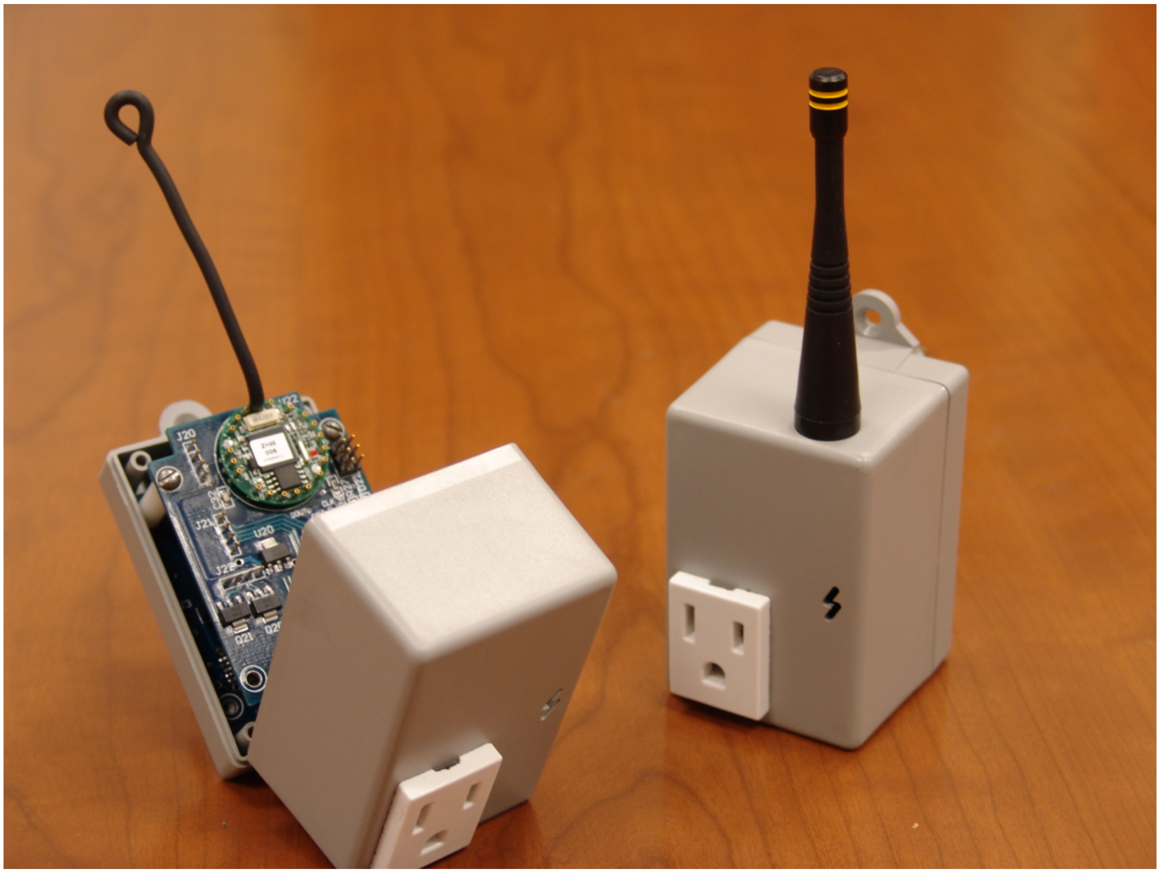

Table of Contents

1. Introduction

1.1. Overall Block Diagram

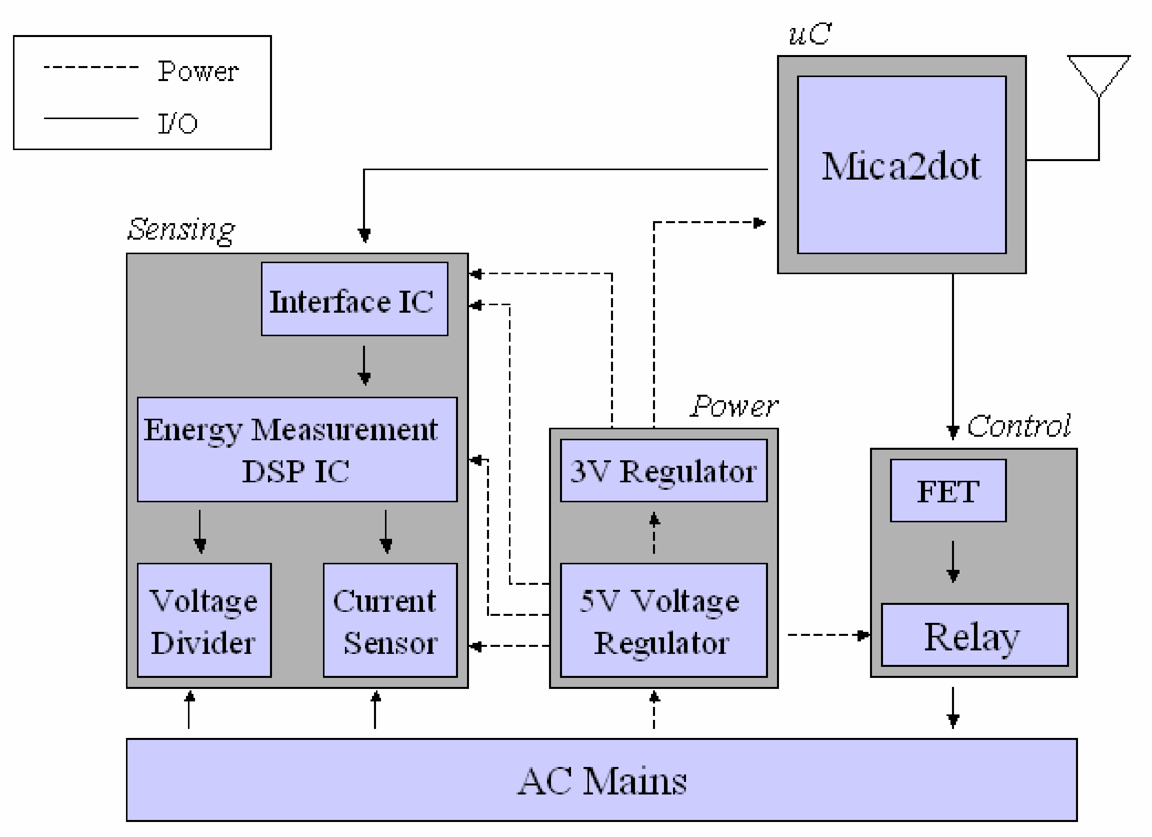

The submeter control outlet is composed of a sensing element, a control element, and a mains powered dc supply circuit all integrated with a Mica2dot wireless module. The sensing unit takes in analog voltage and current samples and calculates relevant energy values in the DSP integrated circuit. The control module consists of a FET controlled latching relay. The power module converts line voltage to a regulated 5V DC. A second 5V to 3V linear regulator is used to provide a 3V dc supply. The Mica2dot wireless module interfaces to the Sensing and Control module through GPIO pins.

1.2. WARNING

Galvanic isolation to the AC line is not provided in this circuit. Therefore, DANGEROUS VOLTAGES are present in all parts of the circuit when it is powered.

Consequently:

DO NOT USE LINE-OPERATED EQUIPMENT TO TEST THIS DEVICE! DO NOT PROGRAM THE WIRELESS MOTE WITHIN THE POWERED CIRCUIT. IT MUST BE REMOVED AND PROGRAMMED EXTERNALLY!

2. Getting Started

2.1. Accessing Hardware

Step 1:

Remove Screws From Back

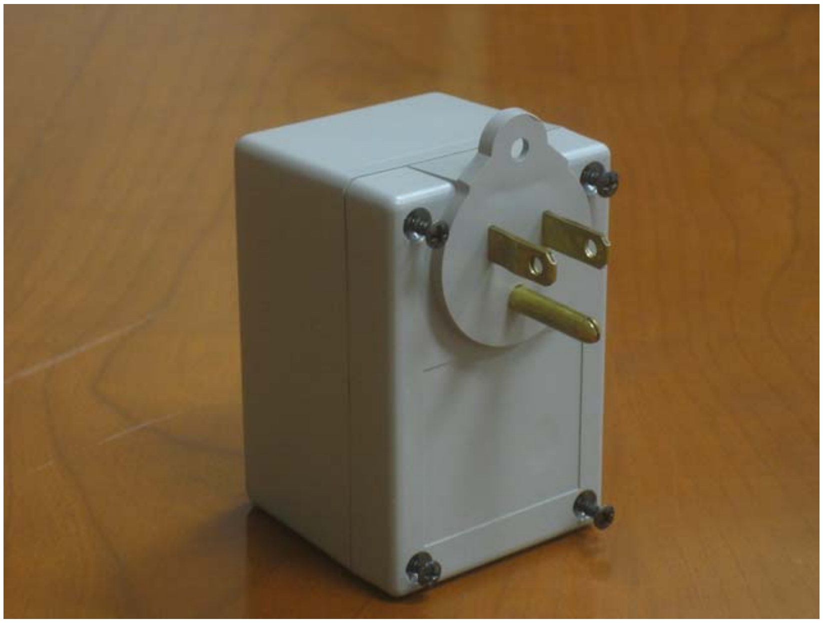

Step 2:

Open enclosure slowly in an arc. Note permanent wiring between enclosure top and enclosure bottom. These are heavy gage wires and they should not be bent too excessively.

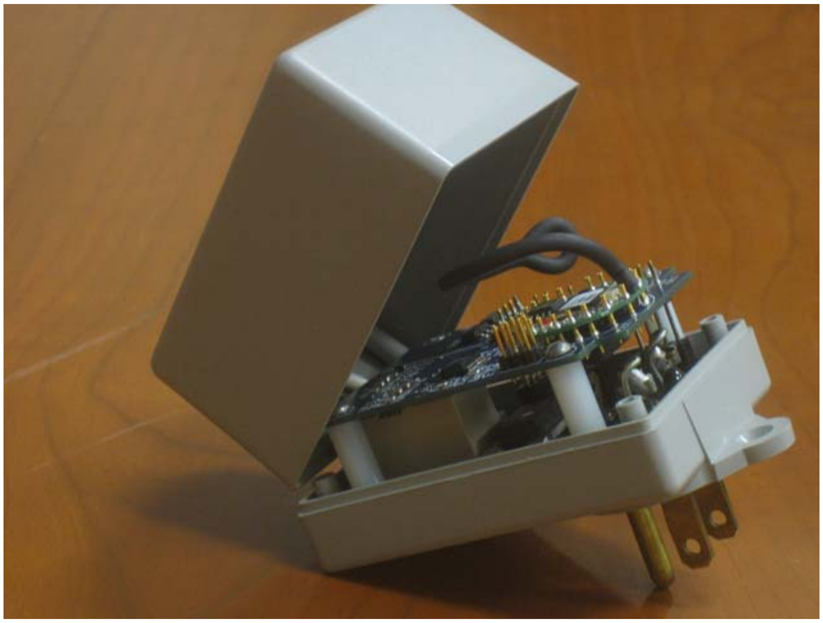

2.2. Programming

2.2.1. Source Code

Source code located in /opt/tinyos-1.x/app/XTestADE7753

2.2.2. External Programming

Do not program the mica2dot mote while the unit is powered through the AC mains. To ensure safe handling, disconnect module from AC mains first. Then extract mica2dot mote from module. Program the mica2dot externally.

2.2.3. AVR ISP

AVR ISP pins are populated on the board. However do not use these pins when the unit is powered through the AC Mains.

3. Hardware Design

3.1. Overview

The design of the submeter control outlet is separated into two boards. The lower board consists of components that need access to higher voltage AC lines. The upper board consists of low voltage elements. In addition there are also pins on the upper board designed to interface with a mica2dot mote.

3.2. Schematic

High Voltage Board

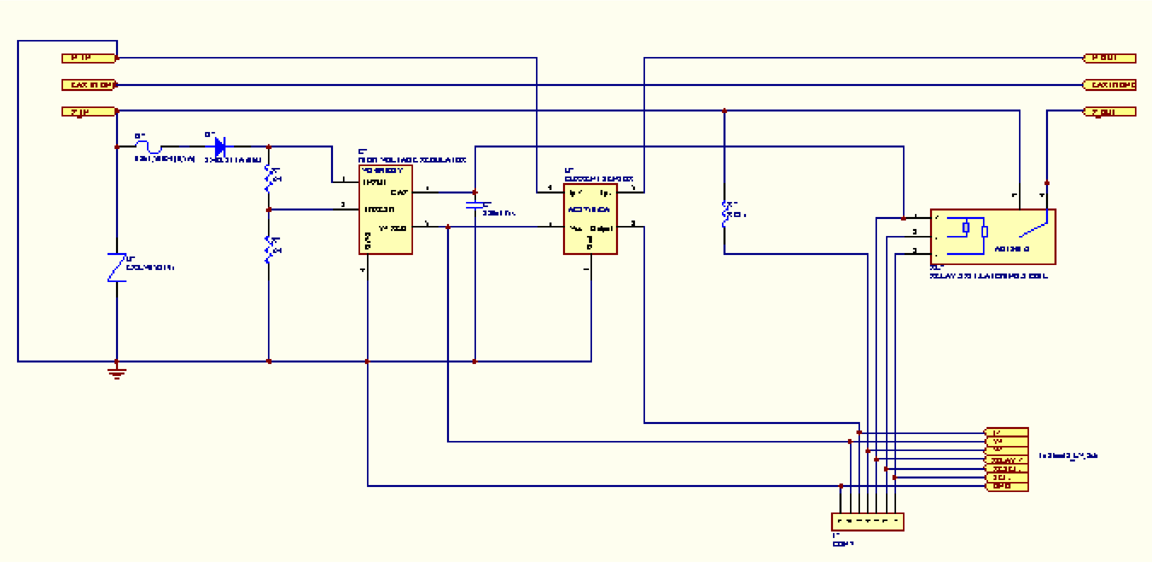

Low Voltage Board

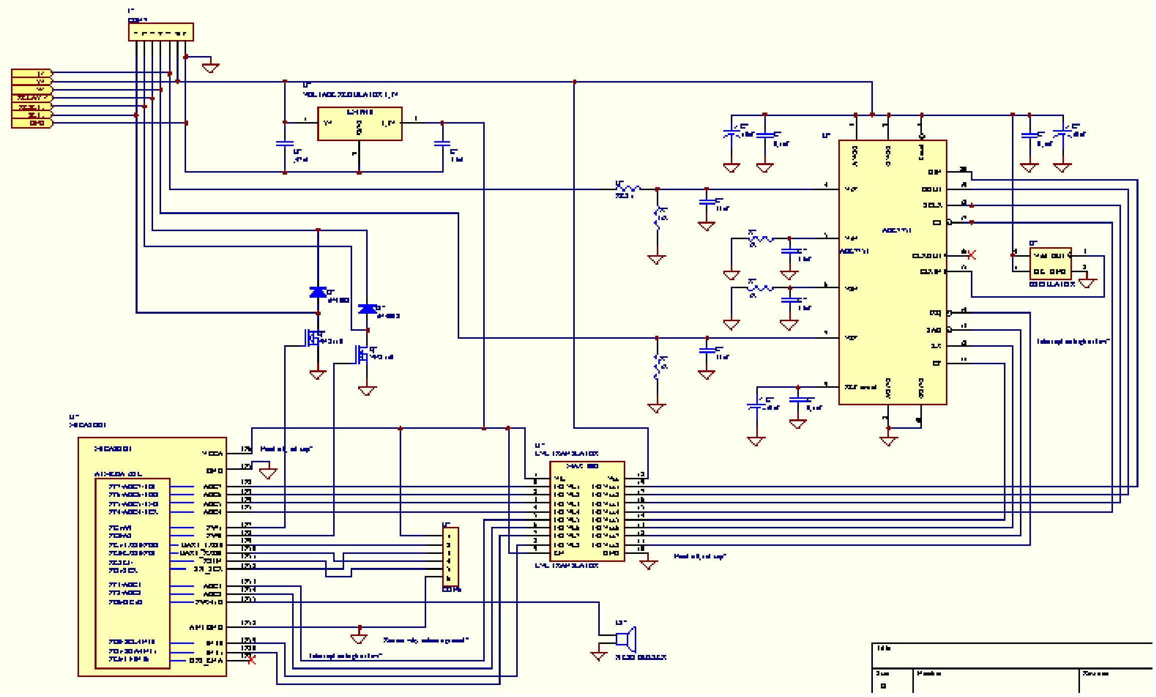

3.3. Layout

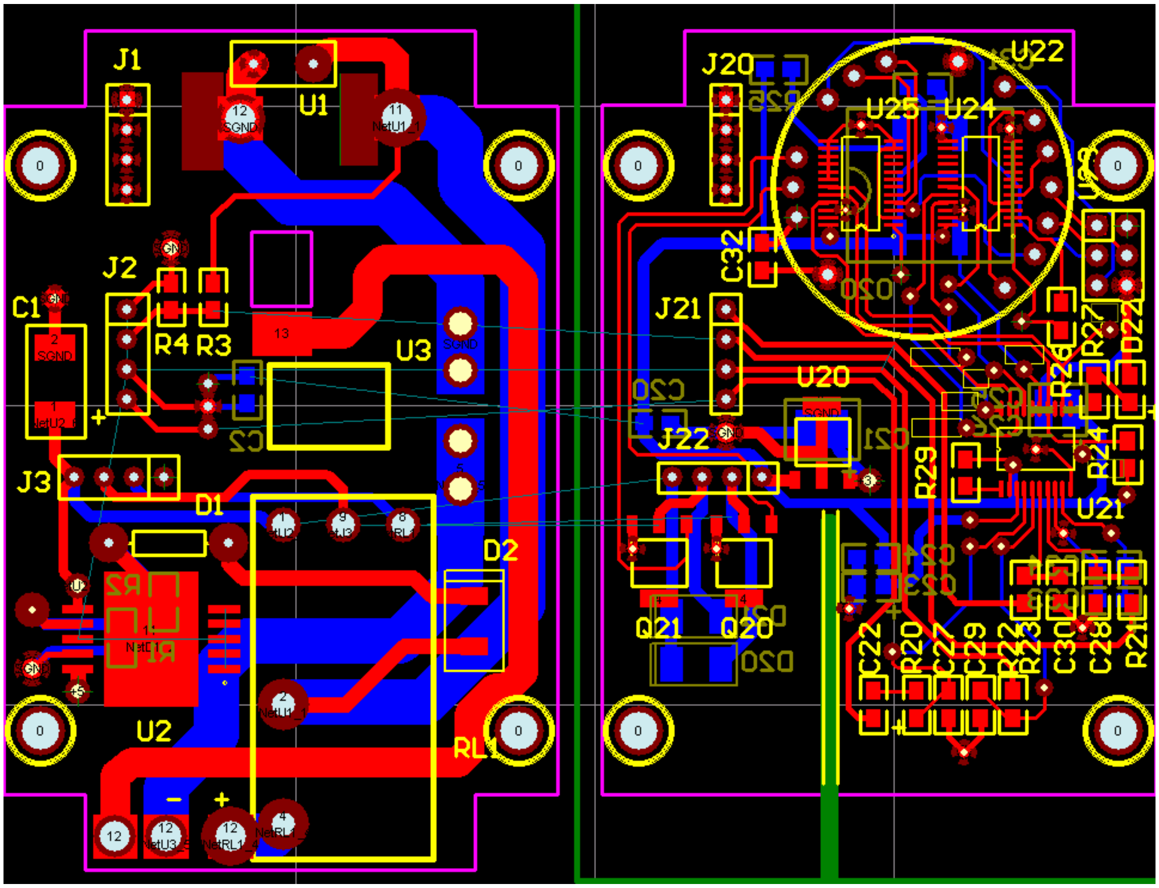
J1
U1
J2
C1
R4
R3
U3
C2
J3
D1
D2
R2
R1
U2
RL1
−
+
SGND
J20
R25
U25
U24
U22
U23
C32
J21
C20
U20
J22
C21
R29
R26
R27
D22
R24
U21
Q21
Q20
D20
C24
C23
C22
R20
C27
C29
R22
R23
C30
C28
R21

3.4. Pictures

Low Voltage Board:

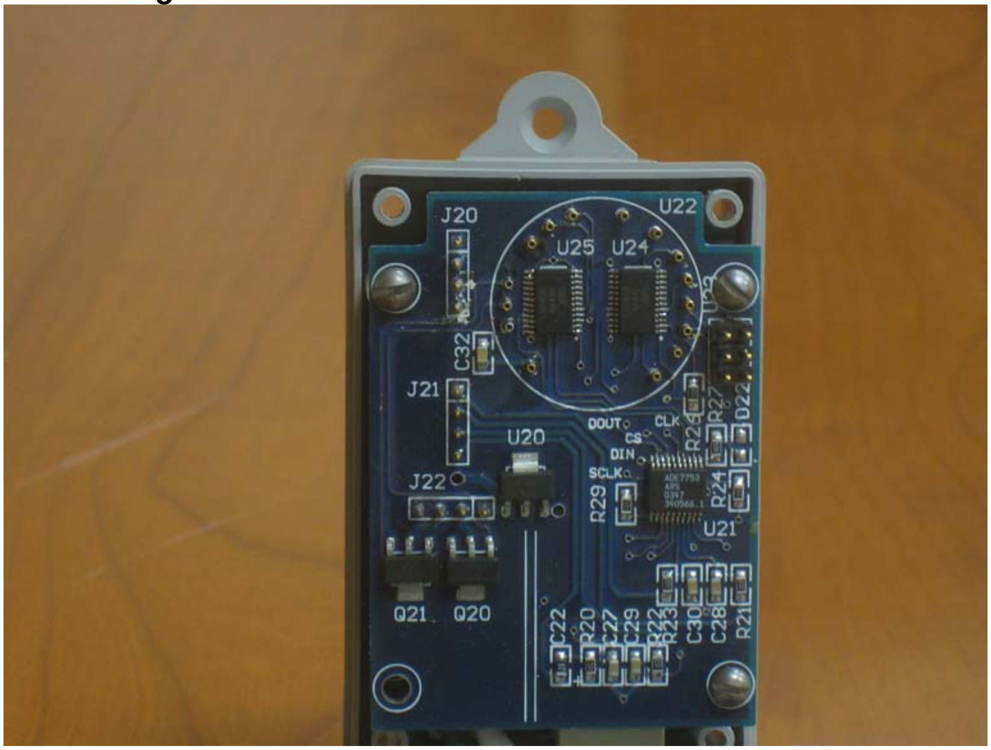

High Voltage Board:

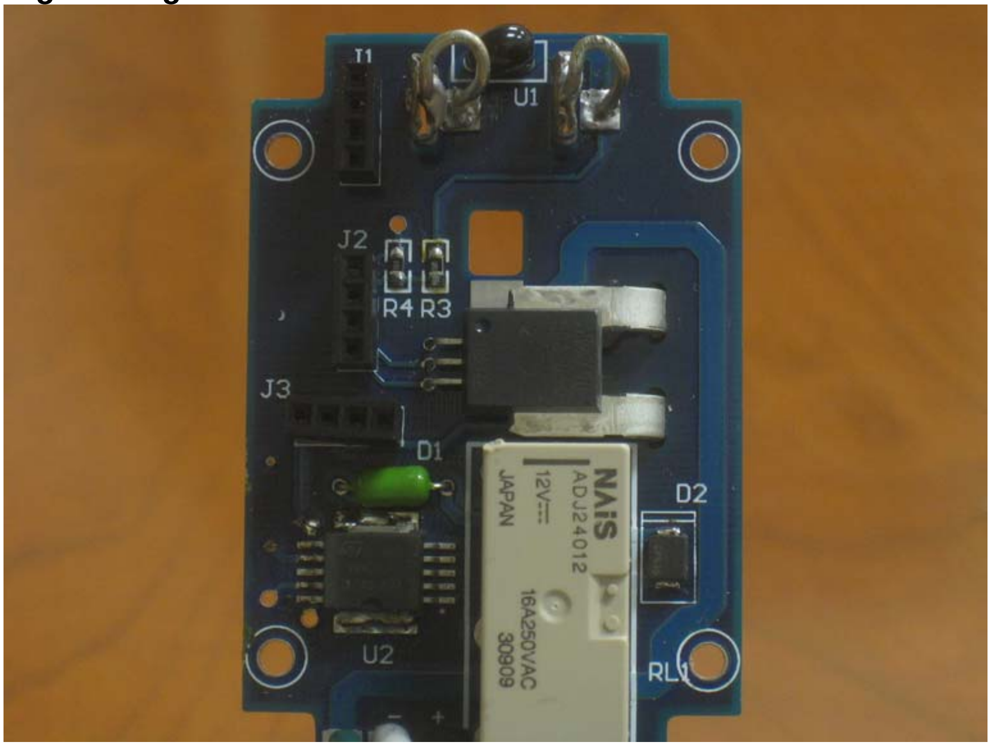

4. Software

4.1. Wiring diagram

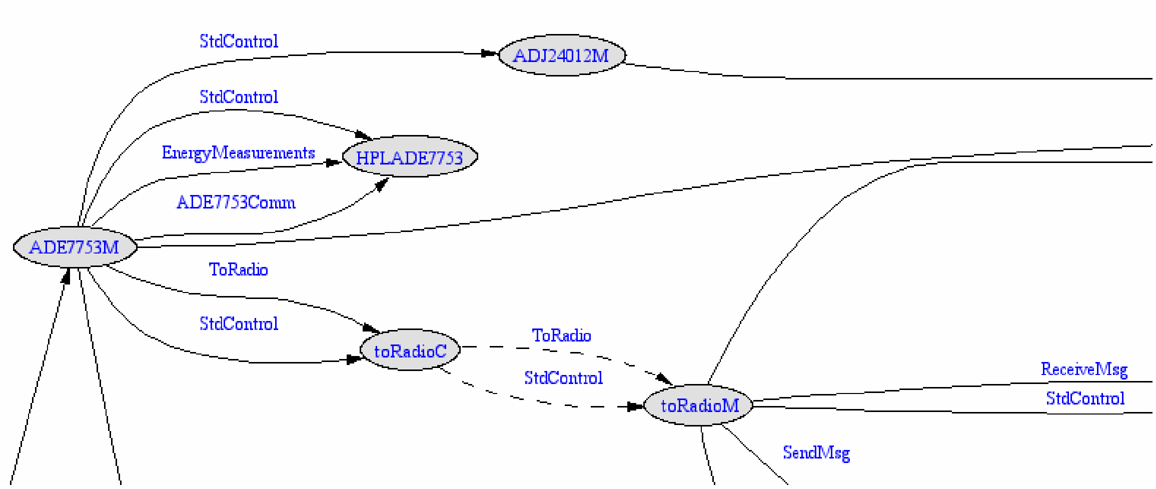

4.2. Packet structure

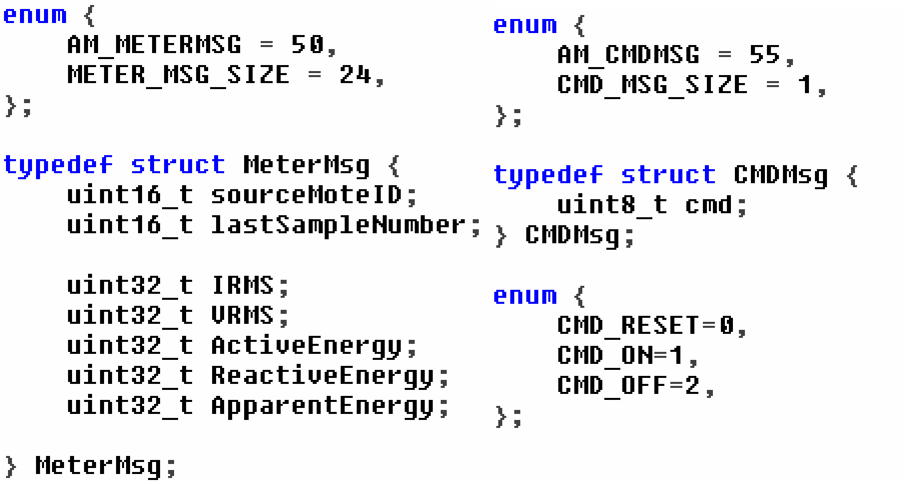

```
enum {
    AM_METERMSG = 50,
    METER_MSG_SIZE = 24,
};

typedef struct MeterMsg {
    uint16_t sourceMoteID;
    uint16_t lastSampleNumber;

    uint32_t IRMS;
    uint32_t VRMS;
    uint32_t ActiveEnergy;
    uint32_t ReactiveEnergy;
    uint32_t ApparentEnergy;

} MeterMsg;
```

```
enum {
    AM_CMDMSG = 55,
    CMD_MSG_SIZE = 1,
};

typedef struct CMDMsg {
    uint8_t cmd;
} CMDMsg;

enum {
    CMD_RESET=0,
    CMD_ON=1,
    CMD_OFF=2,
};
```

4.3. PC Side Test App

A simple test app has been written to graph the calibrated values. Currently only IRMS and VRMS are calibrated. The energy values are still in engineering units. A standard TOSBase application is needed to forward data to the serial port. The source code is located at:

/opt/tinyos-1.x/tools/java/net/tinyos/escope
/opt/tinyos-1.x/apps/TOSBase

Consult rune.sh script for starting the energy scope.

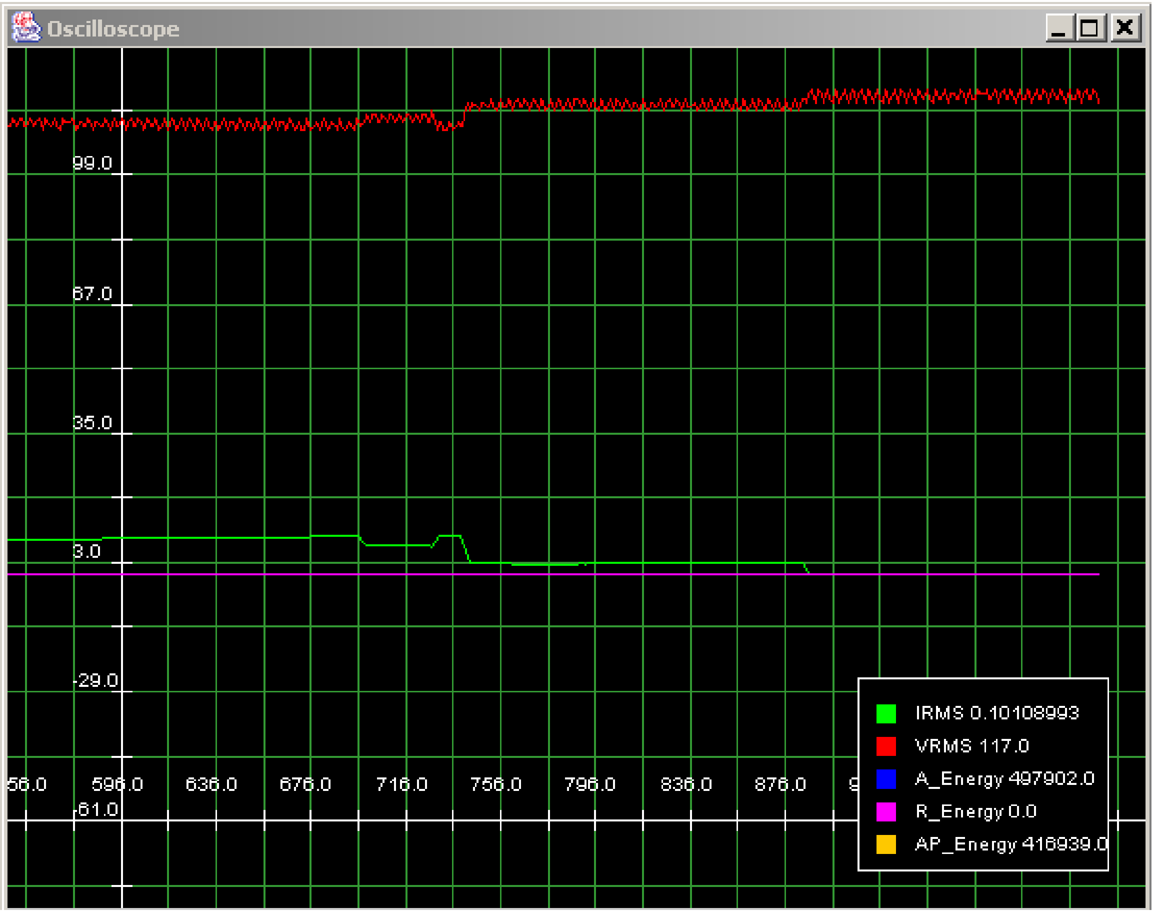

There is also a command window that will turn the relay on the outlet on and off. The default behavior of the outlet on power up is to open the relay. The reset command will software reset the power calculation IC.

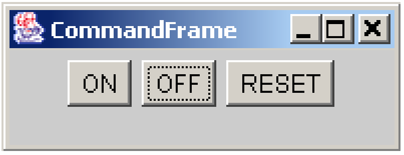

5. Calibration

A rough calibration of the IRMS and VRMS has been performed on the prototype unit. The conversion from raw ADC units to engineering units is performed PC side by the test app.

5.1. IRMS

To obtain the IRMS calibration values, six sample points were taken across 0 to 10 amps range. A linear regression is then performed on the raw ADC and current value pairs to obtain the approximation for the full range.

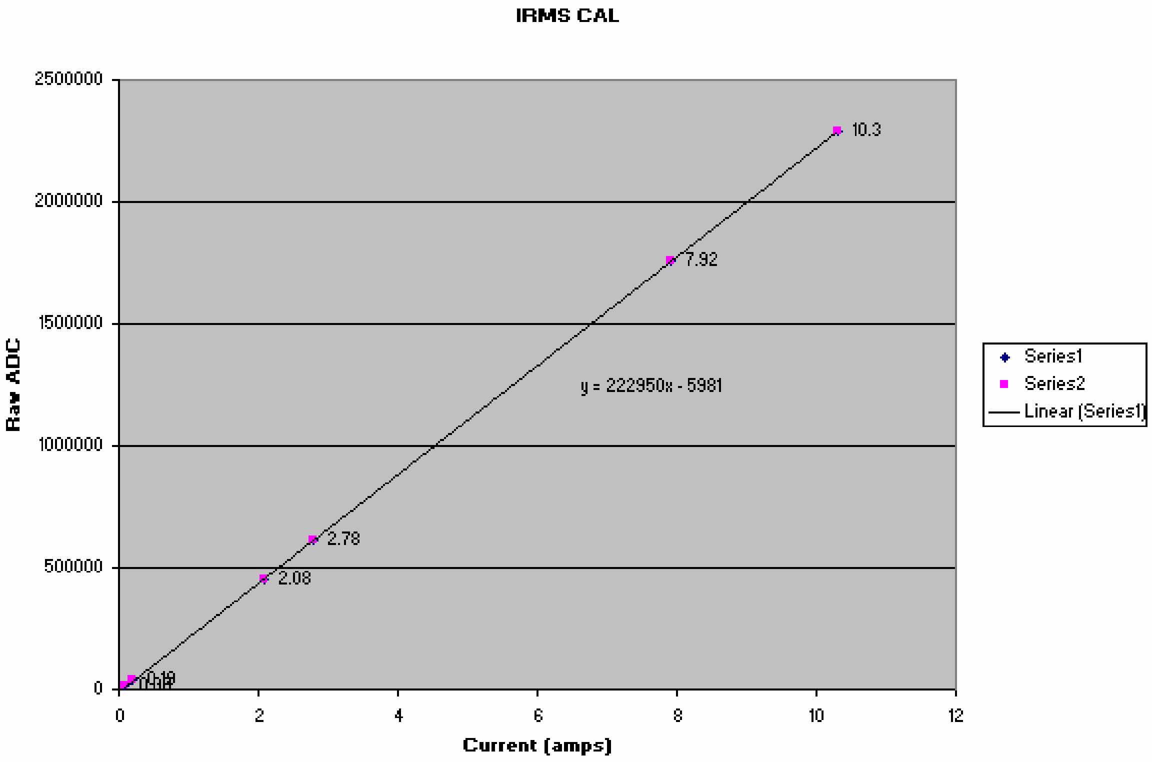

5.2. VRMS

With out the ability to generate arbitrary voltages, the calibration for VRM is done with only one data point. This ratio is then used to extrapolate the voltage value in the test app.

6. Unused features

6.1. Network wide synchronization

The designers of this unit envisioned each unit to be a part of a multi-hop network. Since each unit has line power, they have the potential to serve as a high-powered backbone. In addition, in residential environments where there is only single-phase power, the zero crossing of the 60hz power line is the same. Thus each outlet is designed to have the ability to produce interrupts on each zero crossing. This feature can be used to develop a time synchronization algorithm with very little maintenance.

APPENDIX N: STOP LIGHT NODE DOCUMENTATION

Vikas Bhargava
Electrical Engineering Department

1 Description

The Stoplight system serves primarily as an energy price indicator, lighting up three colored LEDs according to current price levels. The system can be configured as a single stoplight or a dual stoplight system. The dual stoplight system consists of two sets of colored LEDs, ideally placed on both sides of a doorway, whereas the single stoplight system consists of one set of LEDs, and is best placed on a wall.

2 Hardware Functionality

The system has one main board which connects directly to the mote's ADC outputs. The ADC I/O pins, specifically ADC0, ADC1, ADC6, ADC7, GIO2, and GIO3, control the on/off functionality of the LEDs. As seen in Figure 1, connections UART0RX and UART0TX can also be used; however they are not necessary for the stoplight system. They are available to provide extra functionality if necessary. Initial designs do not have any resistors between the ADC I/O pins and the positive terminal of the LEDs, however it is recommended 100 ohm resistance is used between each I/O pin and the LED, as the LEDs draw 20mA of current. The board shown in Figure 1 has the option available for resistor placement.

2.1 LED Board

The LEDs themselves are placed on a separate board. The LEDs are aligned in an array with a common ground. The positive terminal of all three LEDs, along with the ground signal, is then routed to the main board via external wires. The main purpose of this is to provide flexibility in the placement of the LEDs and the mote.

3 Installation

The code provided needs to be installed on the mote connected to the stoplight system and the motes communicating with the system. The motes communicating with the system will send it an integer, which then controls which LEDs turn on and off. The table below shows what integers correspond to what LEDs.

Integer	LED
1	GREEN1
2	YELLOW1
4	RED1
8	GREEN2
16	YELLOW2
32	RED2

Table 1: Integer to LED correlation

The second set of LEDs is only available in the dual stoplight system. To turn on multiple LEDs, the integer values must be summed. For instance, to turn on GREEN1 and GREEN2, the integer value 9 must be sent.

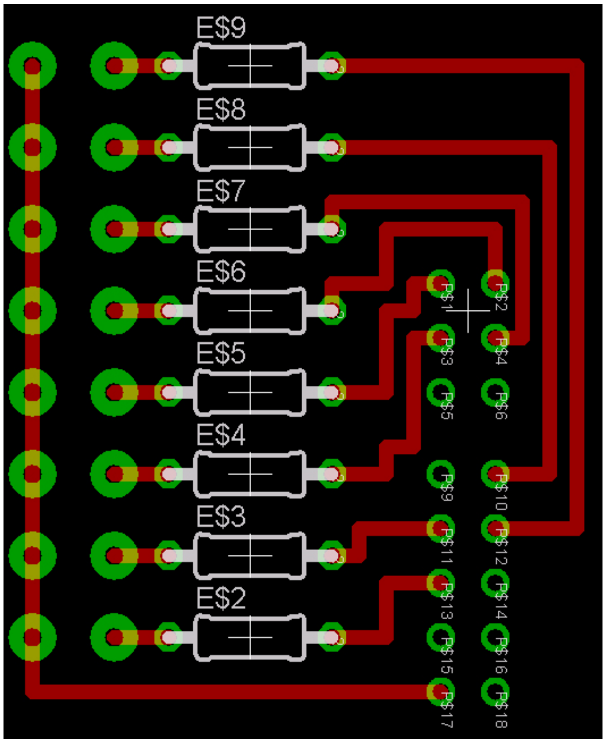

Figure 1: Main Board Layout

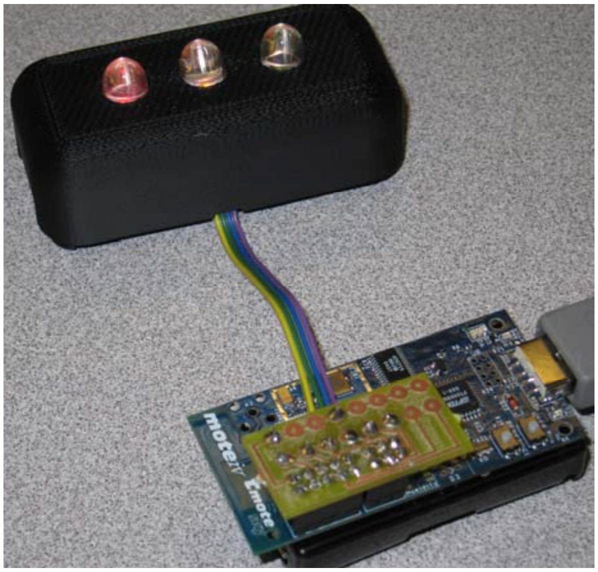

Figure 2: Single Stop